

# Microbial symbionts buffer hosts from the demographic costs of environmental stochasticity

Joshua C. Fowler<sup>1,2\*</sup>, Shaun Ziegler<sup>3</sup>, Kenneth D. Whitney<sup>3</sup>,  
Jennifer A. Rudgers<sup>3</sup>, Tom E.X. Miller<sup>1</sup>

<sup>1</sup>\*Department of BioSciences, Rice University, Houston, 77005, TX, USA.

<sup>2</sup>Department of Biology, University of Miami, Miami, 33146, FL, USA.

<sup>3</sup>Department of Biology, University of New Mexico, Albuquerque, 87131, NM, USA.

\*Corresponding author(s). E-mail(s): [jcf221@miami.edu](mailto:jcf221@miami.edu);

Contributing authors: [shaun.ziegler@gmail.com](mailto:shaun.ziegler@gmail.com); [whitneyk@unm.edu](mailto:whitneyk@unm.edu);

[jrudgers@unm.edu](mailto:jrudgers@unm.edu); [tom.miller@rice.edu](mailto:tom.miller@rice.edu);

Phone: 719-359-2960

## Author Contributions

J.C.F. contributed to data collection, data analysis, and led manuscript drafting. S.Z. contributed to data collection and manuscript revisions. K.D.W. contributed to research conception, data collection, and manuscript revisions. J.A.R. established transplant plots, contributed to research conception, data collection, and manuscript revisions. T.E.X.M. contributed to research conception, data collection, data analysis, and manuscript revisions.

## Data and Code Accessibility

Data will be made accessible as an Environmental Data Initiative package online  
**DOI:** [updated here when available](#). Code for all analysis is available through  
<https://github.com/joshuacfowler/Grass-Endophyte-Stochastic-Demography>

**Article Type:** Letter

**Running Title:** Symbiont-mediated demographic buffering

**Keywords:** stochastic demography, plant-microbe interactions, environmental variability, symbiosis, mutualism, long-term data, life history, Epichloë, Poaceae

**This file contains:** Abstract ( 150 words), Main Text (5397 words), Figures (1-4); Supporting Information - Supplemental Methods, Supplemental Figures A1-A28, Supplemental Tables S1-S3, References (66)

047      Manuscript submitted following PNAS style guidelines and can be  
048                  reformatted upon revision  
049  
050  
051  
052  
053  
054  
055  
056  
057  
058  
059  
060  
061  
062  
063  
064  
065  
066  
067  
068  
069  
070  
071  
072  
073  
074  
075  
076  
077  
078  
079  
080  
081  
082  
083  
084  
085  
086  
087  
088  
089  
090  
091  
092

**Abstract**

Species' persistence in increasingly variable climates will depend on resilience against the fitness costs of environmental stochasticity. Most organisms host microbiota that shield against stressors. Here, we test the hypothesis that, by limiting exposure to environmental extremes, microbial symbionts reduce hosts' demographic variance. We parameterized stochastic models using data from a 14-year symbiont-removal experiment including seven grass species that host *Epichloë* fungal endophytes. Endophytes reduced variance in fitness by > 10%, on average. Hosts with "fast" life history traits that lacked longevity as an intrinsic buffer benefited most from symbiont-mediated variance buffering. Under current climate conditions, contributions of variance buffering were modest compared to symbiont benefits to mean fitness. However, simulations of increased stochasticity amplified benefits of variance buffering and made it the more important pathway of host-symbiont mutualism than elevated mean fitness. Microbial-mediated variance buffering is likely an important, yet cryptic, mechanism of resilience in an increasingly variable world.

093	
094	
095	
096	
097	
098	
099	
100	
101	
102	
103	
104	
105	
106	
107	
108	
109	
110	
111	
112	
113	
114	
115	
116	
117	
118	
119	
120	
121	
122	
123	
124	
125	
126	
127	
128	
129	
130	
131	
132	
133	
134	
135	
136	
137	
138	

139 **Introduction**

140  
141 Global climate change involves increases in environmental variability, including  
142 changes to precipitation patterns and the frequency of extreme weather events [1, 2].  
143 Yet, the ecological consequences of increased variability are less well understood than  
144 those of changing climate means, such as long-term warming or drying. Incorpor-  
145 rating environmental variability into forecasts of population dynamics can improve  
146 predictions of the future [3].

147 Classic theory predicts that long-term population growth rates (equivalently, pop-  
148 ulation mean fitness) will decline under increased environmental stochasticity because  
149 the costs of bad years outweigh the benefits of good years – a consequence of nonlinear  
150 averaging [4, 5]. For example, in unstructured populations, the long-term stochastic  
151 growth rate in a fluctuating environment ( $\lambda_s$ ) will always be lower than the average  
152 growth rate ( $\bar{\lambda}$ ) by an amount proportional to the environmental variance ( $\sigma^2$ ):

153  
154 
$$\log(\lambda_s) \approx \log(\bar{\lambda}) - \frac{\sigma^2}{2\bar{\lambda}^2} \quad (1)$$
  
155

156  
157 Populations structured by size or stage similarly experience costs of variability [6, 7].  
158 There are accordingly two pathways to increase population viability in a variable  
159 environment: increase the mean growth rate and/or dampen temporal fluctuation in  
160 growth rates, also called “variance buffering”.

161 Both the inherent characteristics of species and the external properties of their envi-  
162 ronment can buffer demographic fluctuations. These inherent characteristics include  
163 life history traits [8, 9], negative correlations among vital rates [10], transient shifts in  
164 population structure [11]. For example, theory predicts that long-lived species, those  
165 on the slow end of the slow-fast life history continuum, will be less sensitive to environ-  
166 mental variability than short-lived species [12], a pattern which has empirical support  
167 across plants [13] and animals [9, 14]. Demographic variance is also determined by  
168 external abiotic factors, such as the magnitude of environmental variability [15] or  
169 the degree of environmental autocorrelation [16, 17]. These complex interplay of these  
170 factors determines the risks of extinction faced by populations [18] and underlies man-  
171 agement strategies promoting ecosystem resilience [19]. Yet little is known about how  
172 biotic interactions influence demographic variability or contribute to variance buffer-  
173 ing [20]. Intra-specific interactions, such as parental care, can reduce demographic  
174 variance in birds [21] and in primates [22]. While most research on inter-specific inter-  
175 actions focuses on their effects on mean demographic performance, species interactions  
176 also have the potential to influence demographic variance.

177 Most multicellular organisms host symbiotic microbes that affect growth and per-  
178 formance [23, 24], and many of these are vertically transmitted from maternal hosts to  
179 offspring [25]. Vertical transmission links the fitness of hosts and symbionts in a feed-  
180 back loop that selects for mutual benefits [26]. Many vertically-transmitted microbes  
181 are mutualistic and protect hosts from stressful environmental conditions including  
182 drought, extreme temperatures, or natural enemies [27, 28]. Some of the best studied  
183 examples include bacterial symbionts of insects that provide their hosts with thermal  
184 tolerance through the production of heat-shock proteins [29], and fungal symbionts of

plants that produce anti-herbivore and drought-protective compounds [30–32]. However, these diverse protective symbioses are context-dependent: the magnitude of benefits depends on environmental conditions [33, 34] and thus will vary temporally in a stochastic environment [35]. We hypothesized that context-dependent benefits from symbionts may buffer hosts against variability through strong benefits during harsh periods and neutral or even costly outcomes during benign periods, reducing the impacts of host exposure to extremes and dampening inter-annual variance relative to non-symbiotic hosts. Variance buffering is a previously unexplored mechanism by which symbionts may benefit their hosts instead of or in addition to elevating average fitness, the focus of most previous research.

To test the hypothesis that context-dependent benefits of symbiosis buffer hosts from the fitness costs of environmental stochasticity, we used a combination of long-term field experiments and stochastic demographic modeling. We used cool-season grasses and *Epichloë* fungal endophytes as a tractable experimental model in which non-symbiotic plants can be derived from naturally symbiotic plants through heat treatment, providing a contrast of symbiont effects that controls for the confounding influence of host genetic background. *Epichloë* endophytes are specialized symbionts growing intercellularly in the aboveground tissue of ~ 30% of  $C_3$  grass species [36]. These fungi are primarily transmitted vertically from maternal plants through seeds [37]. They produce a variety of alkaloids that can protect host plants from natural enemies [38] and drought stress [39].

Over 14 years (2007–2021), we collected longitudinal demographic data on the survival, growth, reproduction, and recruitment of all plants within replicated endophyte-symbiotic and endophyte-free populations at our field site in southern Indiana, USA. Through taxonomic replication (seven host-symbiont species pairs) we aimed to understand whether host life history traits could explain inter-specific variation in the magnitude of demographic buffering through symbiosis. We used this long-term data to parameterize stochastic population projection models in a hierarchical Bayesian framework. Specifically, we (1) quantified the effect of symbiosis on the mean and variance of host vital rates (survival, growth and reproduction) and fitness, (2) evaluated the relationship between host life history traits and the magnitude of symbiont-mediated variance buffering, (3) determined the relative contribution of symbiont-mediated mean and variance effects to host fitness, and (4) projected how increased environmental stochasticity (expected under future climates) changes the importance of variance buffering as a pathway of host-symbiont mutualism.

## Materials and Methods

### Study site and species

This study was conducted at Indiana University’s Lilly-Dickey Woods Research and Teaching Preserve (39.238533, -86.218150) in Brown County, Indiana, USA. This site is part of the Eastern broadleaf forests of southern Indiana, where the ranges of many understory cool-season grass species overlap. The experiment focused on seven of these grasses (*Agrostis perennans*, *Elymus villosus*, *Elymus virginicus*, *Festuca subverticillata*, *Lolium arundinaceum*, *Poa alsodes*, and *Poa sylvestris*), each of which hosts a

231 unique species of *Epichloë* endophyte (Table S1). All are native to eastern North  
232 America except the Eurasian species *L. arundinaceum*.

233

#### 234 **Endophyte removal, plant propagation, and field set-up**

235

236 Seeds from naturally symbiotic populations of the seven focal host species were col-  
237 lected during summer-fall 2006 from Lilly-Dickey Woods and the nearby Bayles Road  
238 Teaching and Research Preserve (39.220167, -86.542683). To generate symbiotic (S+)  
239 and symbiont-free (S-) plants from the same genetic lineages, seeds from each species  
240 were disinfected with a heat treatment described in Table S1 or left untreated. The  
241 heat treatment created symbiont-free plants by warming seeds to temperatures at  
242 which the fungus becomes inviable but the host seeds can still germinate. Both heat-  
243 treated and untreated seeds were surface sterilized with bleach to remove epiphyllous  
244 microbes, cold stratified for up to 4 weeks, then germinated in a growth chamber before  
245 transfer to the greenhouse at Indiana University where they grew for ~ 8 weeks. We  
246 confirmed endophyte status by staining thin sections of inner leaf sheath with aniline  
247 blue and examining tissue for fungal hyphae at 200X magnification [40]. We estab-  
248 lished experimental populations with vegetatively propagated clones of similar sizes  
249 (plants ranging from one to six tillers across species). By starting the experiment with  
250 plants of similar sizes and the same number of unique genotypes, we aimed to limit  
251 any potential effects of heat treatments on initial plant growth [41].

252 During the fall of 2007 and spring of 2008, we established 10 3x3 m. plots for *A. perennans*, *E. villosus*, *E. virginicus*, *F. subverticillata*, and *L. arundinaceum* and 18  
253 plots for *P. alsodes* and *P. sylvestris*. Half of the plots were randomly assigned to be  
254 planted with either symbiotic (S+) or symbiont-free (S-) plants, and initiated with  
255 20 evenly spaced individuals labeled with aluminum tags. In spring 2008, we placed  
256 plastic deer net fencing around each plot to limit deer herbivory and disturbance;  
257 damaged fences were regularly replaced.

258

#### 259 **Long-term demographic data collection**

260

261 Each summer (2008–2021) we censused all individuals in each plot for survival,  
262 growth and reproduction, and added new recruits to the census. Plots contained 13.3  
263 individuals/m<sup>2</sup> on average over the course of the experiment. Each census year was a  
264 sample of inter-annual climatic variation (n = 14 years, comprising 13 demographic  
265 transition years). We censused each species during its peak fruiting stage (May: *Poa*  
266 *alsodes*, *Poa sylvestris*; June: *Festuca subverticillata*; July: *Elymus villosus*, *Elymus vir-*  
267 *ginicus*, *Lolium arundinaceum*; September: *Agrostis perennans*), such that the censuses  
268 were pre-breeding and new recruits came from the previous years' seed production.  
269 Leaf litter was cleared out of each plot prior to the census, to aid in locating plants.  
270 For each plant remaining from the previous year, we determined survival, measured  
271 its size as a count of tillers, and collected reproductive data as counts of reproductive  
272 tillers and seed-bearing spikelets on all reproductive tillers to a maximum of three. We  
273 also tagged all unmarked individuals that were recruits from the previous years' seed  
274 production and collected the same demographic data. New recruits typically had one  
275 tiller and were non-reproductive. In 2008 through 2010, we took additional counts of  
276

seeds per inflorescence for all reproducing individuals in the plots to relate inflorescence and spikelet counts to seed production. In 2018, we stopped collecting data for the exotic *L. arundinaceum*, which had very high survival and low recruitment, and consequently very low variation across years. In total across 14 years, the dataset included demographic information for 16,789 individual host-plants and 31,216 transition-year observations.

We expected plots to maintain their endophyte status (symbiotic or symbiont-free) because these fungal symbionts are almost exclusively vertically transmitted, and plots were spaced a minimum of 5 m apart, limiting seed dispersal or horizontal transmission of the symbiont between plots. However, we regularly confirmed endophyte treatment throughout the lifetime of the experiment by opportunistically taking subsets of seeds from reproductive individuals and scoring them for their endophyte status with microscopy as above. Overall, these scores reflected 98% faithfulness of recruits to their expected endophyte status across species and plots (Fig. S23; Supplement data). Additionally, we have rarely observed fungal stromata, the fruiting bodies by which *Epichloë* are potentially transmitted horizontally, provided the fly vector is also present [42]. For *A. perennans*, *F. subverticillata*, *L. arundinaceum*, and *P. alsodes*, we never observed stromata. We observed stromata only infrequently for *E. villosus*, and even more rarely for *E. virginicus* and *P. sylvestris* (Table S2). For these species, stromata have only been observed irregularly across years on 35, 4, and 6 plants respectively, making up < 0.3% of all censused plants.

## Vital rate modeling

Equipped with these demographic data, we fit statistical models for survival, growth, flowering (yes or no), fertility of flowering plants (number of flowering tillers), production of seed-bearing spikelets (number per inflorescence), the average number of seeds per spikelet, and the recruitment of seedlings from the preceding year's seed production. We fit these vital rates as generalized linear mixed models in a hierarchical Bayesian framework using RStan [43] which allowed us to isolate endophyte effects on vital rate means and variances, borrow strength across species for some variance components, and propagate uncertainty from the individual-level vital rates to population projection models [44]. All vital rate models included random plot and year effects, with separate estimates of year-to-year variance for symbiotic and symbiont-free plants, to quantify the effect of endophytes on inter-annual variance. All parameters were given vague priors [45]. We ran each vital rate model for 2500 warm-up and 2500 MCMC sampling iterations with three chains. We assessed model convergence with trace plots of posterior chains and checked for  $\hat{R}$  values less than 1.01, indicating low within- and between-chain variation [46, 47]. For those models that showed poor convergence, we extended the MCMC sampling to include 5000 warm-up and 5000 sampling iterations, which was only necessary for seedling growth. We graphically checked vital rate model fit with posterior predictive checks comparing simulated and observed data (Fig. S19-S20).

*Survival* - We modeled survival as a Bernoulli process, where the survival ( $S$ ) of an individual  $i$  in plot  $p$  and census year  $t$  was predicted by the plot-level endophyte

323 status ( $e$ ), host species ( $h$ ), size in the preceding census, and the plant's origin status  
324 (whether it was initially transplanted or naturally recruited into the plot).

325

326

327  $S_{i,p,e,h,t} \sim Bernoulli(\hat{S}_{i,p,e,h,t})$  (2a)

328  $\text{logit}(\hat{S}_{i,p,e,h,t}) = \beta_{0_h} + \beta_1 * \text{origin}_i$  (2b)

329  $+ \beta_{2_h} * \text{endo}_e + \beta_{3_h} * \text{size}_{i,t-1} + \tau_{e,h,t} + \rho_p$  (2c)

330  $\tau_{e,h,t} \sim \text{Normal}(0, \sigma_{\tau_{e,h}}^2)$  (2d)

331  $\rho_p \sim \text{Normal}(0, \sigma_\rho^2)$  (2e)

332

333

334 Here,  $\hat{S}$  is the survival probability,  $\beta_{0_h}$  is an intercept specific to each host species,  
335  $\beta_1$  is the effect of the plant's recruitment origin,  $\beta_{2_h}$  is the endophyte effect,  $\beta_{3_h}$  is the  
336 size effect,  $\tau_{e,h,t}$  is a normally distributed year effect for each species and endophyte  
337 status with variance  $\sigma_{\tau_{e,h}}^2$ , and  $\rho_p$  is a normally distributed plot effect with variance  
338  $\sigma_\rho^2$  ( $p(e)$  indicates that plot identity is uniquely associated with an endophyte status).  
339 We assume that origin effect  $\beta_1$  and plot-to-plot variance  $\sigma_\rho^2$  are shared across host  
340 species, allowing us to "borrow strength" across the multi-species dataset; other model  
341 parameters are unique to host species. We separately modeled the survival of newly  
342 recruited seedlings with a similar model but omitting previous size dependence and  
343 origin status.

344 *Growth* - We modeled plant size in census year  $t$  ( $G$ ) with the same linear pre-  
345 dictor for the mean as described for survival. Because we measured size as positive  
346 integer-valued counts of tillers, we modeled it with a zero-truncated Poisson-inverse  
347 Gaussian distribution. This distribution includes a shape parameter  $\lambda_G$  to account for  
348 overdispersion in the data. We additionally modeled the growth of newly recruited  
349 seedlings separately with a Poisson-inverse Gaussian model omitting size structure  
350 and the plants' origin status as with seedling survival.

351 *Flowering* - We modeled whether or not a plant was flowering during the census ( $P$ )  
352 as a Bernoulli process, with the same linear predictor for the mean as described above  
353 for survival except that size dependence for reproductive vital rates was determined  
354 by the individual's size during the same census year as opposed to its size during the  
355 previous year.

356 *Fertility* - For a plant that was flowering during the census, its fertility was the  
357 number of reproductive tillers produced ( $F$ ), which we modeled as a function of size in  
358 the same census period with a zero-truncated Poisson-Inverse Gaussian distribution,  
359 with the same linear predictor for the mean as described above.

360 *Spikelets per Inflorescence* - Spikelet production ( $K$ ) was recorded as integer counts  
361 on up to three inflorescences per reproducing plant. We modeled these data with a neg-  
362 ative binomial distribution, with the same linear predictor for the mean as described  
363 above.

364 *Seed Production per Spikelet* - For individuals with recorded counts of seed pro-  
365 duction, we calculated the number of seeds per spikelet from our counts of seeds and  
366 spikelets per inflorescence, and then modeled seeds per spikelet ( $D$ ) as means of a  
367 Gaussian distribution for each species and endophyte status. Because we had less

detailed data across years and plants for seed production than for other reproductive vital rates, we omitted both plot and year random effects. 369  
370

*Seedling Recruitment* - We used a binomial distribution to model the recruitment of new seedlings ( $R$ ) into the plots from seeds produced in the preceding year, assuming no long-lived seed bank. We included an intercept specific to each host and endophyte status and the same random effects structure as in other models. We estimated the number of seeds per plot in the preceding year by multiplying the total number of reproductive tillers per plant by the mean number of spikelets per inflorescence and mean number of seeds per spikelet ( $D$ ). For plants with missing fertility or spikelet data, we used the expected number of reproductive tillers ( $F$ ) or of spikelets per inflorescence from ( $K$ ), drawing from the full posteriors of our models. We rounded this value to get the estimated seed production for each individual, and finally summed across all reproductive plants in each year and plot to get the total number of seeds produced. 371  
372  
373  
374  
375  
376  
377  
378  
379  
380  
381  
382  
383  
384  
385  
386  
387  
388  
389  
390  
391  
392  
393  
394  
395  
396  
397  
398

## Stochastic population model

We parameterized stochastic matrix projection models using the fitted statistical vital rate models. Each matrix projection model included two state variables:  $r_t$  (the number of newly recruited individuals in year  $t$  which we assume to be non-reproductive), and  $\mathbf{n}_t$  (a vector including all non-seedling individuals of sizes  $x \in \{1, 2, \dots, U\}$ , ranging from one to the maximum number of tillers  $U$ ). We use these two state variables to avoid having to assume demographic equivalence between seedling and non-seedling one-tiller plants. We used the same model structure for each species and endophyte status (not shown in model notation for readability). See Fig. S21 for a generalized life cycle graph. 399  
400  
401  
402  
403  
404  
405  
406  
407  
408  
409  
410  
411  
412  
413  
414

The number of recruits in year  $t + 1$  is given by:

$$r_{t+1} = \sum_{x=1}^U P(x; \boldsymbol{\tau}_P) F(x; \boldsymbol{\tau}_F) K(x; \boldsymbol{\tau}_K) D R(\boldsymbol{\tau}_R) n_t^x \quad (3)$$

The total number of seeds produced by a maternal plant of size  $x$  is the product of the size-specific probability of flowering  $P$ , the number of reproductive tillers  $F$ , the number of spikelets per inflorescence  $K$ , and the number of seeds per spikelet  $D$ . Multiplying by the probability of transitioning from seed to seedling  $R$  gives a per-capita rate of seedling production, which is multiplied by the number of plants of size  $x$  ( $n_t^x$ , the  $x^{\text{th}}$  element of  $\mathbf{n}_t$ ) and summed over all sizes. Each function also depends on the species- and endophyte-specific year random effects for that vital rate ( $\boldsymbol{\tau}$ , a vector of year-specific values derived from the statistical models).

The number of  $y$ -sized plants in year  $t + 1$  is given by:

$$n_{t+1}^y = Z(y; \boldsymbol{\tau}_Z) B(\boldsymbol{\tau}_B) r_t + \sum_{x=1}^U S(x; \boldsymbol{\tau}_S) G(x, y; \boldsymbol{\tau}_G) n_t^x \quad (4)$$

where  $n_{t+1}^y$  is the  $y^{\text{th}}$  element of vector  $\mathbf{n}_{t+1}$ . The first term on the right hand side of Eqn. 4 represents growth ( $Z$ ) and survival ( $B$ ) of seedling recruits. The second term

415 includes the survival of previously  $x$ -sized plants and the growth of survivors from size  
 416  $x$  to  $y$ , summed over all  $x$ . To avoid predictions of unrealistic growth outside of the  
 417 observed size distribution, we set a ceiling on the growth function for plants at the  
 418 97.5<sup>th</sup> percentile of observed sizes for each host species [48].

419 Each of the vital rate functions in Eqns. 3 and 4 have separate intercepts and year  
 420 random effects for symbiotic and symbiont-free populations, allowing us to calculate  
 421 the effect of endophyte symbiosis on the mean, variance, and coefficient of variation  
 422 (CV) of  $\lambda$ , the dominant eigenvalue of the year- and endophyte-specific projection  
 423 matrix. This model treats climate drivers implicitly through year-specific random  
 424 effects. We also developed a climate-explicit version with the addition of parameters  
 425 defining the relationship between either annual or growing season drought index and  
 426 each vital rate. A full description of climate-explicit methods can be found in the  
 427 *Supporting Information Supplemental Methods*.

428

## 429 Life History Analysis

430

431 We collected metrics describing each host species' life history to test the relationship  
 432 between pace of life and variance buffering (Table S2). Using the Rage package [49],  
 433 we calculated  $R_0$ , longevity, and generation time from the mean transition matrix for  
 434 symbiont-free populations. We recorded seed size as the average lemma length from  
 435 the Flora of North America [50]. We also calculated the 99th percentile of maximum  
 436 observed age for symbiont-free plants from the census data for each species. Next, we  
 437 fit Bayesian phylogenetic mixed-effects models using the brms package [51] to test the  
 438 relationship between each life history trait and the effect of symbiosis on the CV of  $\lambda$   
 439 (a measure of variance buffering) while controlling for phylogenetic non-independence  
 440 between host and symbiont species. We pruned species-level phylogenies of plants  
 441 [52] and *Epichloë* fungi [53] to include the focal species. *Agrostis perennans* was not  
 442 included in the tree, and so we used the congener *A. hyemalis*. We defined separate  
 443 phylogenetic covariance matrices for each pruned tree. We propagated uncertainty in  
 444 the estimated variance buffering effect  $V$  with a measurement error model:

445

446

$$V_{MEAN,h} \sim Normal(V_{EST,h}, V_{SD,h}) \quad (5a)$$

448

$$V_{EST,h} \sim Normal(\mu_h, \sigma) \quad (5b)$$

449

$$\mu = \alpha + \beta * trait + \pi_j \quad (5c)$$

450

$$\alpha \sim Normal(0, .5) \quad (5d)$$

451

$$\beta \sim Normal(0, .1) \quad (5e)$$

452

$$\sigma \sim Half-Normal(.04, .01) \quad (5f)$$

453

$$\pi_h \sim MVN(0, \sigma_\pi \mathbf{A}) \quad (5g)$$

454

$$\sigma_\pi \sim Half-Normal(0, .1) \quad (5h)$$

455

456

457 Here,  $V_{EST}$  is the variance buffering effect for host species  $h$ , estimated from the  
 458 posterior mean ( $V_{MEAN}$ ) and standard deviation ( $V_{SD}$ ), propagating uncertainty asso-  
 459 ciated with the effect of symbiosis. The model includes an intercept ( $\alpha$ ) and a slope  
 460

( $\beta$ ) defining the relationship between the variance buffering effect and the life history trait. The residual standard deviation is given by ( $\sigma$ ). We used weakly informative priors to aid model convergence. Each prior was centered at zero, except for the residual standard deviation, which we centered at the standard deviation of the estimated variance buffering effect, .04. The phylogenetic random effect ( $\pi$ ), which is modeled as a multivariate normal distribution, has a between-species standard deviation ( $\sigma_\pi$ ) structured by the phylogenetic covariance matrix  $\mathbf{A}$ . We ran each MCMC sampling chain for 8000 warmup iterations and 2000 sampling iterations. We assessed model convergence as described for the vital rate models.

## Mean-variance decomposition

To calculate stochastic population growth rates ( $\lambda_s$ ) for each host species and endophyte status we simulated population dynamics for 1000 years by randomly sampling from the 13 annual transition matrices, discarding the first 100 years to minimize the influence of initial conditions. Sampling observed transition matrices produces models that realistically capture inter-annual variation by preserving correlations between vital rates [54]. We tallied the total population size at each time step as  $N_t = r_t + \sum_{x=1}^U n_t^x$  and calculated the stochastic growth rate as  $\log(\lambda_s) = E[\log(\frac{N_t}{N_{t+1}})]$  [55, 56]. We calculated the total effect of endophyte symbiosis as the difference in  $\lambda_s$  between S+ and S- populations. We propagated uncertainty from the vital rate models to the calculation of  $\lambda_s$  using 500 draws from the posterior distribution of model parameters.

We decomposed the total endophyte effect on  $\lambda_s$  into contributions from effects on vital rate means, variances, and their interaction. Specifically, we repeated the calculation of  $\lambda_s$  for two additional “treatments”: (1) endophyte effects on mean vital rates only, with inter-annual variances shared between S+ and S- at the S- reference level for all vital rates, and (2) endophyte effects on vital rate variances only, with vital rate means shared between S+ and S- at the S- reference level. The combination of all four  $\lambda_s$  treatments (S+ vital rate means and variances, S- means and variances, S+ means with S- variances, S- means with S+ variances) allowed us to quantify to what extent the overall effect of symbiosis derives from changes in vital rates means, variances, and their interaction. The interaction occurs because the variance penalty to stochastic growth is proportional to the arithmetic mean of annual growth rates (see Eq. 1) such that variance is more detrimental for populations with lower average growth rates.

To create scenarios of increased variance relative to that observed during the study period, we repeated the stochastic growth rate decomposition, but sampling only subsets of the 13 observed annual transition matrices. We created two scenarios of increased environmental variance by sampling the transition matrices associated with the set of either six or two most extreme  $\lambda$  values. These extreme  $\lambda$  values represent the best and worst years experienced by the plants, using the S- populations as the reference condition. By sampling away from an average year in both directions, the six- and two- years scenarios increased the standard deviation of yearly host growth rates by 1.3 and 2.1 times, respectively, without changing mean growth rates (< 2.3% difference in  $\bar{\lambda}$  between simulation treatments, Fig. S22). We performed the same

507 mean-variance decomposition for these scenarios as for the ambient conditions (all 13  
508 years sampled) for all host species described above.

509

## 510 **Results**

511

### 512 **Symbionts buffer host demographic variance**

513

514 Across the 14 census years, endophytes reduced inter-annual variance for 66% (37/56)  
515 of host species-vital rate combinations (average Cohen's D for effects on vital rate stan-  
516 dard deviation: -0.15) (Fig 1A; Fig. S6 - Fig. S18). Endophytes also increased mean  
517 vital rates for the majority (36/56) of host species-vital rate combinations (average  
518 Cohen's D for effects on vital rate mean: 0.15), and benefits were particularly strong  
519 for host survival, plant growth and recruitment (Fig. 1A; Fig. S1 - Fig. S5). The magni-  
520 tude of mean and variance effects differed among host species and vital rates. Symbiont  
521 effects on vital rate variance are as large and even exceed effects on vital rate means  
522 for certain species. For example, endophytes modestly increased mean adult survival  
523 (Fig. 1C) and strongly reduced variance in survival (Fig. 1D) for *Festuca subverticil-  
524 lata*, while for *Poa alsodes*, variance buffering was more apparent in seedling growth  
525 and inflorescence production (Fig 1E). Interestingly, certain vital rates showed costs  
526 of endophyte symbiosis. Symbiotic individuals of *A. perennans* grew larger than those  
527 without endophytes (Fig. 1B), yet endophytes also reduced this species' mean recruit-  
528 ment rates (Fig. 1A). Similarly, variance was increased for certain species' vital rates,  
529 such as in seedling growth for *Elymus villosus* and *Festuca subverticillata* (Fig. 1A).

530

531 Because not all vital rates contribute equally to fitness, we used stochastic matrix  
532 models to integrate the diverse effects on vital rates described above into comprehen-  
533 sive measures for the mean and variance of year-to-year fitness ( $\lambda_t$ ) and the long-run  
534 stochastic fitness that integrates both mean and variance ( $\lambda_S$ ). On average across host  
535 species, S+ populations had greater mean fitness (> 92% confidence that endophytes  
536 increased  $\bar{\lambda}$ ) and lower inter-annual variability in fitness (> 86% confidence that endo-  
537 phytes decreased the coefficient of variation of  $\lambda_t$ ) than S- populations (Fig. 2). For  
538 some host species, the CV of  $\lambda_t$  declined by as much as 170% (*P. alsodes*, *F. subverti-  
539 cillata*), while for others, endophyte effects on variance were substantially smaller (6%  
540 lower for *E. villosus*, 16% lower for *A. perennans*), or even positive (27% increase for  
*E. virginicus*).  
541

542

### 543 **Faster life histories predict stronger symbiont-mediated variance buffering**

544

545 Maybe need to bring up the "prediction" here or in introduction, but I moved it to  
the discussion<sup>1</sup>

546

547 In support of the prediction that hosts with long lifespans, which are intrinsically  
548 buffered from environmental variability, should benefit less from symbiont-mediated  
549 variance buffering, we found that hosts with trait values representing faster life history  
550 strategies experienced greater variance buffering from endophytes than those with  
551 slow life histories (Fig. 3). Bayesian phylogenetic mixed-effects models, controlling for  
552

---

1

species' relatedness, indicated that variance buffering was stronger for host species with shorter lifespan (Fig. 3A; 75% probability of positive relationship with empirically observed maximum plant age) and smaller seeds (Fig. 3B; 73% probability of positive relationship with seed length). Other life history traits similarly had positive, but weaker, support for the prediction that faster life history traits correlate with stronger variance buffering (Fig. S26-S28).

## Contributions from variance buffering are weak relative to mean effects

To evaluate the relative importance of mean fitness benefits and variance buffering as alternative pathways of mutualism, we decomposed the overall effect of the symbiosis on the stochastic growth rate  $\lambda_S$  using simulations from the population models in four configurations<sup>2</sup>. These included either the full symbiosis effect (both mean and variance buffering effects), mean effects alone, variance effects alone, or neither mean nor variance effects. Overall, the full effect of symbiosis on  $\lambda_S$ , averaged across host species, provided strong evidence of grass-endophyte mutualism (99% certainty of a positive total effect on  $\lambda_S$ ) (Fig. 4; see Fig. S22 for individual host species). Contributions to this full effect derived from both mean and variance buffering effects, as well as a slightly negative interaction (i.e., the combined influence of mean and variance effects) was smaller than the sum of their individual effects). Endophytes' contributions to  $\lambda_S$  from mean effects were four times greater, averaged across species, than contributions from variance buffering (Fig. 4), suggesting that, under the regime of environmental variability represented by our 14-year study, damped fluctuations in fitness via variance buffering was a far less important element of the benefits of symbiosis than increased mean fitness. Results for individual host species were largely consistent with the cross-species trends (Fig S22). The full effect of symbiosis on  $\lambda_S$  was positive for seven out of eight host species, with statistical confidence ranging from 66% to > 99% certainty. The one exception was the host species *P. sylvestris*, for which our analysis indicated that fungal endophytes were effectively neutral in their overall fitness effect (45% and 55% posterior probability of positive and negative effects; Fig S22).

## Variance buffering strengthens under increased environmental variability

To simulate increased variability, we repeated the decomposition of  $\lambda_S$  for two alternative forecast scenarios, randomly sampling transition matrices that represented either the six most extreme years experienced by each species or the two most extreme years, subsets of the thirteen transition matrices across the 14-year study period. Increased variability elicited stronger mutualistic benefits of endophyte symbiosis (Fig. 3) than ambient variability (overall effect of the symbiosis increased by > 130%). This increase was driven by increased contributions from the variance buffering mechanism (from a 24% contribution in the ambient scenario to a 66% contribution in the most variable scenario) rather than from greater mean effects. In the most variable scenario,

---

<sup>2</sup> Could update this to include the VR decomposition

599 the relative importance of mean and variance effects reversed, with variance buffering  
600 contributions that were 1.5 times greater than contributions from mean benefits,  
601 averaged across species (Fig. 4).

602

## 603 Discussion

604

605 Across seven host species, eight vital rates, 14 years, and 16,789 individual plants, our  
606 analysis provided the first empirical evidence of symbiont-mediated variance buffering.  
607 When mean and variance effects of symbionts were considered together, none of the  
608 host-symbiont pairings were antagonistic (i.e., with endophytes that both decreased  
609 mean fitness and increased variance) (Fig. 2C), suggesting that variation across host  
610 species and vital rates in mean and variance effects may reflect alternative strategies  
611 that yield similar net benefits of endophyte symbiosis. These alternative strategies  
612 may to the long-term stability of these mutualism

613 Therefore, host species with long lifespans that produce few, large offspring should  
614 benefit less from symbiont-mediated variance buffering than species with fast life cycles  
615 that produce many smaller offspring with low per-capita chance of success [57, 58].

616 Considering fungal life history traits, the three host species for which the net mutualism  
617 benefit was weakest (*Elymus villosus*, *Elymus virginicus*, and *Poa sylvestris*)  
618 (Fig. 2C) were the only hosts for which we observed fungal stromata, fruiting bodies  
619 capable of horizontal (contagious) transmission (Table S2). This result supports the  
620 theoretical expectation that strict vertical transmission drives the evolution of strong  
621 host-symbiont mutualism [26, 59]. Conclusions about life histories are somewhat con-  
622 strained by the narrow range of trait values among closely related species in the grass  
623 sub-family Pooideae and their co-evolving symbionts. Our understanding of how life his-  
624 tory variation modulates the fitness consequences of microbial symbiosis would profit  
625 from tests across a wider span of taxonomic groups [60].

626 Simulations of increased environmental variability, a key prediction of climate  
627 change forecasts [2], indicated that mutualism with microbial symbionts, and their  
628 variance buffering effects in particular, will take on increased importance for hosts in  
629 a more variable future climate.

630 Reduced sensitivity to drought, as has been reported for some *Epichloë* symbioses  
631 [39], is a candidate mechanism that could generate a signature of variance buffering:  
632 drought conditions may have weaker fitness costs for S+ hosts, reducing fluctuations in  
633 fitness through time. Accordingly, analysis of climate-explicit matrix models indicated  
634 that, for five of seven taxa, S+ populations were less sensitive to annual or growing  
635 season drought (12-month or 3- month drought index; Standardized Precipitation-  
636 Evapotranspiration Index [61]) than S- populations (Supporting Information Text;  
637 Fig. S24-S25; Table S3). However, we did not find a strong relationship between the  
638 magnitude of variance buffering and relative drought sensitivities, suggesting that  
639 other climatic factors or other temporally-varying aspects of the environment may  
640 elicit benefits of endophyte symbiosis, including documented resistance to herbivory  
641 for six of these host taxa [62, 63].

642 To forecast how symbionts may affect hosts in future climates across their ranges,  
643 we need to consider that this is a field experiment in one location.

644

Thus, variance buffering – a cryptic microbial influence that manifests only over long time scales – is poised to become the dominant way in which grasses benefit from symbiosis with fungal endophytes in more variable climates of the future.	645
	646
	647
To DO: remake size-struct plot for each species	648
Remake size structure for only recruit plantsecoles	649
- The fact that this is a field experiment in one location	650
SPEI analysis? and climate; implicit to explicit treatment of drivers; types of envrionemtnal variability	651
- Evolutionary context: i.e. different alternative strategies of mean and variance; diverse microbiome, bet-hedging	652
S+ and S- independent	653
	654
	655
	656
	657
<b>Conclusion</b>	658
Ecologists increasingly recognize the importance of symbiotic microbes for host organisms and the populations, communities, and ecosystems in which their hosts reside [64–67]. Despite awareness of these ubiquitous interactions, long-term studies of microbial symbiosis are very rare. Our analysis of taxonomically-replicated, long-term field experiments that manipulated the presence/absence of fungal symbionts in plants demonstrates for the first time that heritable microbes can commonly benefit hosts not only through improved mean fitness – the focus of most previous research – but also through buffering against environmental variance. Our results provide an important advance to improve forecasts of the responses of populations (and symbiota) to increasing environmental stochasticity under global change, suggesting that, for some host species, microbial symbiosis may compensate for the lack of intrinsic tolerance of variability conferred by “slow” life history traits. We found that, relative to mean fitness benefits, symbiont-mediated variance buffering made weak contributions to host-symbiont mutualism under the current regime of environmental variability. However, variance buffering is likely to become the dominant benefit that fungal endophytes confer to grass hosts in more variable future environments. This result emerges from the context-dependent nature of grass-endophyte interactions, combined with the observation that environmental stochasticity generates fluctuation in context. These key ingredients, and thus the potential for symbiont-mediated variance buffering, similarly apply to the diverse host-microbe symbioses across the tree of life.	659
	660
	661
	662
	663
	664
	665
	666
	667
	668
	669
	670
	671
	672
	673
	674
	675
	676
	677
	678
	679
	680
	681
	682
	683
	684
	685
	686
	687
	688
	689
	690

691 **Acknowledgments.** We thank Mark Sheehan, Ali Campbell, Kyle Dickens, Blaise  
692 Willis, and Sar Lindner for contributions to field data collection. We also thank Volker  
693 Rudolf, Daniel Kowal, Lydia Beaudrot and Judie Bronstein for helpful comments on  
694 and discussion of this project. This research was supported by the National Science  
695 Foundation (grants 1754468 and 2208857).

696 **Supplementary information.** Supplementary information for this paper includes  
697 Supplementary Methods, Figs. A1 to A28, and Tables A1 to A3.  
698

699

700

701

702

703

704

705

706

707

708

709

710

711

712

713

714

715

716

717

718

719

720

721

722

723

724

725

726

727

728

729

730

731

732

733

734

735

736

## Figures

737  
738  
739  
740  
741  
742  
743  
744  
745  
746  
747  
748  
749  
750  
751  
752  
753  
754  
755  
756  
757  
758  
759  
760  
761  
762  
763  
764  
765  
766  
767  
768  
769  
770  
771  
772  
773  
774  
775  
776  
777  
778  
779  
780  
781  
782

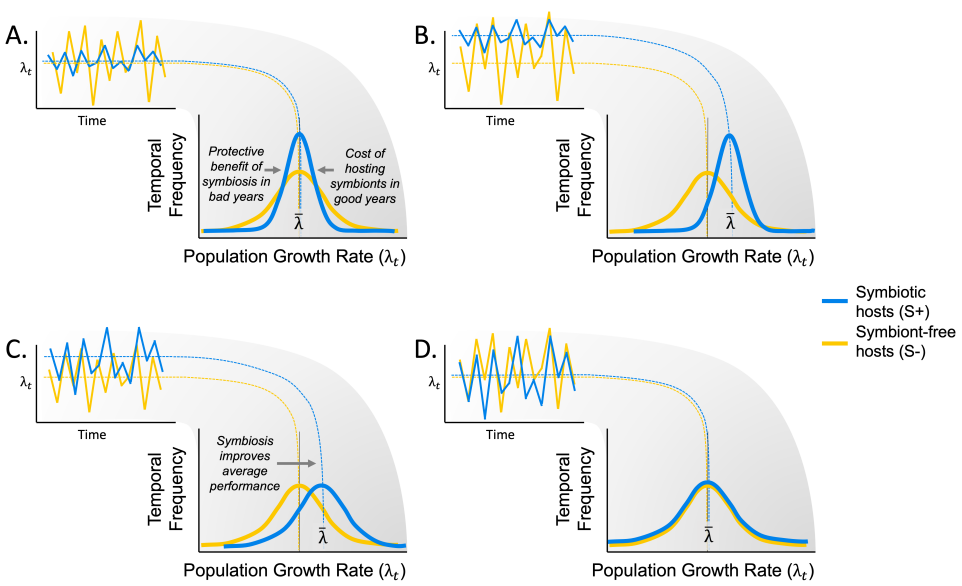


**Fig. 1** Hypothesized effects of symbiosis on the mean and variance of annual population growth rates. (A) Context-dependent symbiosis may provide benefits to hosts during harsh years while being neutral or costly during benign years. Temporal variance in populations growth rates of symbiotic host populations (S+; blue lines) is expected to decrease relative to symbiont-free hosts (S-; yellow lines). (B) Symbiosis may improve average performance across years in addition to reducing temporal variance. (C) Consistent benefits of symbiosis could improve average performance across years with no influence on temporal variance. (D) Symbiosis may have an effectively neutral effect on population growth rates.

783  
 784  
 785  
 786  
 787  
 788  
 789  
 790  
 791  
 792  
 793  
 794  
 795  
 796  
 797  
 798  
 799  
 800  
 801  
 802  
 803  
 804  
 805  
 806  
 807  
 808  
 809  
 810  
 811  
 812  
 813  
 814  
 815  
 816  
 817  
 818  
 819  
 820  
 821  
 822  
 823  
 824  
 825  
 826  
 827  
 828

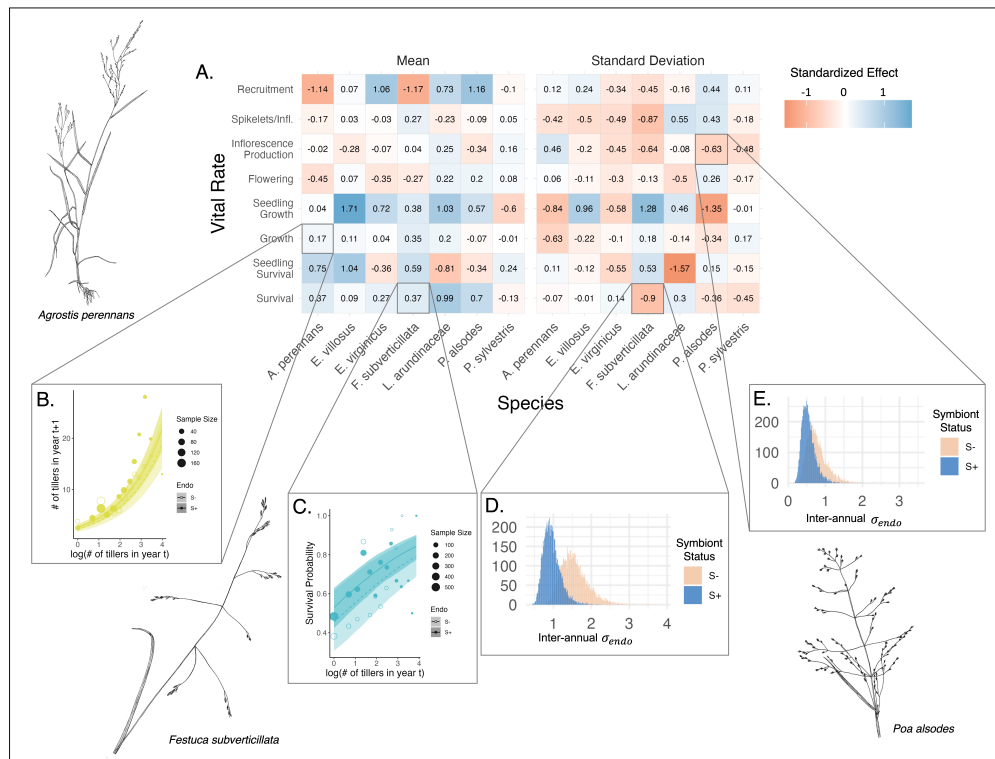


**Fig. 2** Endophyte symbiosis altered host vital rates.(A) Shading represents the posterior mean standardized effect size (Cohen's D) of endophyte symbiosis on mean or standard deviation of host vital rates (blue indicates that symbiosis increased the mean or standard deviation and red indicates a reduction). Endophytes' diverse vital rate effects include increased (B) mean growth of *A. perennans* and (C) mean survival probability of *F. subverticillata*. Endophyte presence also reduced inter-annual standard deviation in (D) the survival of *F. subverticillata* and (E) the fertility of *P. alsodes*. In panels B-C, mean vital rate estimates are shown with 80% credible intervals along with data binned by size for symbiotic (S+) and symbiont-free (S-) plants, while panels D-E show estimated posterior distributions of endophyte-status specific inter-annual standard deviation ( $\sigma_{\tau_{e,h}}^2$ ) for each vital rate for S+ (blue) and S- (beige) populations. Organism silhouettes modified from "Festuca subverticillata" by Cindy Roché and "Agrostis hyemalis" and "Poa alsodes" by Sandy Long ©Utah State University.

829  
 830  
 831  
 832  
 833  
 834  
 835  
 836  
 837  
 838  
 839  
 840  
 841  
 842  
 843  
 844  
 845  
 846  
 847  
 848  
 849  
 850  
 851  
 852  
 853  
 854  
 855  
 856  
 857  
 858  
 859  
 860  
 861  
 862  
 863  
 864  
 865  
 866  
 867  
 868  
 869  
 870  
 871  
 872  
 873  
 874

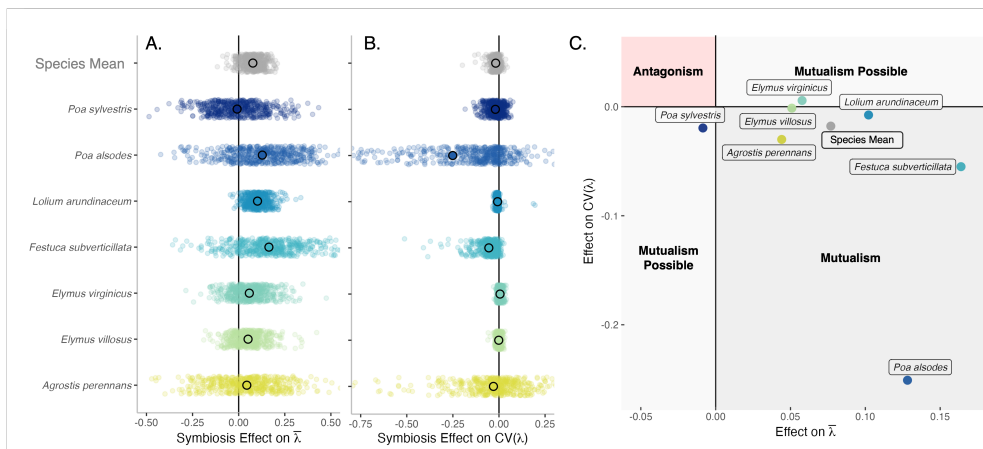


**Fig. 3** Mean and variance-buffering effects on fitness. Black circles indicate the average effect of endophytes along with 500 posterior draws (smaller colored circles) on the (A) mean and (B) coefficient of variation in  $\lambda$  for each host species as well as a cross species mean. (C) For all hosts, endophytes either reduce variance, increase the mean, or both, and consequently when considering stochastic environments, the interactions are always at least potentially mutualistic.

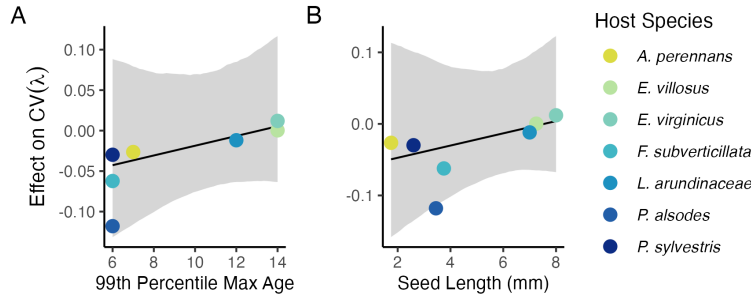
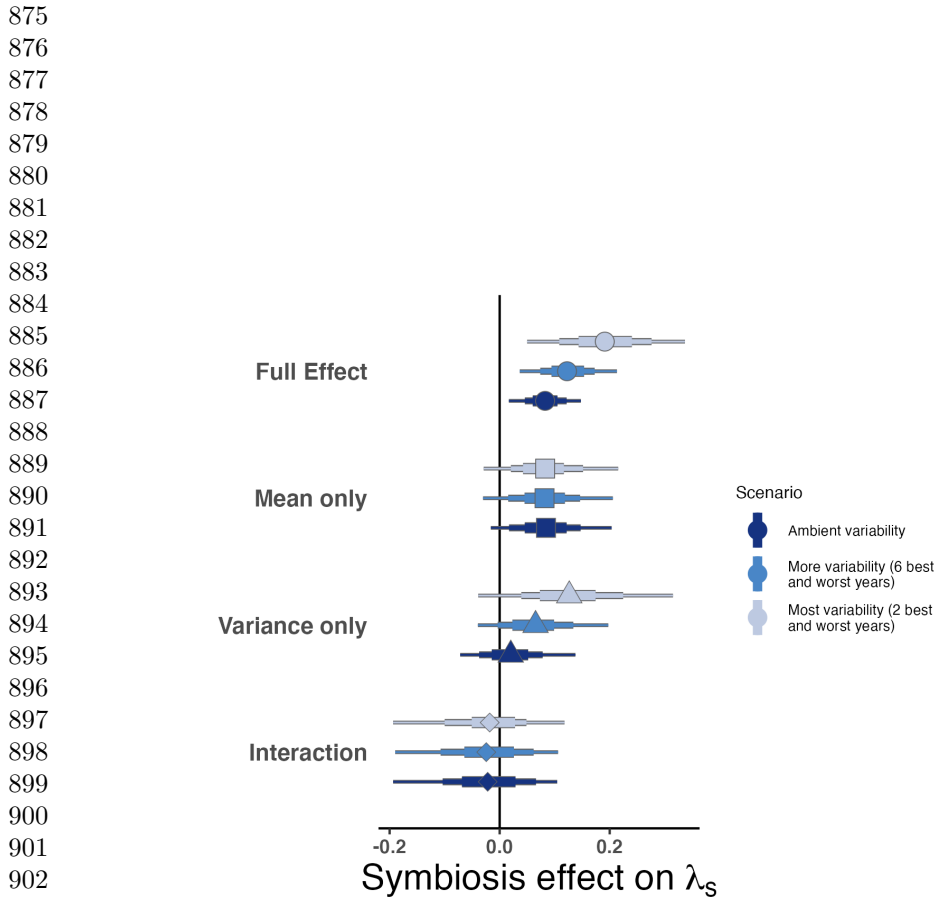


**Fig. 4** Host species with faster life history traits experience stronger effects of symbiont-mediated variance buffering. Regressions between life history traits describing the fast-slow life history continuum ((A) 99th percentile maximum age observed during long term censuses in years; (B) Seed size) and the effect of endophyte symbiosis on the coefficient of variation in population growth rate ( $\lambda$ ). Each panel shows the fitted mean relationship (line) along with the 95% credible interval.



904 **Fig. 5** Cross-species average endophyte contributions to stochastic growth rates under observed and  
 905 elevated variance. Endophyte symbiosis contributes to the total effect of mutualism on  $\lambda_S$  through  
 906 benefits to mean growth rates and through variance buffering as well as the interaction between  
 907 mean and variance effects. Shapes indicate the posterior mean of each contribution averaged across  
 908 the seven focal symbiota, along with bars for the 50, 75 and 95% credible intervals. The full effect of  
 909 the symbiosis (circles) becomes more mutualistic under scenarios of increased variance (represented  
 910 by color shading). Relative to the ambient scenario sampling transition matrices for all 13 transition  
 911 years during the study period, simulations increased variance by sampling the most extreme six or  
 912 two years, leading to increased contributions from variance buffering effects (triangles) and a  
 913 constant contribution from mean effects (squares).

914  
 915  
 916  
 917  
 918  
 919  
 920

<b>Supporting Information</b>	921
	922
<b>Supplemental Methods</b>	923
<b>Estimating climate drivers of environmental context-dependence</b>	924
	925
To connect the variance buffering effects of endophytes with inter-annual variability in climate, we built climate-explicit stochastic matrix population models from the vital rate data in addition to the climate-implicit model described in the main text.	926
Identifying the potentially complex relationships between vital rates and environmental drivers remains a key challenge for accurate forecasts of the ecological impacts of environmental stochasticity [68]. We first downloaded temperature and precipitation data from a weather station in Bloomington, IN, approx. 27 km from our study site, using the rnoaa package [69]. Compared to other weather stations in the area, the measurements from Bloomington contain the most complete climate record across the study period and are correlated with more local measurements from Nashville, IN for years in which local data are available (total daily precipitation: $R^2 = .76$ ; mean daily temperature: $R^2 = .94$ ). The mean annual temperature across the study period was $11.9 C^\circ$ (SD: $1.05 C^\circ$ ) and the average annual precipitation was 1237.9 mm/year (SD: 204.89 mm/year) (Fig. S24). Given the known role of endophytes in promoting host drought tolerance, we calculated the Standardised Precipitation-Evapotranspiration Index (SPEI) for 3 and 12 months preceding each annual censuses, reflecting drought during the growing season and across the year [61]. To calculate SPEI, we used the Thornthwaite equation to model potential evapotranspiration as implemented in the SPEI R package [70]	927
We repeated the process of fitting statistical models for each vital rate as described in <b>Materials and Methods</b> with the inclusion of a parameter describing the influence of SPEI. We fit separate vital rate models incorporating either the growing season or annual drought index for each vital rate, except for the model describing the mean number of seeds per inflorescence. This model was fit without climate effects because the data came from only a few years. Initial analyses indicated similar fits for models including only a linear term and those with both linear and quadratic terms describing the relationship between the climate driver and the vital rate response, and so we proceeded with models including only the linear term. We expected that including climate predictors into the models would explain some inter-annual variance in vital rates, shrinking the variance associated with the fitted year random effects. We assessed model fit with graphic posterior predictive checks and convergence diagnostics as described for the climate-implicit analysis. Finally, we next built matrix projection models incorporating the climate-dependent vital rate functions to assess the response of symbiotic (S+) vs symbiont-free (S-) populations to drought. The model is as described in <b>Materials and Methods</b> with the inclusion of parameters describing the slope of the relationship with SPEI. We compared the sensitivity of $\lambda$ to either annual or seasonal SPEI of S+ populations ( $\frac{\Delta\lambda^+}{\Delta SPEI}$ ) with those of S- populations ( $\frac{\Delta\lambda^-}{\Delta SPEI}$ ) (Fig. S25; Table S).	928
Most species were slightly more responsive to growing season rather than annual drought conditions, and for most species symbiotic populations were less sensitive to	929
	930
	931
	932
	933
	934
	935
	936
	937
	938
	939
	940
	941
	942
	943
	944
	945
	946
	947
	948
	949
	950
	951
	952
	953
	954
	955
	956
	957
	958
	959
	960
	961
	962
	963
	964
	965
	966

967 SPEI than symbiont-free populations (Fig. S25; Table S3). However, these drought  
968 indices did not explain the full extent of inter-annual variability in demographic  
969 vital rates. For example, flowering in *A. perennans* had one of the strongest climate  
970 signals (82% probability of a positive relationship with SPEI), yet the estimated inter-  
971 annual variance  $\sigma_{\tau_p}^2$  for symbiont-free plants shrank from 6.7 to 6.1 after including  
972 3-month SPEI as a covariate, suggesting that other factors contribute to inter-annual  
973 variability.

974

975

976

977

978

979

980

981

982

983

984

985

986

987

988

989

990

991

992

993

994

995

996

997

998

999

1000

1001

1002

1003

1004

1005

1006

1007

1008

1009

1010

1011

1012

## Supplemental Figures S1-S28

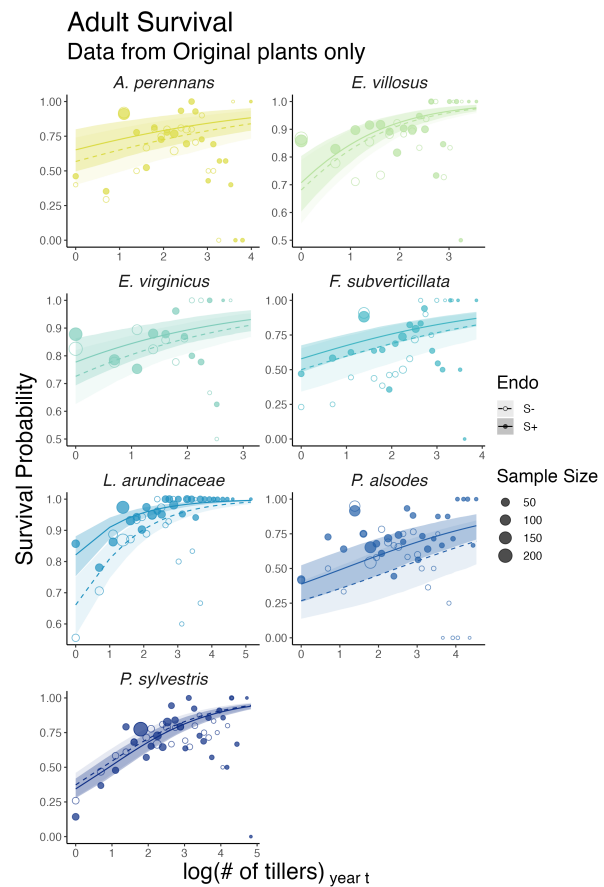
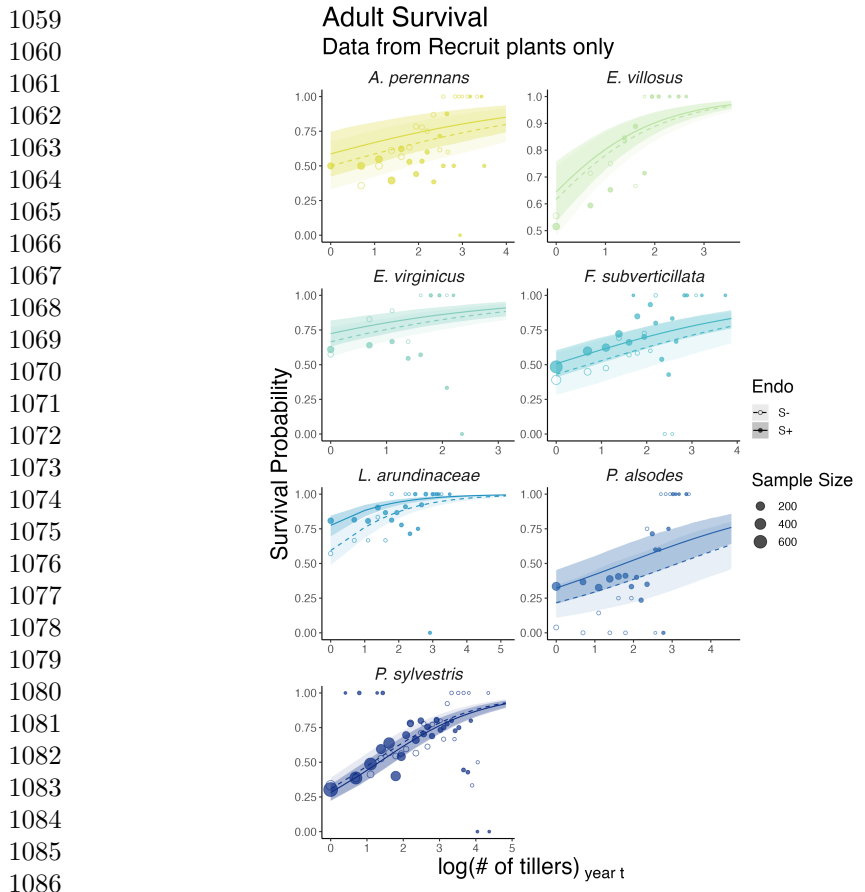


**Fig. S1** Effect of endophyte symbiosis on mean adult survival. Fitted curves represent the size-specific mean survival probability for original plants along with data binned by size shown as open circles with a dashed line for symbiont-free (S-) plants, while the solid line and filled circles represent symbiotic (S+) plants. 80% credible intervals are shown with dark shading for S+, or light shading for S-.

1013  
1014  
1015  
1016  
1017  
1018  
1019  
1020  
1021  
1022  
1023  
1024  
1025  
1026  
1027  
1028  
1029  
1030  
1031  
1032  
1033  
1034  
1035  
1036  
1037  
1038  
1039  
1040  
1041  
1042  
1043  
1044  
1045  
1046  
1047  
1048  
1049  
1050  
1051  
1052  
1053  
1054  
1055  
1056  
1057  
1058



1087 **Fig. S2** Effect of endophyte symbiosis on mean adult survival. Fitted curves represent the size-  
1088 specific mean survival probability for recruited plants along with data binned by size shown as open  
1089 circles with a dashed line for symbiont-free (S-) plants, while the solid line and filled circles represent  
1090 symbiotic (S+) plants. 80% credible intervals are shown with dark shading for S+, or light shading  
1091 for S-.

1092  
1093  
1094  
1095  
1096  
1097  
1098  
1099  
1100  
1101  
1102  
1103  
1104

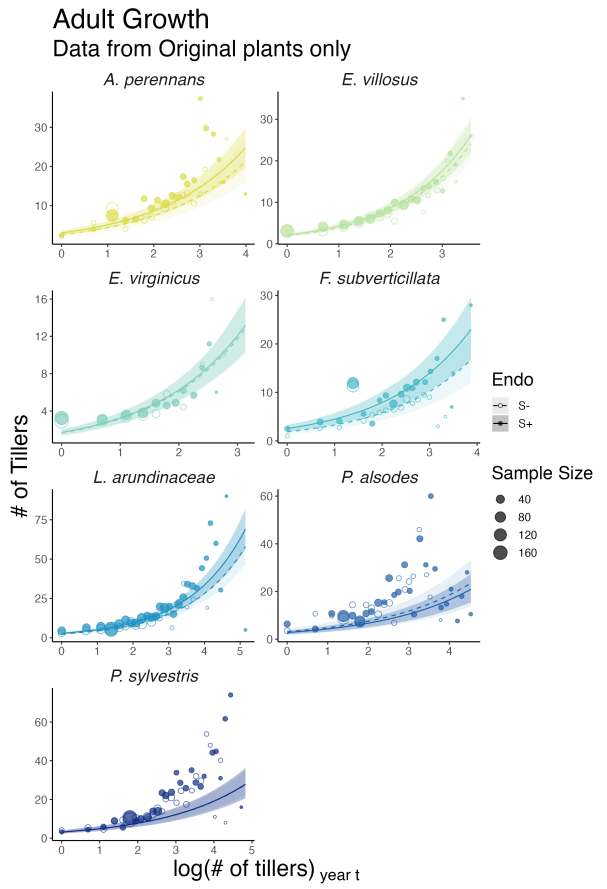
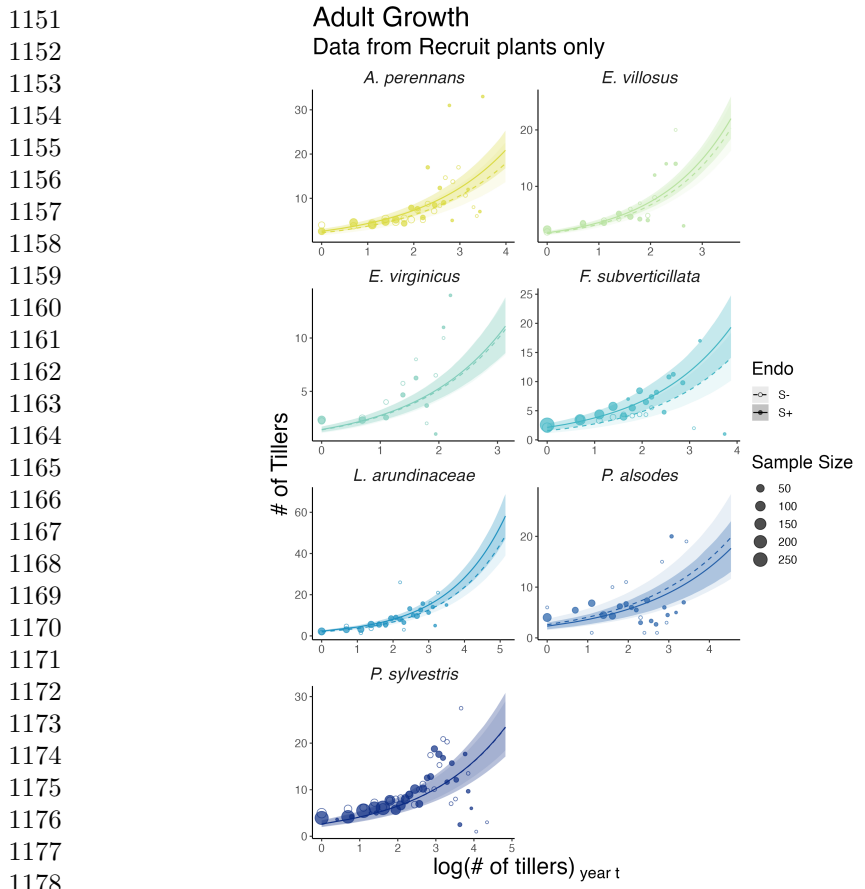


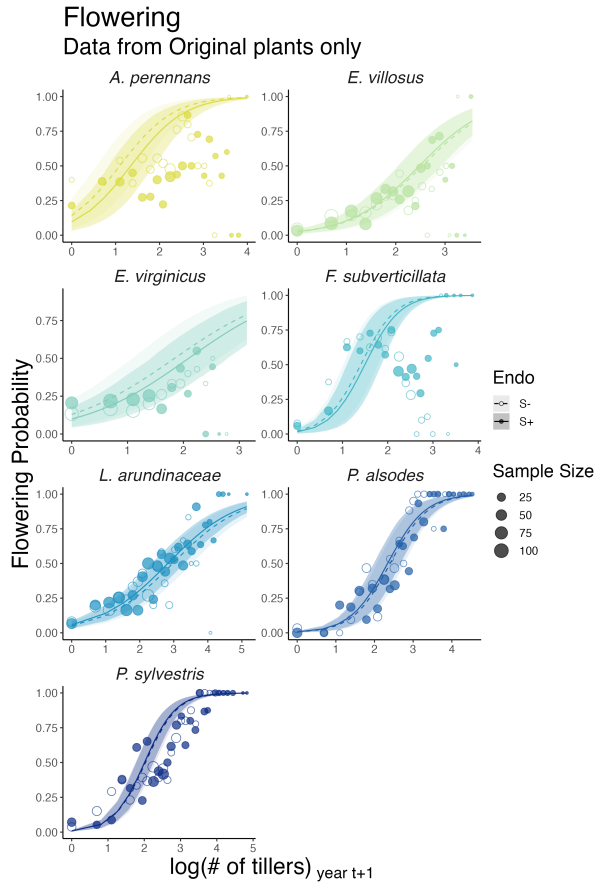
**Fig. S3** Effect of endophyte symbiosis on mean adult growth. Fitted curves represent the size-specific mean expected plant size for original plants along with data binned by size shown as open circles with a dashed line for symbiont-free (S-) plants, while the solid line and filled circles represent symbiotic (S+) plants. 80% credible intervals are shown with dark shading for S+, or light shading for S-.

1105  
1106  
1107  
1108  
1109  
1110  
1111  
1112  
1113  
1114  
1115  
1116  
1117  
1118  
1119  
1120  
1121  
1122  
1123  
1124  
1125  
1126  
1127  
1128  
1129  
1130  
1131  
1132  
1133  
1134  
1135  
1136  
1137  
1138  
1139  
1140  
1141  
1142  
1143  
1144  
1145  
1146  
1147  
1148  
1149  
1150

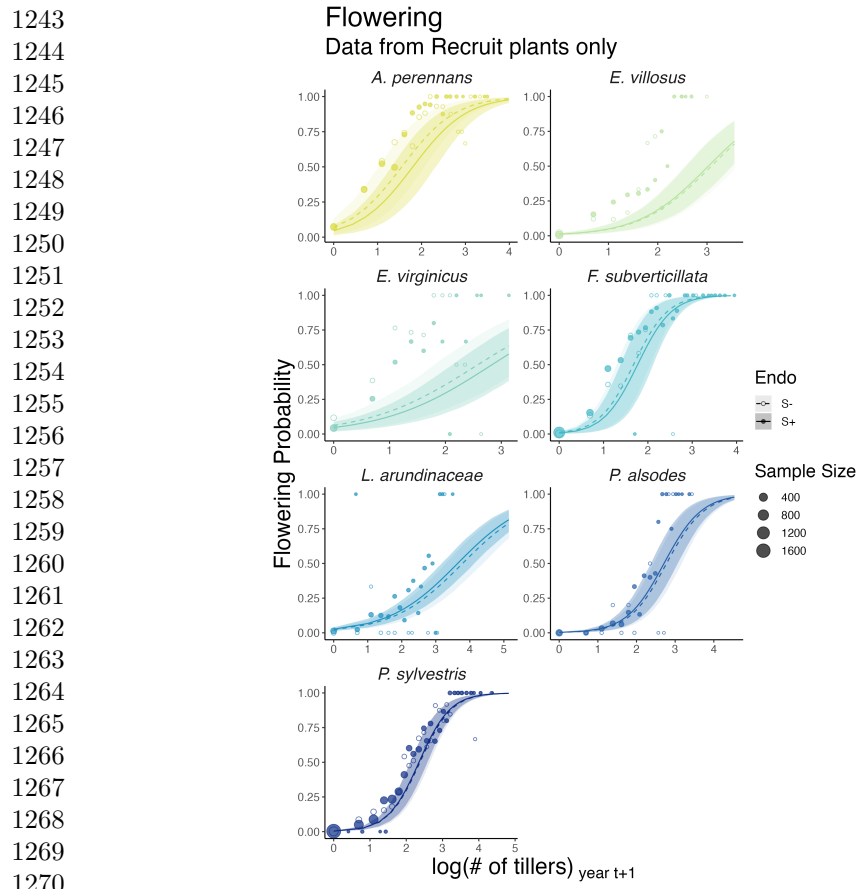


1179 **Fig. S4** Effect of endophyte symbiosis on mean adult growth. Fitted curves represent the size-  
1180 specific mean expected plant size for recruited plants along with data binned by size shown as open  
1181 circles with a dashed line for symbiont-free (S-) plants, while the solid line and filled circles represent  
1182 symbiotic (S+) plants. 80% credible intervals are shown with dark shading for S+, or light shading  
1183 for S-.

1184  
1185  
1186  
1187  
1188  
1189  
1190  
1191  
1192  
1193  
1194  
1195  
1196

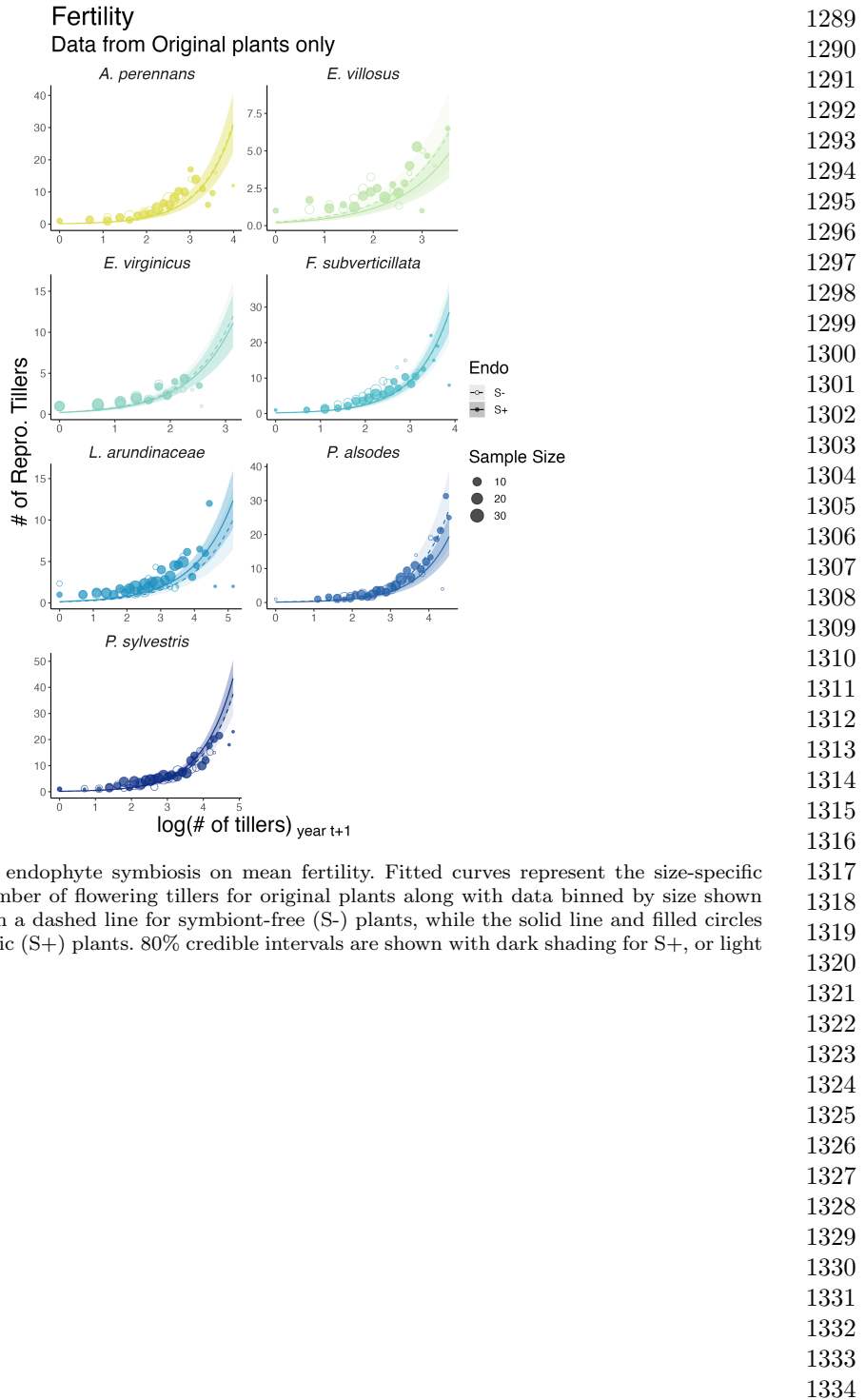


1197  
1198  
1199  
1200  
1201  
1202  
1203  
1204  
1205  
1206  
1207  
1208  
1209  
1210  
1211  
1212  
1213  
1214  
1215  
1216  
1217  
1218  
1219  
1220  
1221  
1222  
1223  
1224  
1225  
1226  
1227  
1228  
1229  
1230  
1231  
1232  
1233  
1234  
1235  
1236  
1237  
1238  
1239  
1240  
1241  
1242

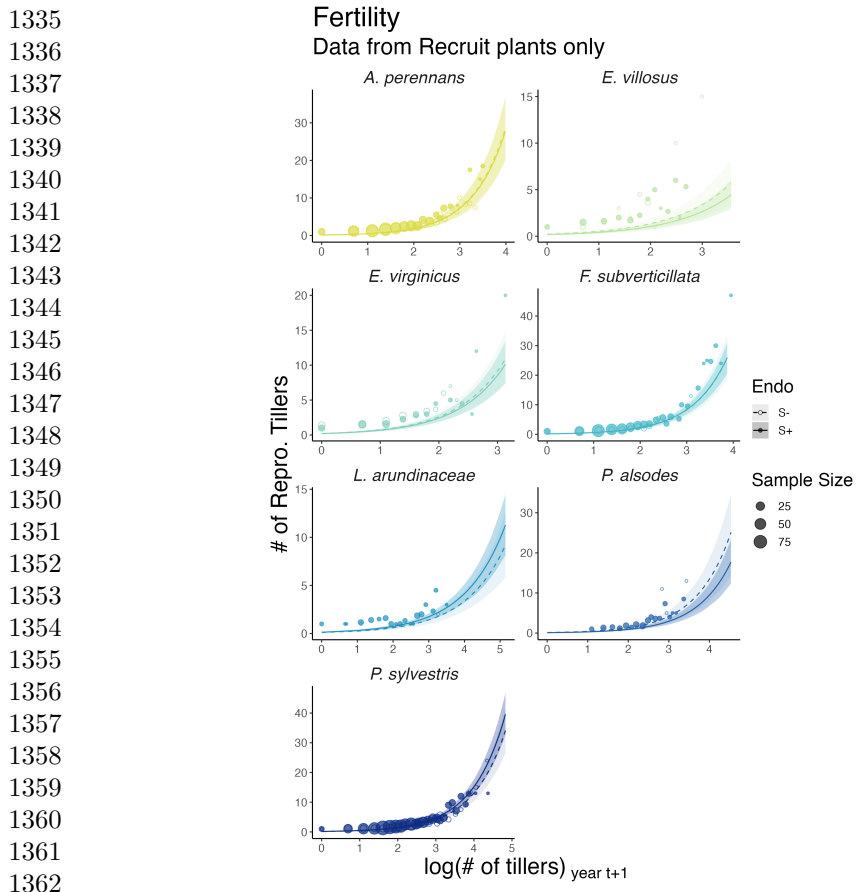


1271 **Fig. S6** Effect of endophyte symbiosis on mean flowering. Fitted curves represent the size-specific  
1272 mean flowering probability for recruited plants along with data binned by size shown as open circles  
1273 with a dashed line for symbiont-free (S-) plants, while the solid line and filled circles represent  
1274 symbiotic (S+) plants. 80% credible intervals are shown with dark shading for S+, or light shading  
1274 for S-.

1275  
1276  
1277  
1278  
1279  
1280  
1281  
1282  
1283  
1284  
1285  
1286  
1287  
1288



**Fig. S7** Effect of endophyte symbiosis on mean fertility. Fitted curves represent the size-specific mean expected number of flowering tillers for original plants along with data binned by size shown as open circles with a dashed line for symbiont-free (S-) plants, while the solid line and filled circles represent symbiotic (S+) plants. 80% credible intervals are shown with dark shading for S+, or light shading for S-.



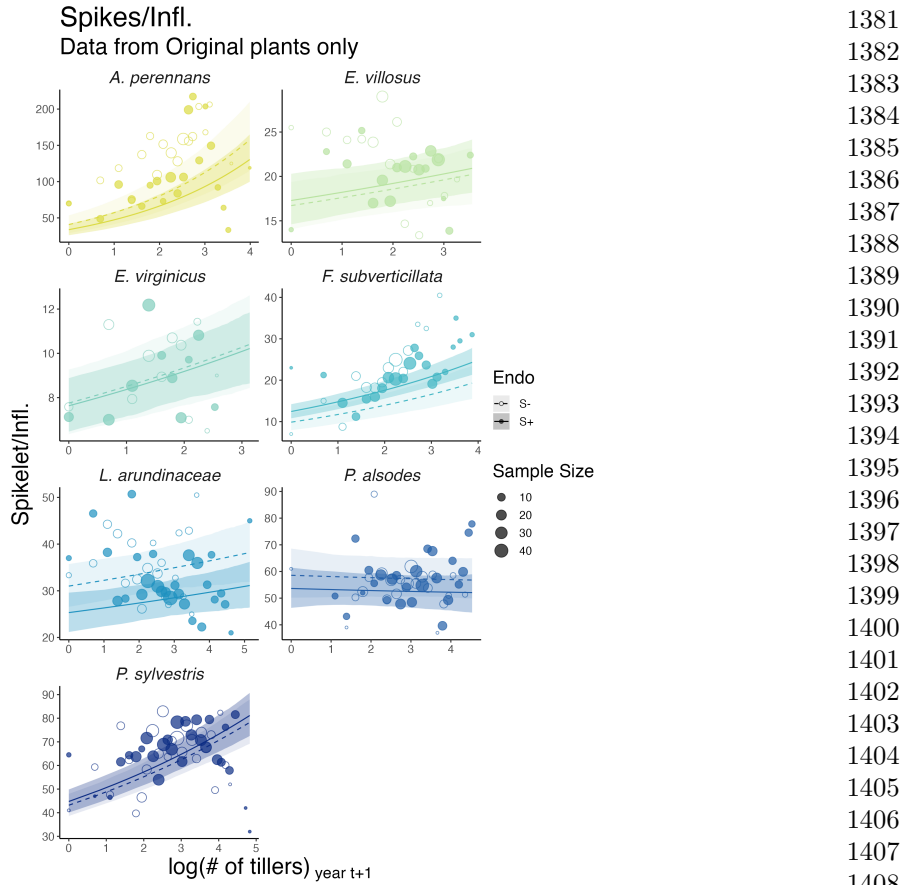


**Fig. S9** Effect of endophyte symbiosis on mean spikelet production. Fitted curves represent the size-specific mean expected number of spikelets per inflorescence for original plants along with data binned by size shown as open circles with a dashed line for symbiont-free (S-) plants, while the solid line and filled circles represent symbiotic (S+) plants. 80% credible intervals are shown with dark shading for S+, or light shading for S-.

1427

1428

1429

1430

1431

1432

1433

1434

1435

1436

1437

1438

1439

1440

1441

1442

1443

1444

1445

1446

1447

1448

1449

1450

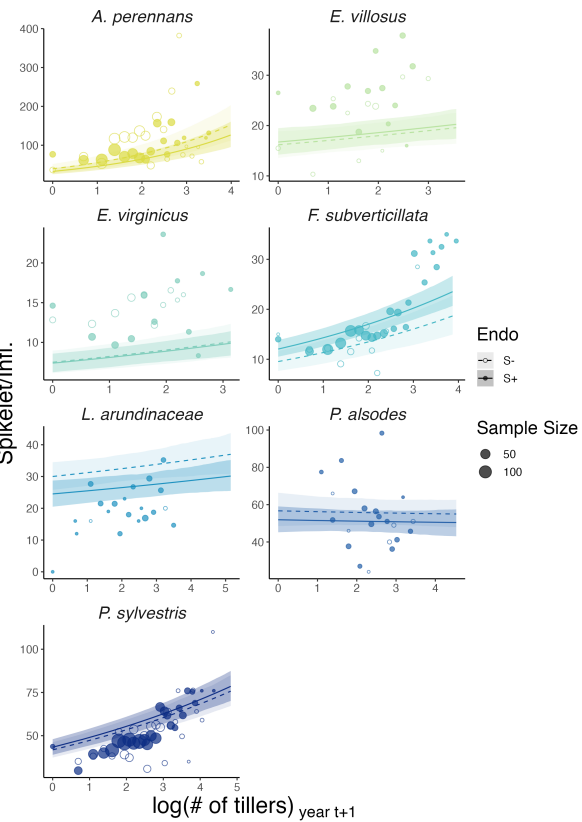
1451

1452

1453

1454

**Spikes/Infl.  
Data from Recruit plants only**



1455 **Fig. S10** Effect of endophyte symbiosis on mean spikelet production. Fitted curves represent the  
1456 size-specific mean expected number of spikelets per inflorescence for recruited plants along with data  
1457 binned by size shown as open circles with a dashed line for symbiont-free (S-) plants, while the solid  
1458 line and filled circles represent symbiotic (S+) plants. 80% credible intervals are shown with dark  
1459 shading for S+, or light shading for S-.

1460

1461

1462

1463

1464

1465

1466

1467

1468

1469

1470

1471

1472

**Adult Survival**  
Data from Original plants only

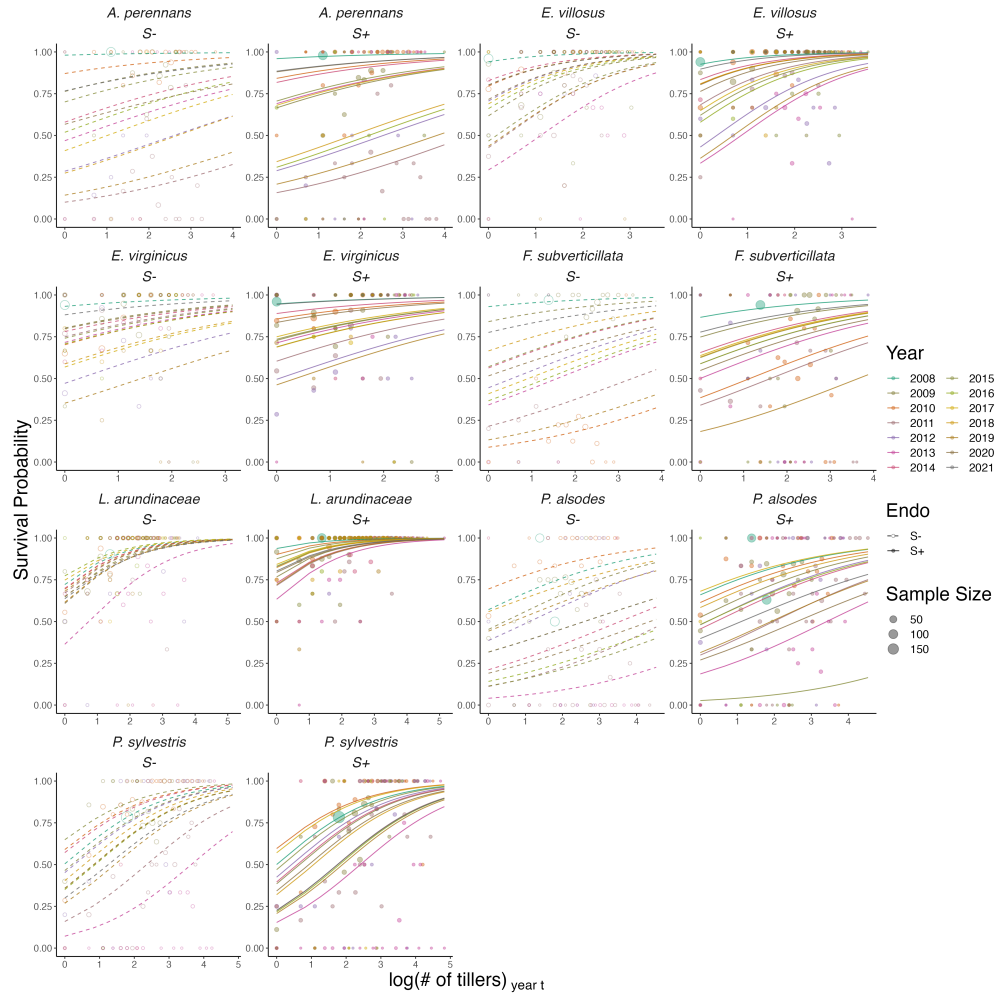
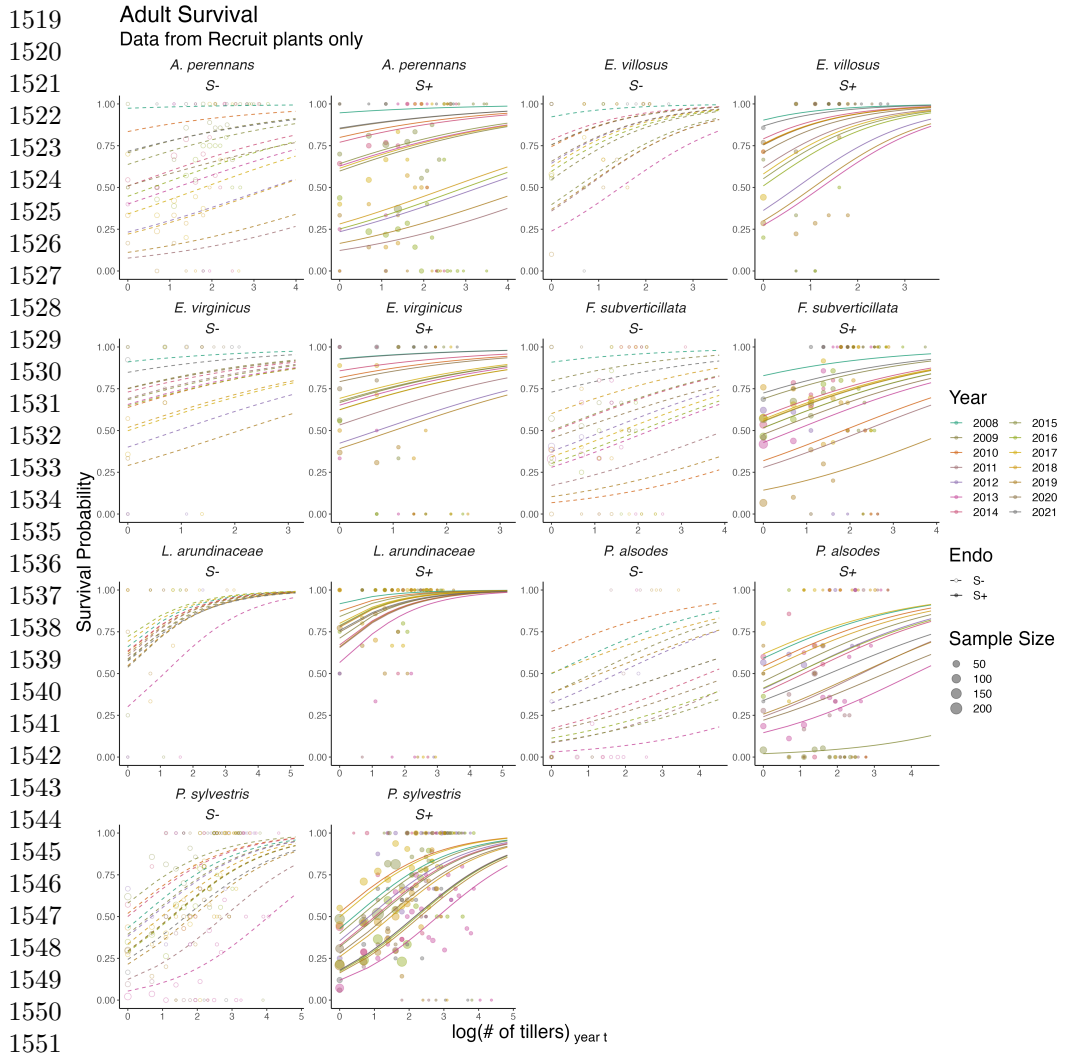


**Fig. S11** Effect of endophyte symbiosis on yearly adult survival. Fitted curves represent the size-specific annual survival probability for original plants along with data binned by size and census year shown as open circles with a dashed line for symbiont-free (S-) plants, while the solid line and filled circles represent symbiotic (S+) plants.

1473  
1474  
1475  
1476  
1477  
1478  
1479  
1480  
1481  
1482  
1483  
1484  
1485  
1486  
1487  
1488  
1489  
1490  
1491  
1492  
1493  
1494  
1495  
1496  
1497  
1498  
1499  
1500  
1501  
1502  
1503  
1504  
1505  
1506  
1507  
1508  
1509  
1510  
1511  
1512  
1513  
1514  
1515  
1516  
1517  
1518



1553 **Fig. S12** Effect of endophyte symbiosis on yearly adult survival. Fitted curves represent the size-  
1554 specific annual survival probability for recruited plants along with data binned by size and census  
1555 year shown as open circles with a dashed line for symbiont-free (S-) plants, while the solid line and  
1556 filled circles represent symbiotic (S+) plants.

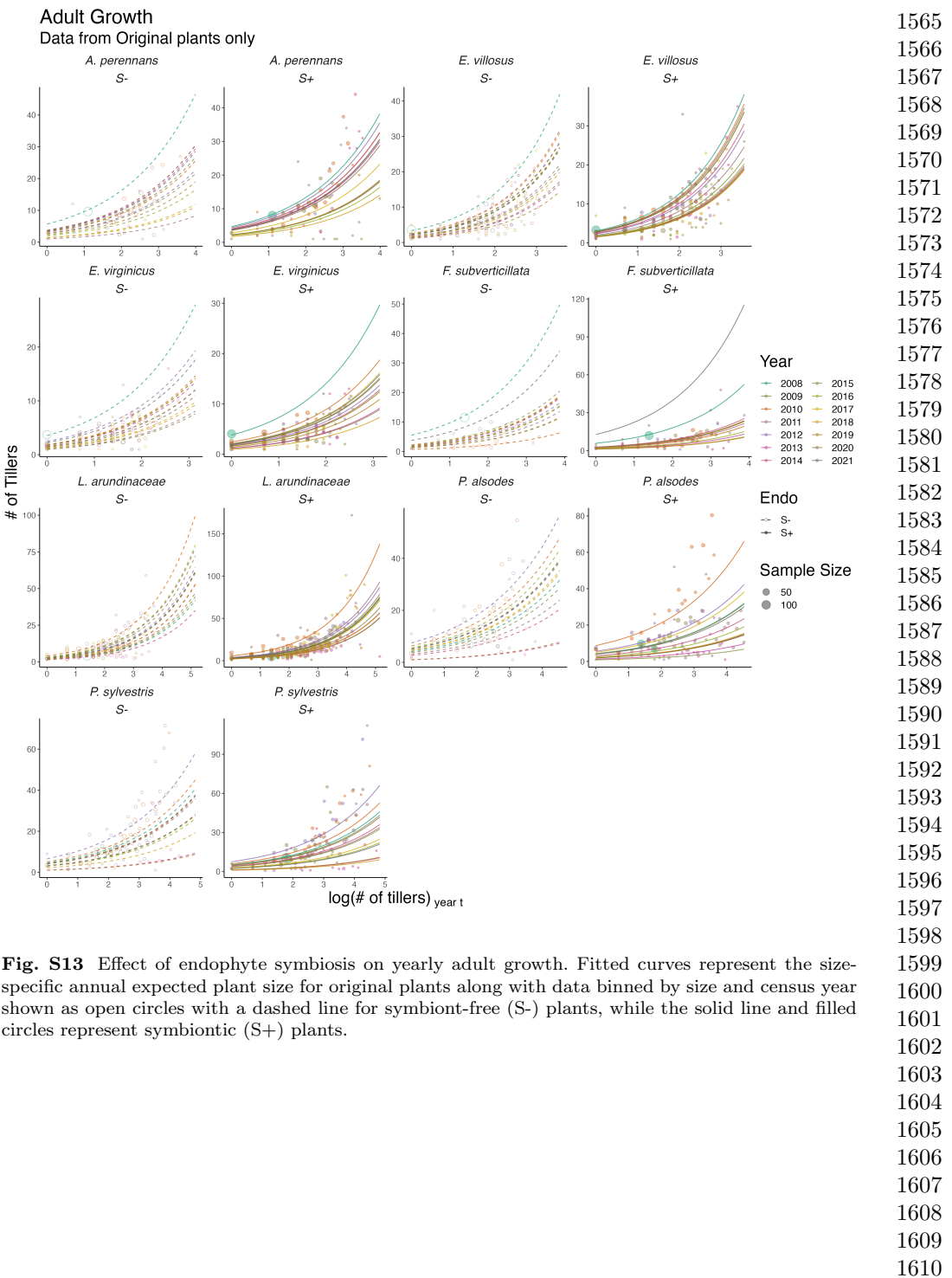
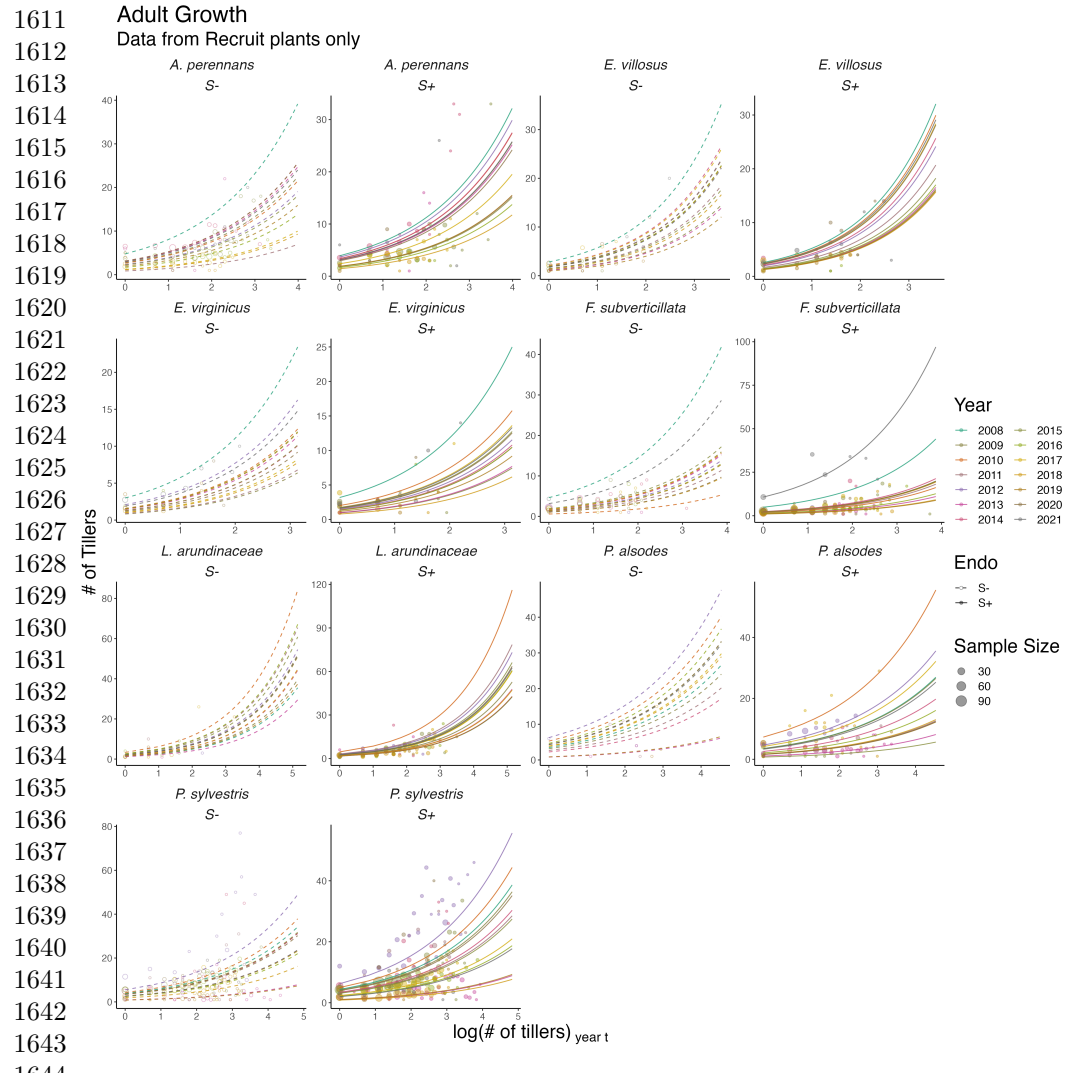


**Fig. S13** Effect of endophyte symbiosis on yearly adult growth. Fitted curves represent the size-specific annual expected plant size for original plants along with data binned by size and census year shown as open circles with a dashed line for symbiont-free (S-) plants, while the solid line and filled circles represent symbiotic (S+) plants.



1645 **Fig. S14** Effect of endophyte symbiosis on yearly adult growth. Fitted curves represent the size-  
1646 specific annual expected plant size for recruited plants along with data binned by size and census  
1647 year shown as open circles with a dashed line for symbiont-free (S-) plants, while the solid line and  
1648 filled circles represent symbiotic (S+) plants.

1649  
1650  
1651  
1652  
1653  
1654  
1655  
1656

**Flowering**  
Data from Original plants only

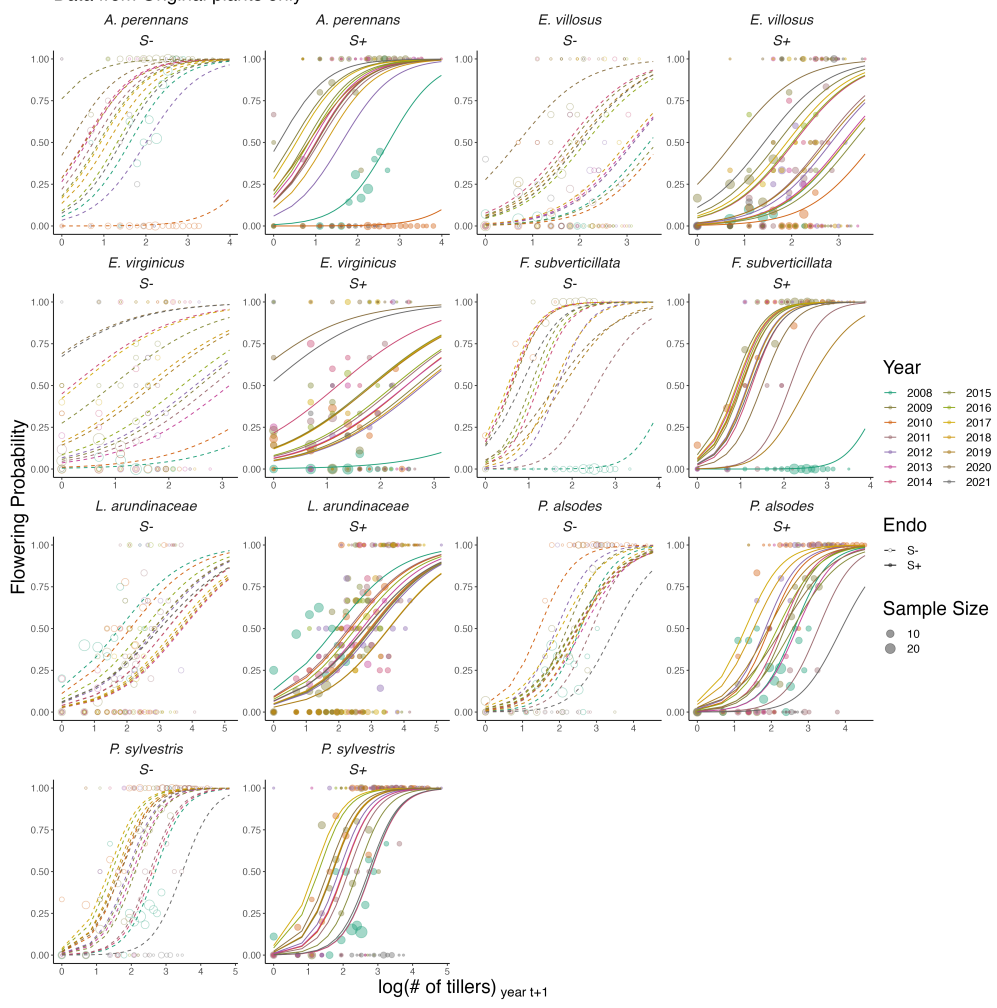
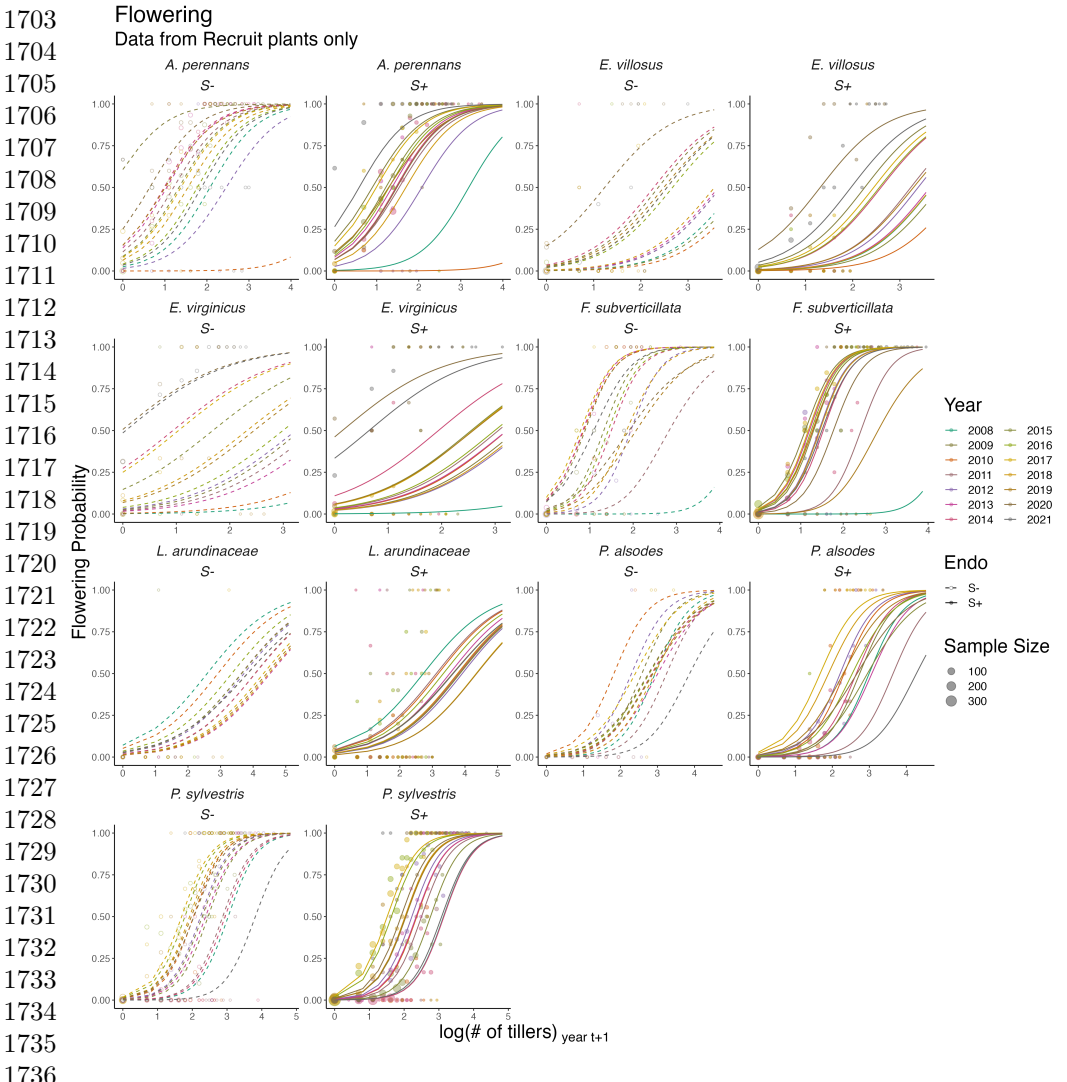


**Fig. S15** Effect of endophyte symbiosis on yearly flowering. Fitted curves represent the size-specific annual flowering probability for original plants along with data binned by size and census year shown as open circles with a dashed line for symbiont-free (S-) plants, while the solid line and filled circles represent symbiotic (S+) plants.

1657  
1658  
1659  
1660  
1661  
1662  
1663  
1664  
1665  
1666  
1667  
1668  
1669  
1670  
1671  
1672  
1673  
1674  
1675  
1676  
1677  
1678  
1679  
1680  
1681  
1682  
1683  
1684  
1685  
1686  
1687  
1688  
1689  
1690  
1691  
1692  
1693  
1694  
1695  
1696  
1697  
1698  
1699  
1700  
1701  
1702



1737 **Fig. S16** Effect of endophyte symbiosis on yearly flowering. Fitted curves represent the size-specific  
1738 annual flowering probability for recruited plants along with data binned by size and census year  
1739 shown as open circles with a dashed line for symbiont-free (S-) plants, while the solid line and filled  
1740 circles represent symbiotic (S+) plants.

1740  
1741  
1742  
1743  
1744  
1745  
1746  
1747  
1748

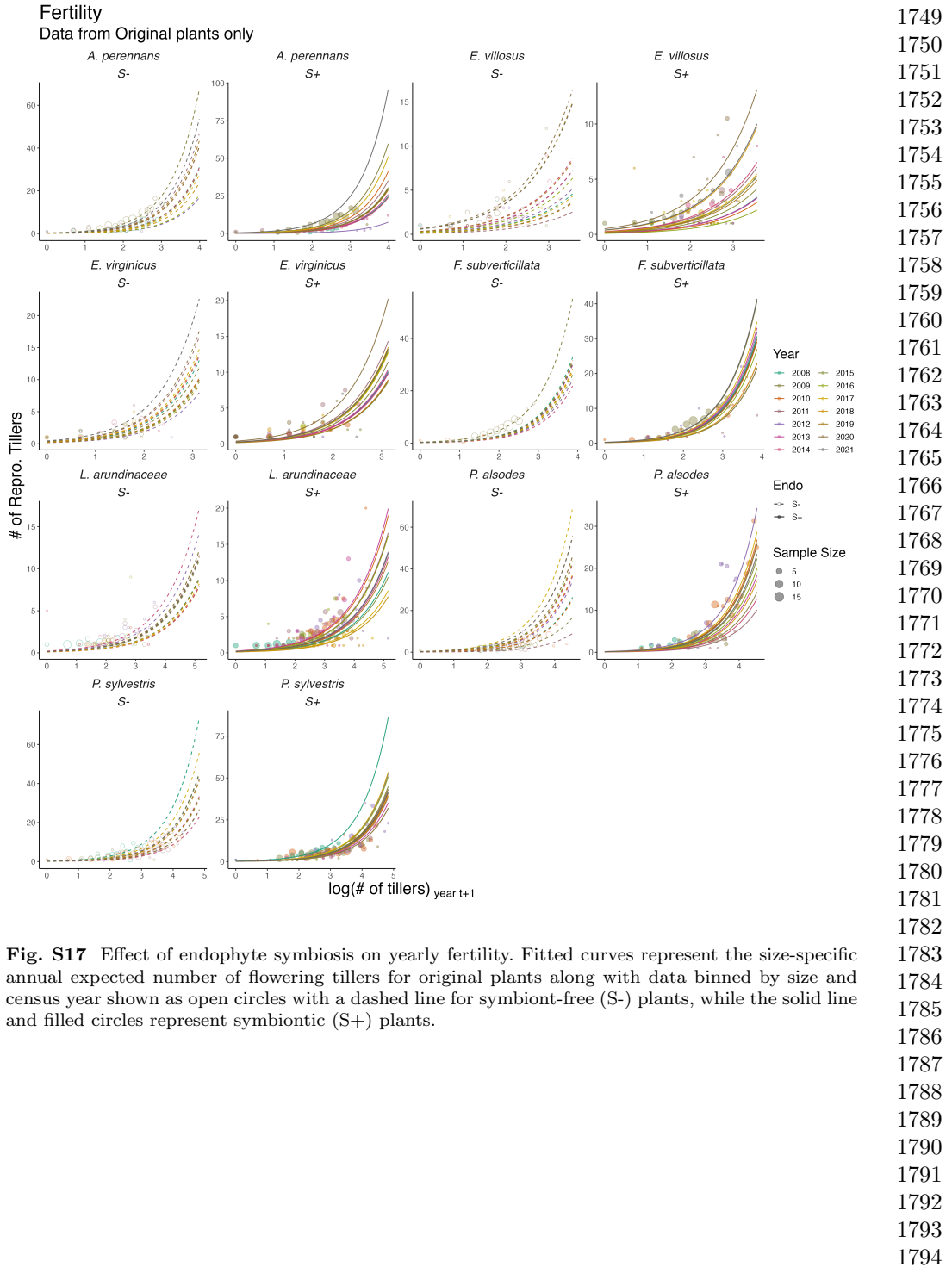
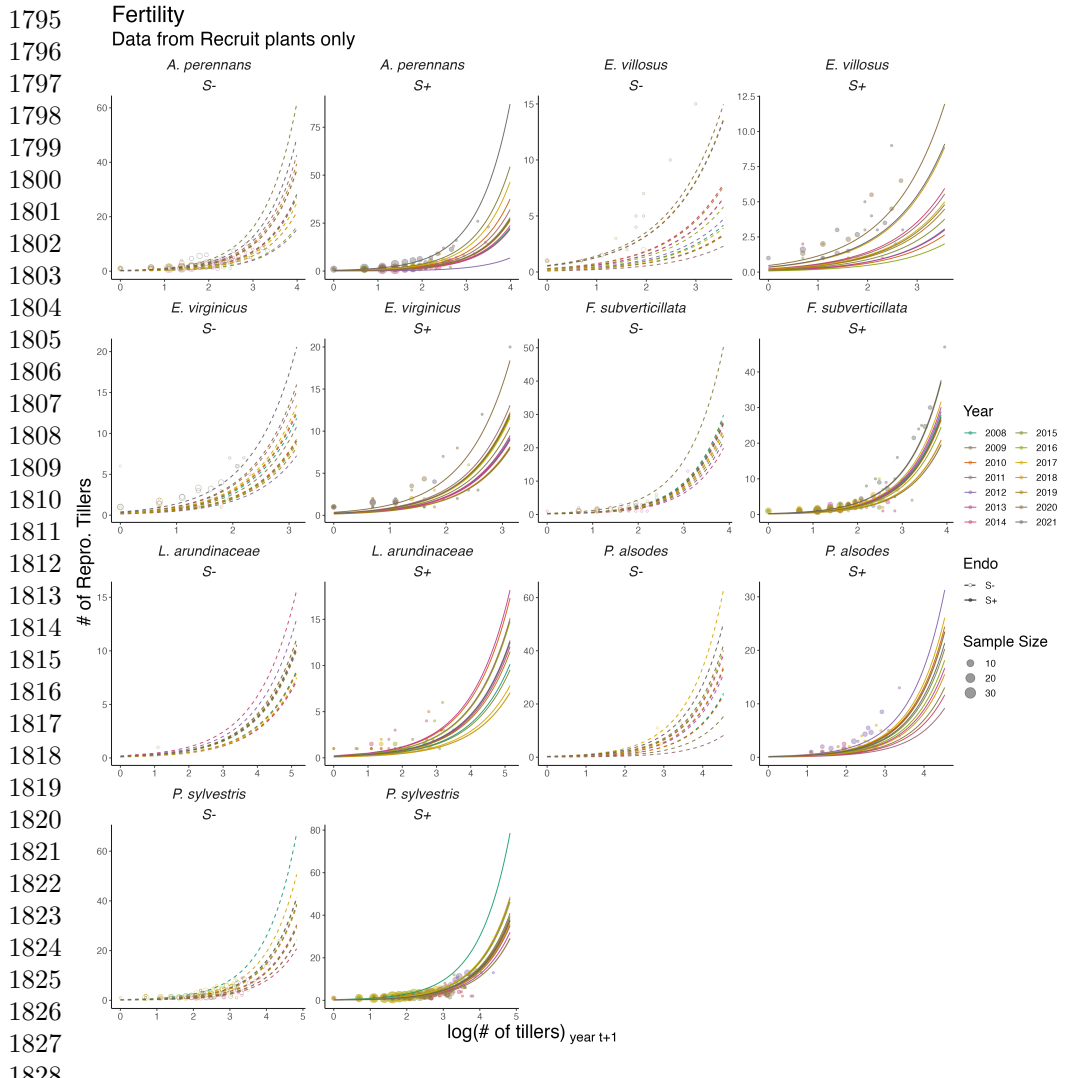
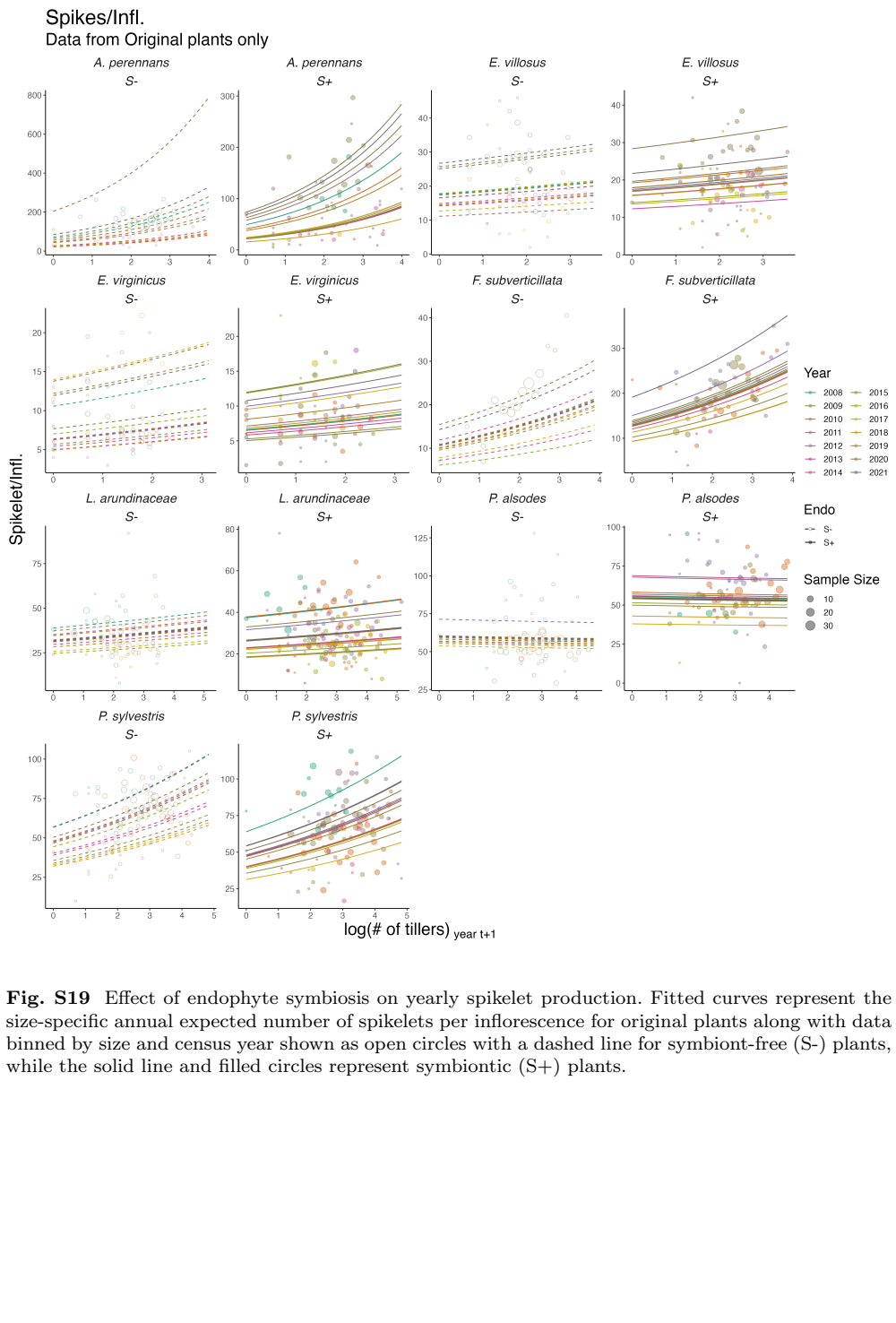


**Fig. S17** Effect of endophyte symbiosis on yearly fertility. Fitted curves represent the size-specific annual expected number of flowering tillers for original plants along with data binned by size and census year shown as open circles with a dashed line for symbiont-free (S-) plants, while the solid line and filled circles represent symbiotic (S+) plants.

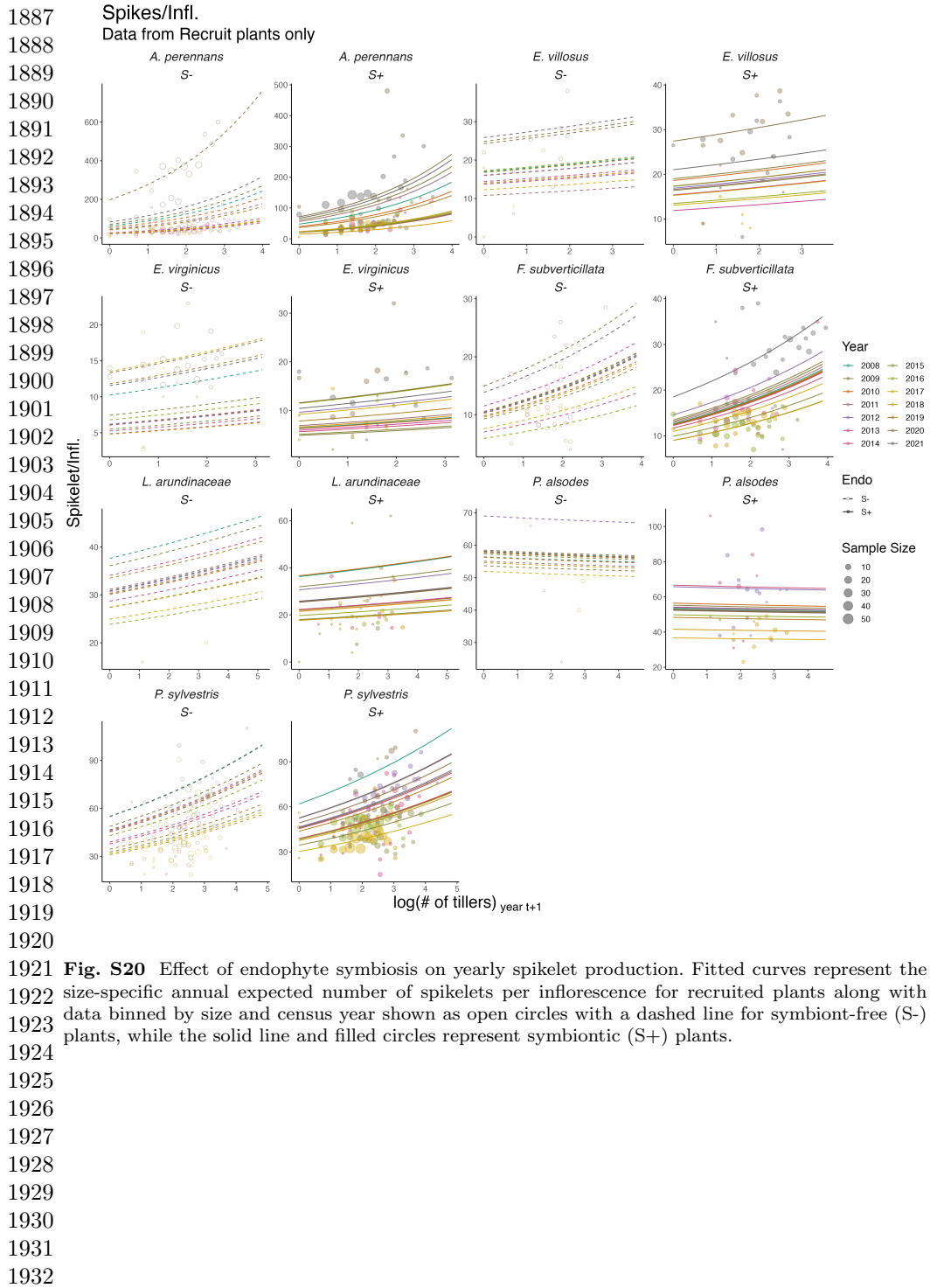


1829 **Fig. S18** Effect of endophyte symbiosis on yearly fertility. Fitted curves represent the size-specific  
 1830 annual expected number of flowering tillers for recruited along with data binned by size and census  
 1831 year shown as open circles with a dashed line for symbiont-free (S-) plants, while the solid line and  
 1832 filled circles represent symbiotic (S+) plants.

1833  
 1834  
 1835  
 1836  
 1837  
 1838  
 1839  
 1840



**Fig. S19** Effect of endophyte symbiosis on yearly spikelet production. Fitted curves represent the size-specific annual expected number of spikelets per inflorescence for original plants along with data binned by size and census year shown as open circles with a dashed line for symbiont-free (S-) plants, while the solid line and filled circles represent symbiotic (S+) plants.



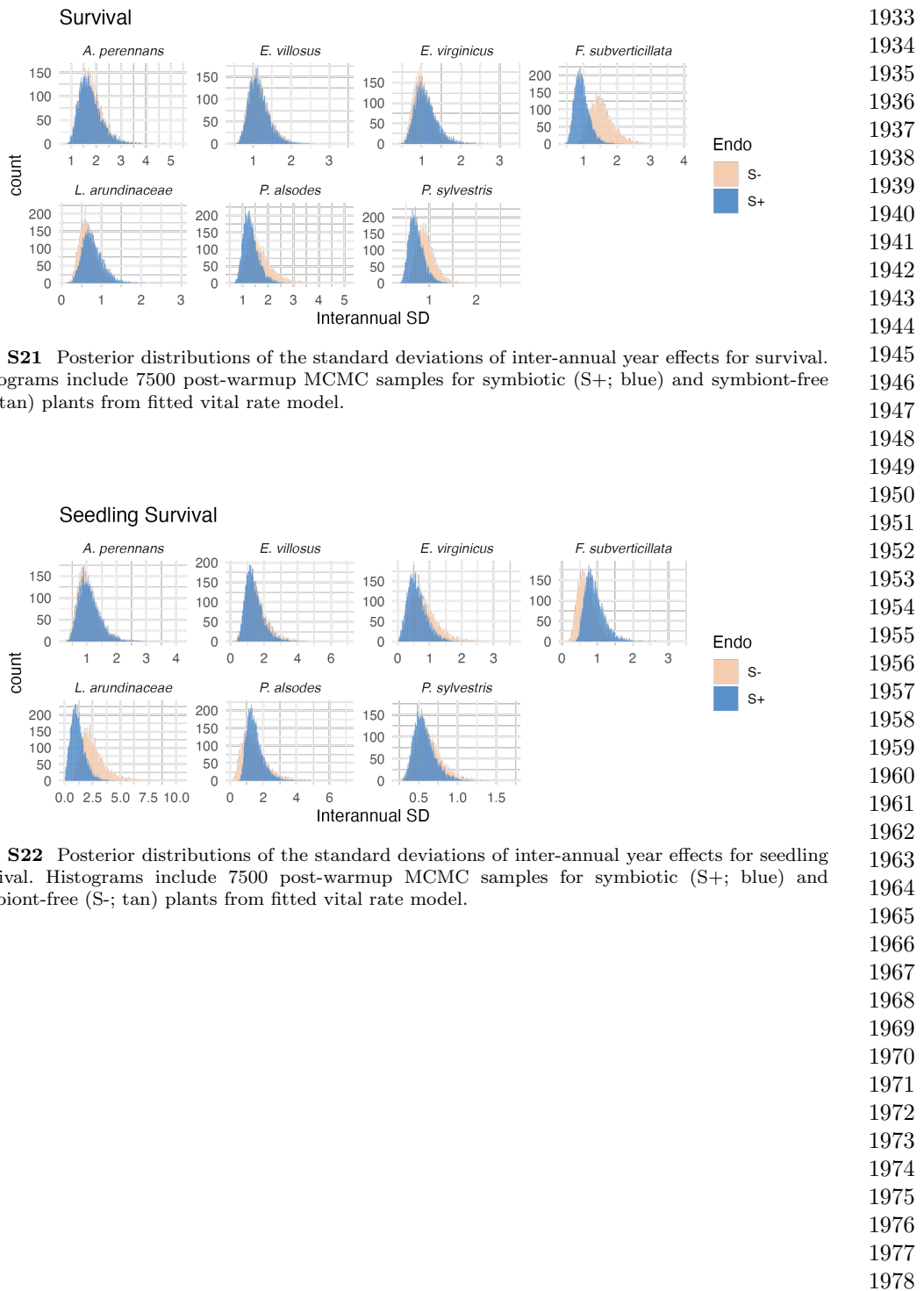
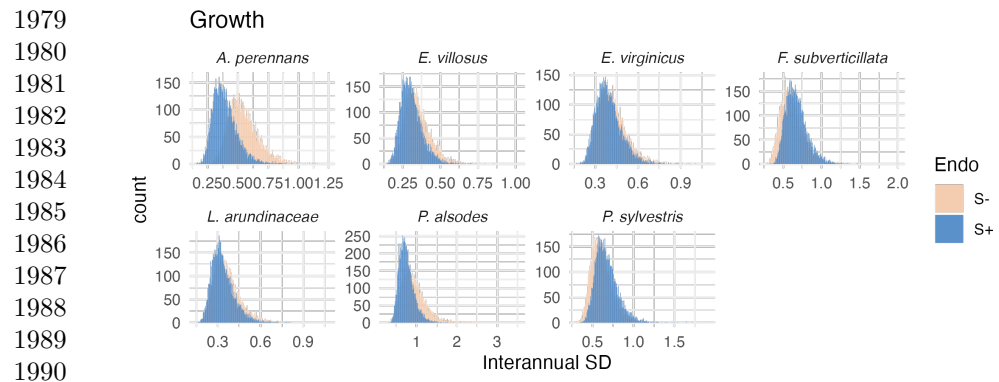
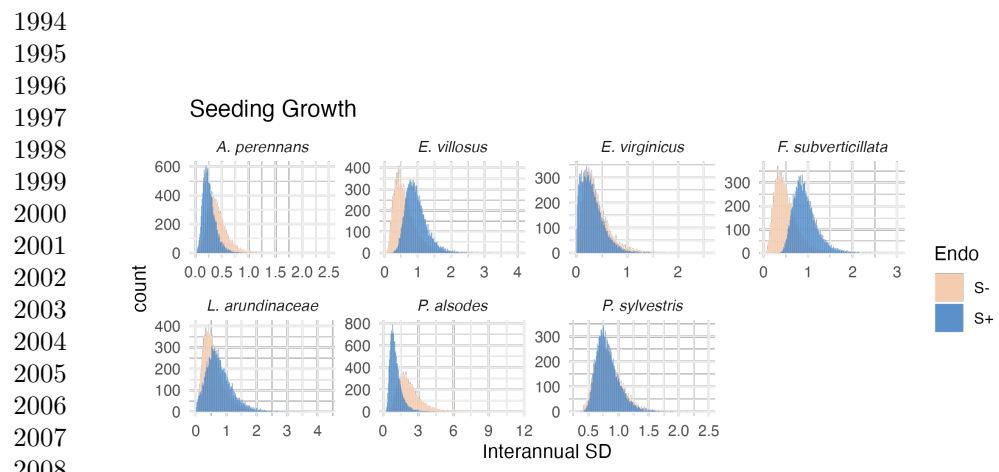


**Fig. S21** Posterior distributions of the standard deviations of inter-annual year effects for survival. Histograms include 7500 post-warmup MCMC samples for symbiotic (S+; blue) and symbiont-free (S-; tan) plants from fitted vital rate model.

**Fig. S22** Posterior distributions of the standard deviations of inter-annual year effects for seedling survival. Histograms include 7500 post-warmup MCMC samples for symbiotic (S+; blue) and symbiont-free (S-; tan) plants from fitted vital rate model.



1991 **Fig. S23** Posterior distributions of the standard deviations of inter-annual year effects for growth.  
 1992 Histograms include 7500 post-warmup MCMC samples for symbiotic (S+; blue) and symbiont-free  
 1993 (S-; tan) plants from fitted vital rate model.



2009 **Fig. S24** Posterior distributions of the standard deviations of inter-annual year effects for seedling growth. Histograms include 7500 post-warmup MCMC samples for symbiotic (S+; blue) and symbiont-free (S-; tan) plants from fitted vital rate model.

2011  
 2012  
 2013  
 2014  
 2015  
 2016  
 2017  
 2018  
 2019  
 2020  
 2021  
 2022  
 2023  
 2024

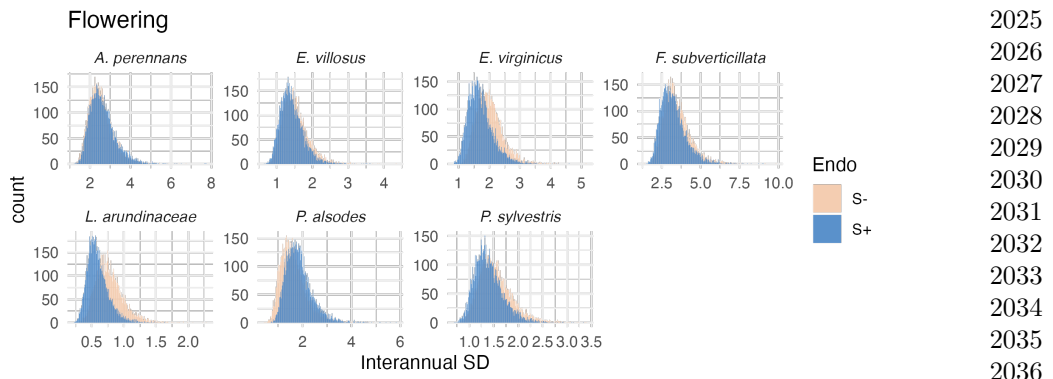


**Fig. S25** Posterior distributions of the standard deviations of inter-annual year effects for flowering probability. Histograms include 7500 post-warmup MCMC samples for symbiotic (S+; blue) and symbiont-free (S-; tan) plants from fitted vital rate model.

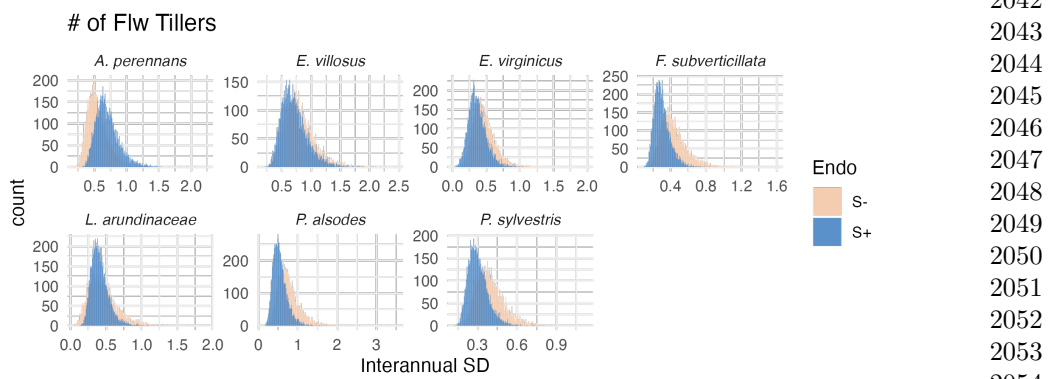
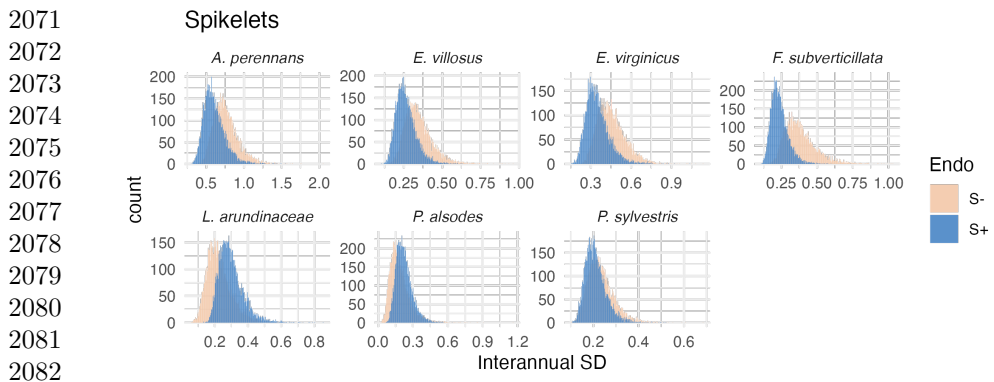
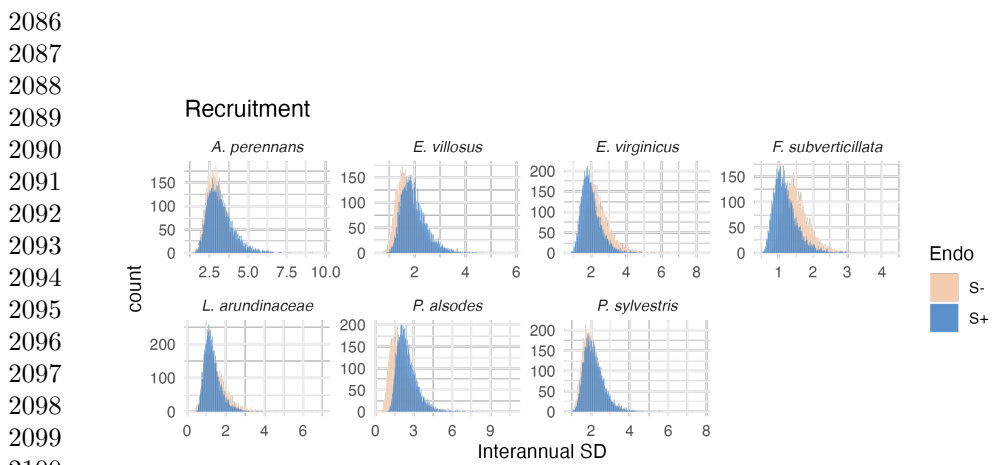


**Fig. S26** Posterior distributions of the standard deviations of inter-annual year effects for fertility (no. of flowering tillers). Histograms include 7500 post-warmup MCMC samples for symbiotic (S+; blue) and symbiont-free (S-; tan) plants from fitted vital rate model.

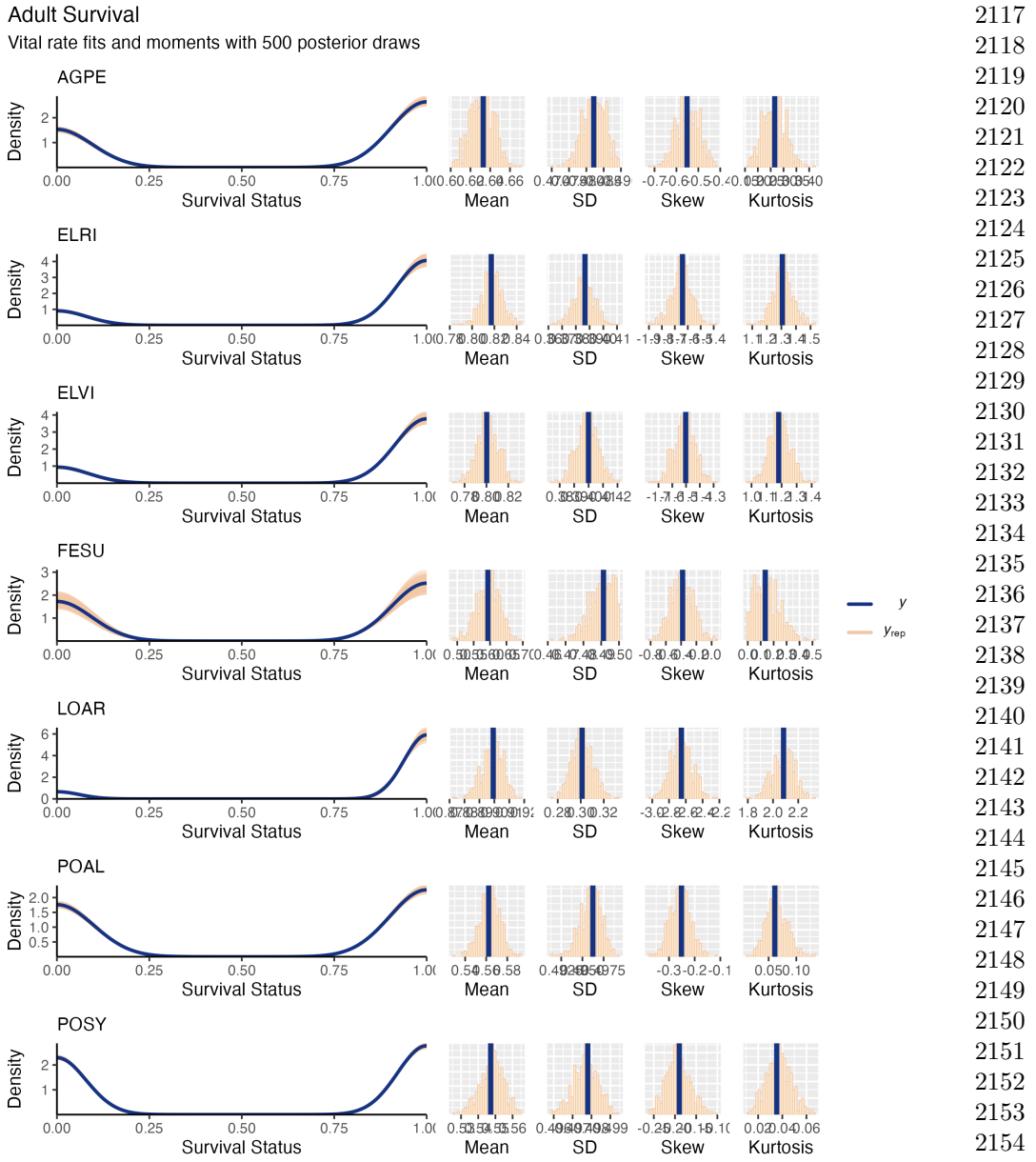
	2025
	2026
	2027
	2028
	2029
Endo	2030
S-	2031
S+	2032
	2033
	2034
	2035
	2036
	2037
	2038
	2039
	2040
	2041
	2042
	2043
	2044
	2045
	2046
Endo	2047
S-	2048
S+	2049
	2050
	2051
	2052
	2053
	2054
	2055
	2056
	2057
	2058
	2059
	2060
	2061
	2062
	2063
	2064
	2065
	2066
	2067
	2068
	2069
	2070



2083 **Fig. S27** Posterior distributions of the standard deviations of inter-annual year effects for spikelets  
2084 per inflorescence. Histograms include 7500 post-warmup MCMC samples for symbiotic (S+; blue)  
2085 and symbiont-free (S-; tan) plants from fitted vital rate model.

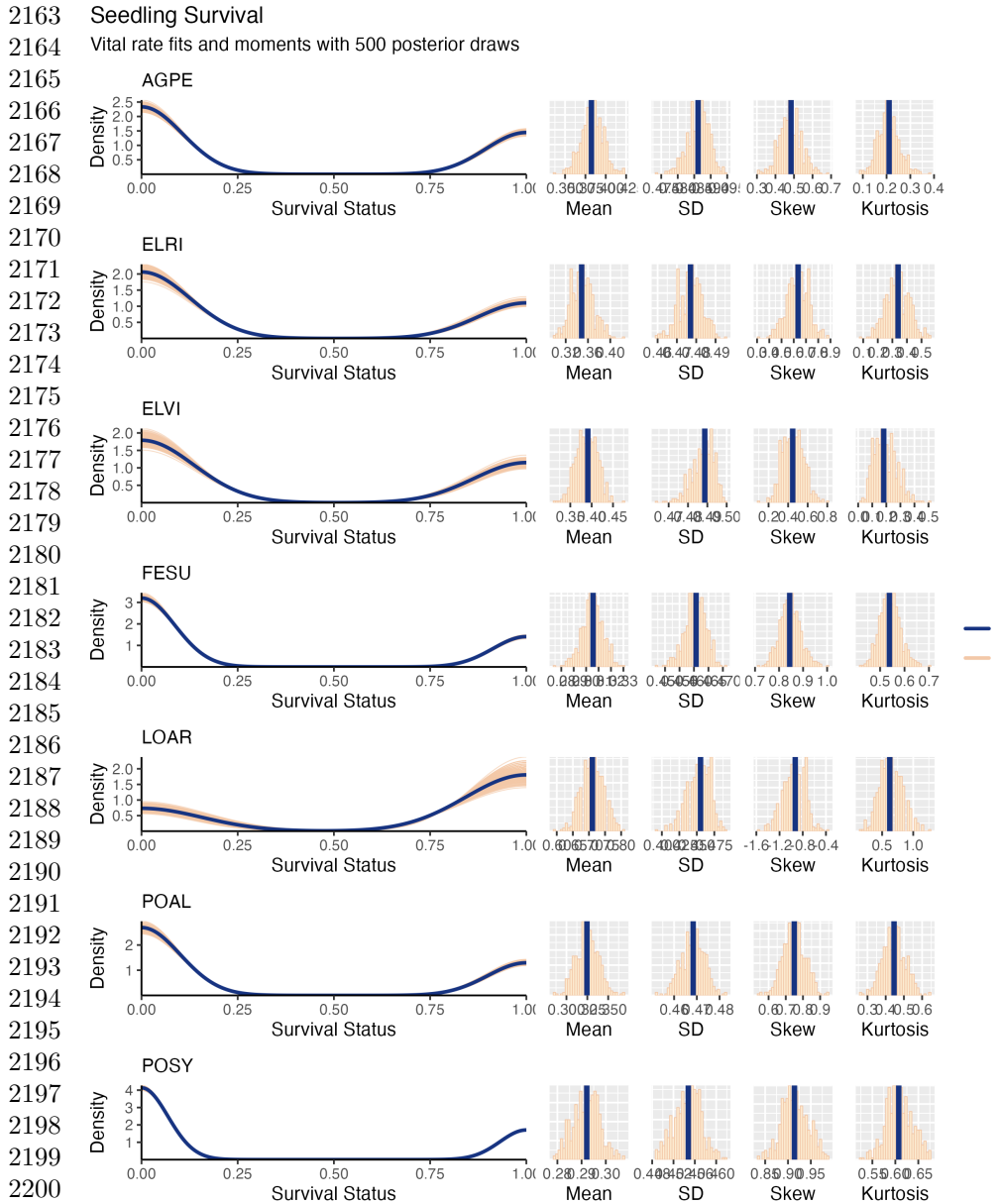


2101 **Fig. S28** Posterior distributions of the standard deviations of inter-annual year effects for  
2102 recruitment. Histograms include 7500 post-warmup MCMC samples for symbiotic (S+; blue) and  
2103 symbiont-free (S-; tan) plants from fitted vital rate model.  
2104  
2105  
2106  
2107  
2108  
2109  
2110  
2111  
2112  
2113  
2114  
2115  
2116



**Fig. S29** Posterior predictive check for statistical model of Adult Survival. Consistency between real data and simulated values indicates that fitted models describe the data well. Lines show density distributions of observed data (blue line) compared to data simulated from fitted models (tan lines) generated from 500 draws from posterior distributions of model parameters along with the distribution's moments.

2117  
2118  
2119  
2120  
2121  
2122  
2123  
2124  
2125  
2126  
2127  
2128  
2129  
2130  
2131  
2132  
2133  
2134  
2135  
2136  
2137  
2138  
2139  
2140  
2141  
2142  
2143  
2144  
2145  
2146  
2147  
2148  
2149  
2150  
2151  
2152  
2153  
2154  
2155  
2156  
2157  
2158  
2159  
2160  
2161  
2162



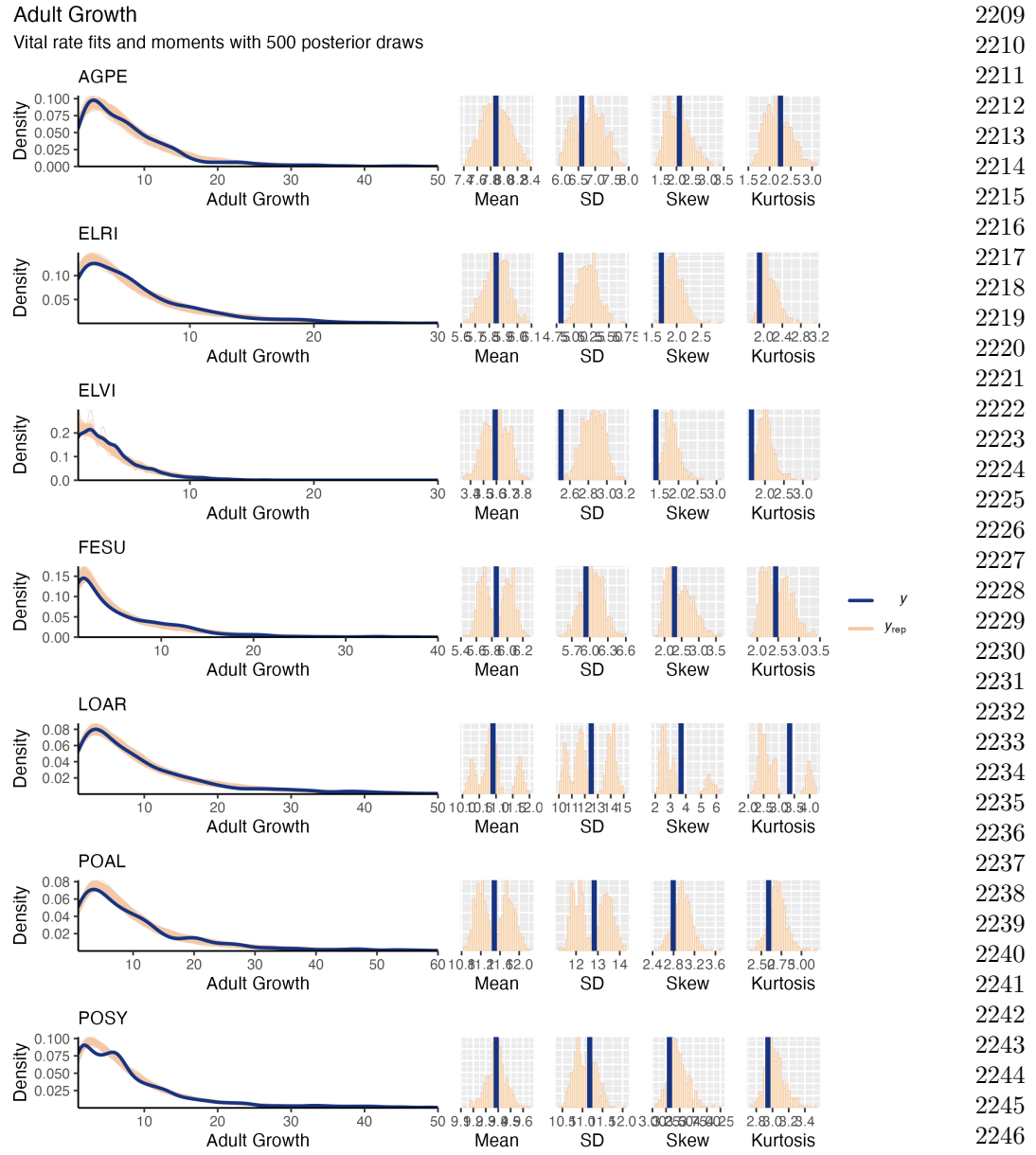
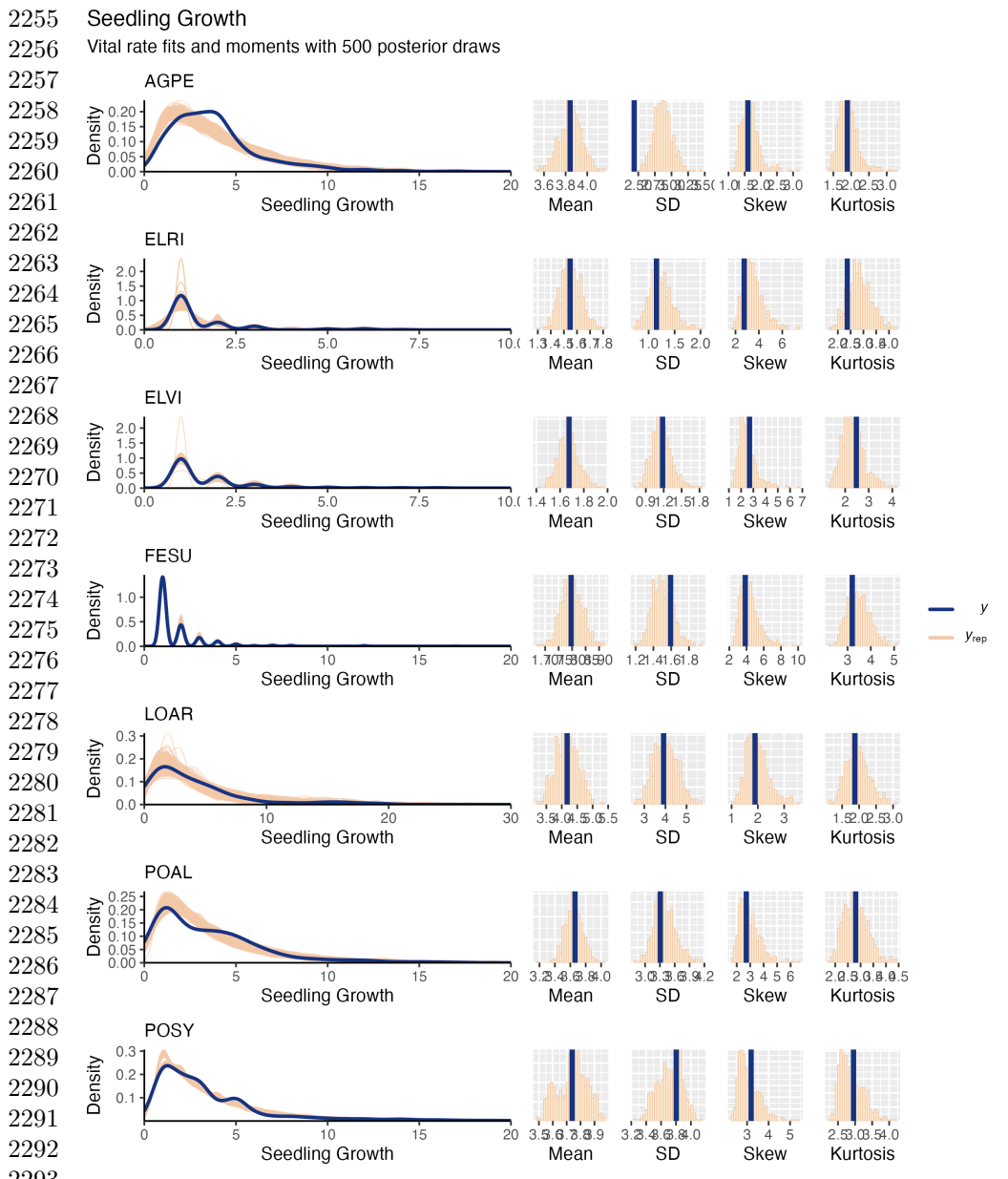


**Fig. S31** Posterior predictive check for statistical model of Adult Growth. Consistency between real data and simulated values indicates that fitted models describe the data well. Lines show density distributions of observed data (blue line) compared to data simulated from fitted models (tan lines) generated from 500 draws from posterior distributions of model parameters along with the distribution's moments.



2295 **Fig. S32** Posterior predictive check for statistical model of Seedling Growth. Consistency between  
 2296 real data and simulated values indicates that fitted models describe the data well. Lines show den-  
 2297 sity distributions of observed data (blue line) compared to data simulated from fitted models (tan  
 2298 lines) generated from 500 draws from posterior distributions of model parameters along with the  
 2299 distribution's moments.

2299  
 2300

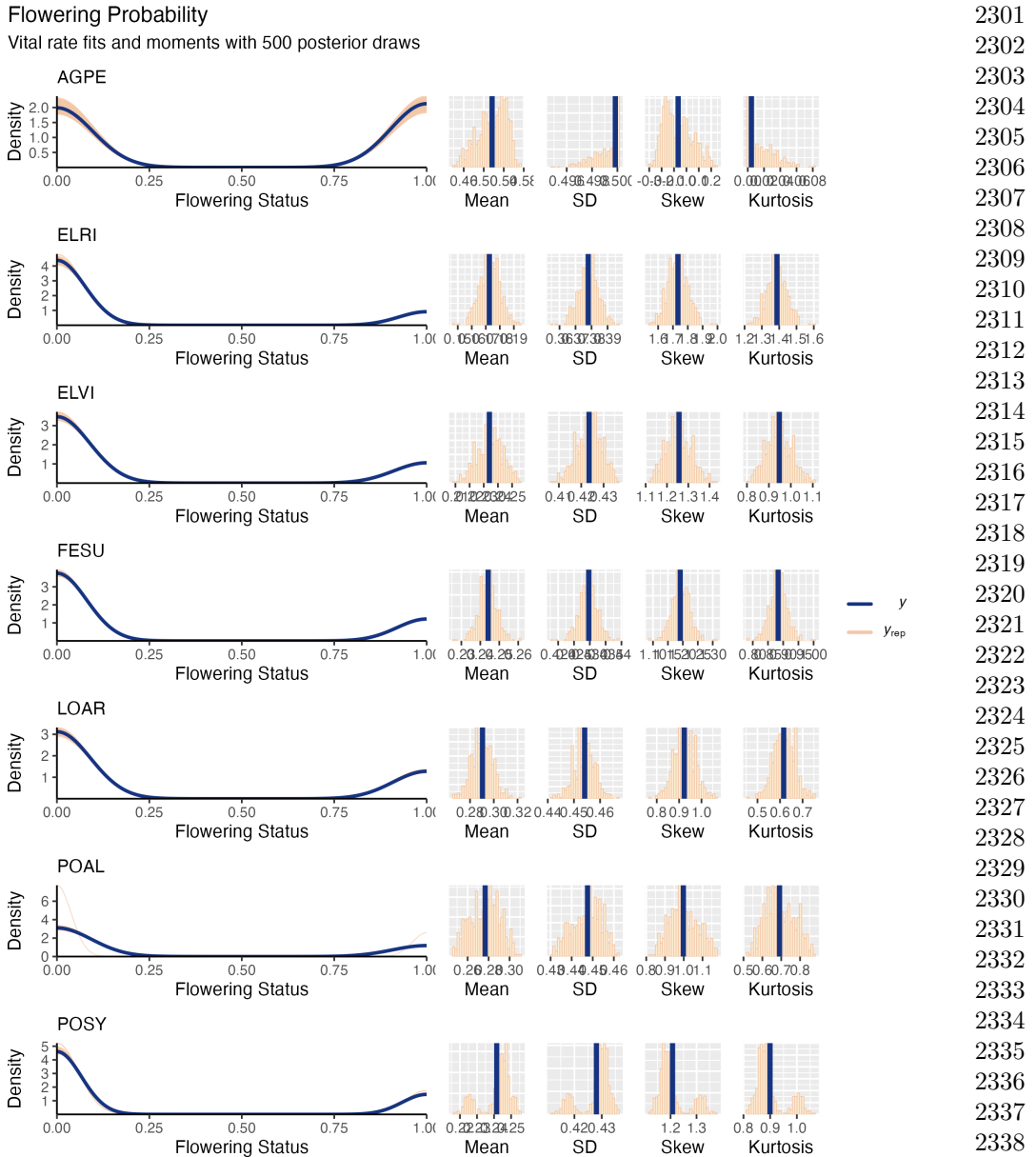
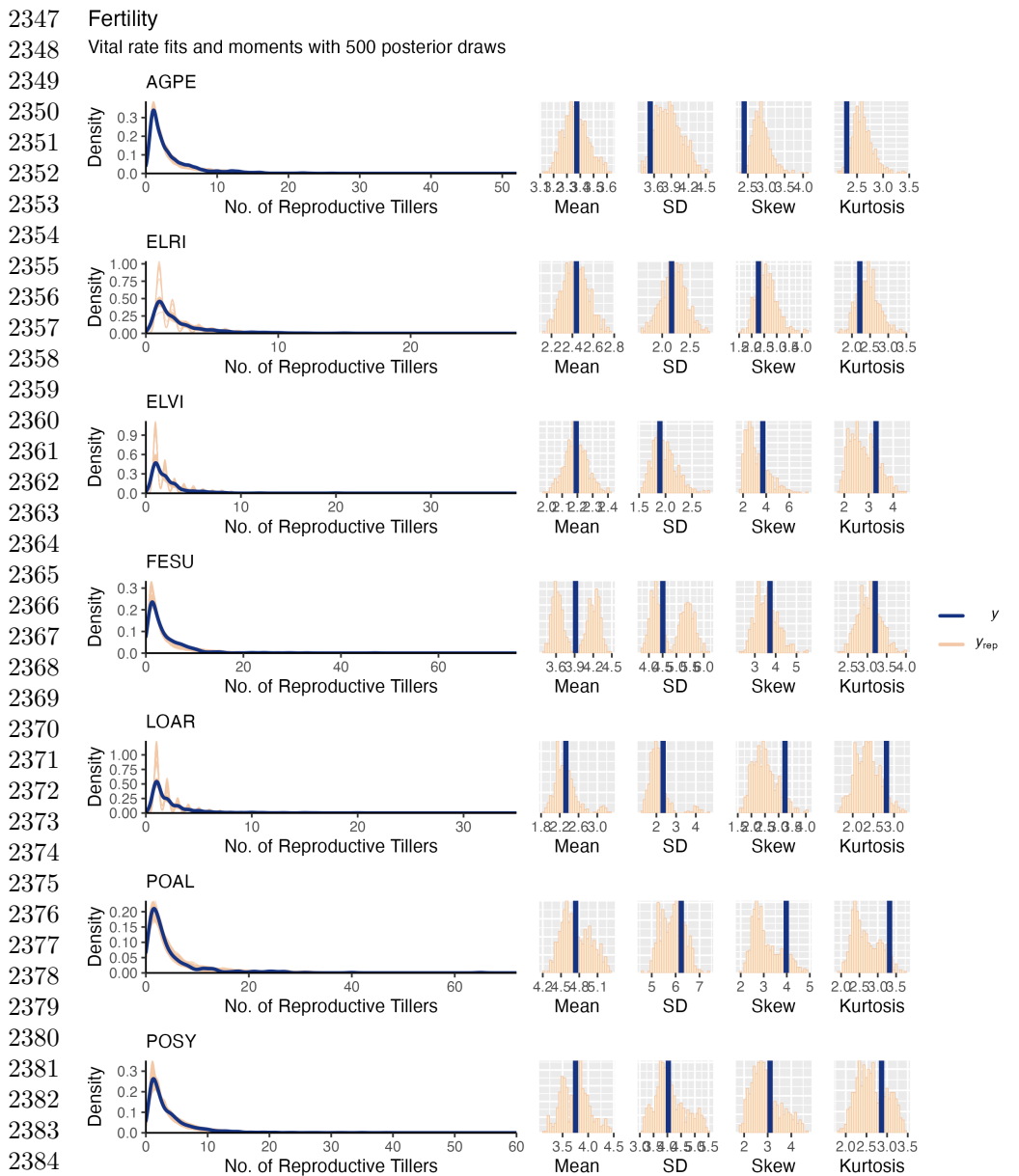


**Fig. S33** Posterior predictive check for statistical model of Flowering Probability. Consistency between real data and simulated values indicates that fitted models describe the data well. Lines show density distributions of observed data (blue line) compared to data simulated from fitted models (tan lines) generated from 500 draws from posterior distributions of model parameters along with the distribution's moments.



2385  
 2386 Fig. S34 Posterior predictive check for statistical model of Flowering Tiller production. Consistency  
 2387 between real data and simulated values indicates that fitted models describe the data well. Lines  
 2388 show density distributions of observed data (blue line) compared to data simulated from fitted models  
 2389 (tan lines) generated from 500 draws from posterior distributions of model parameters along with the  
 2390 distribution's moments.

2391  
 2392

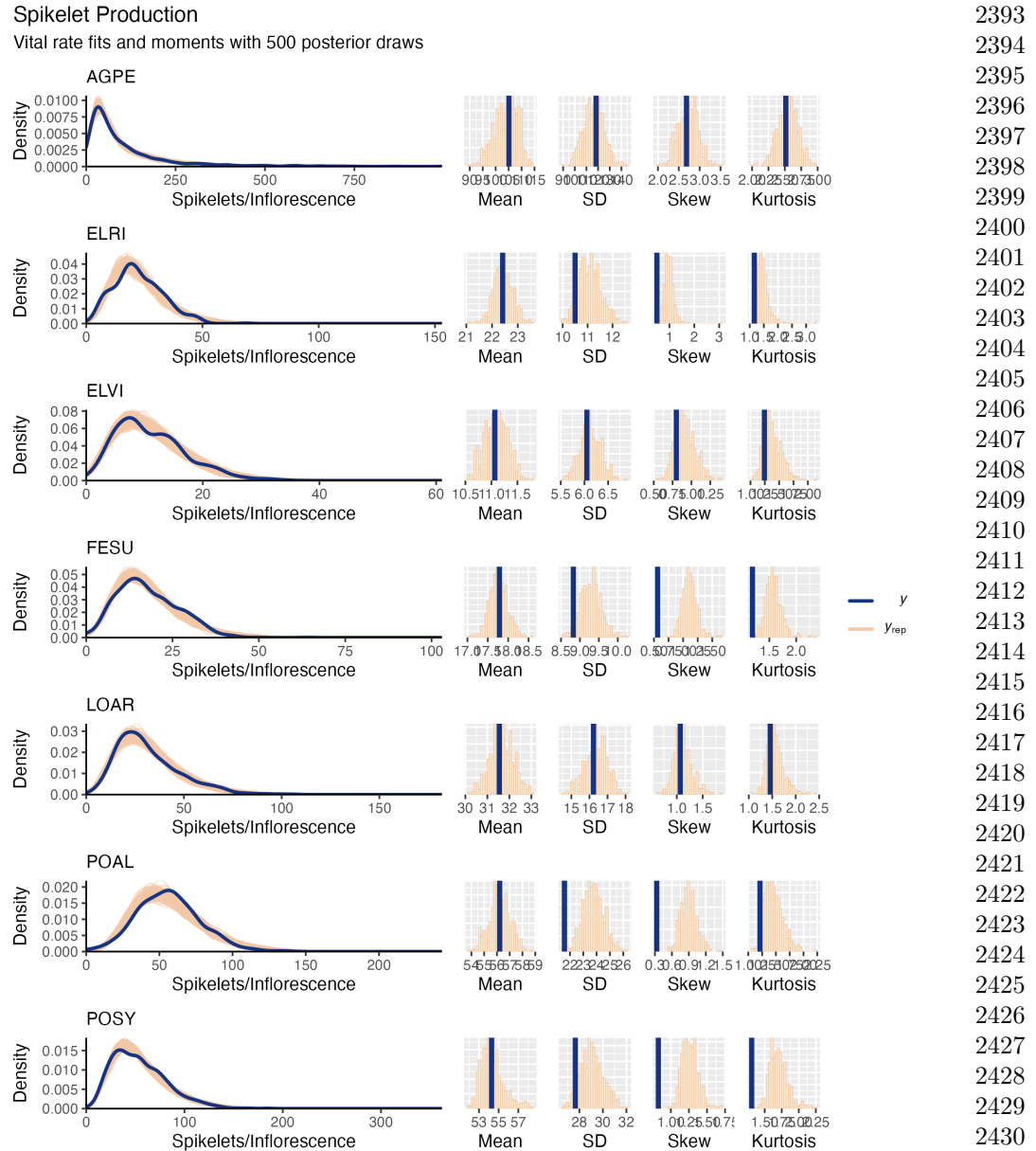
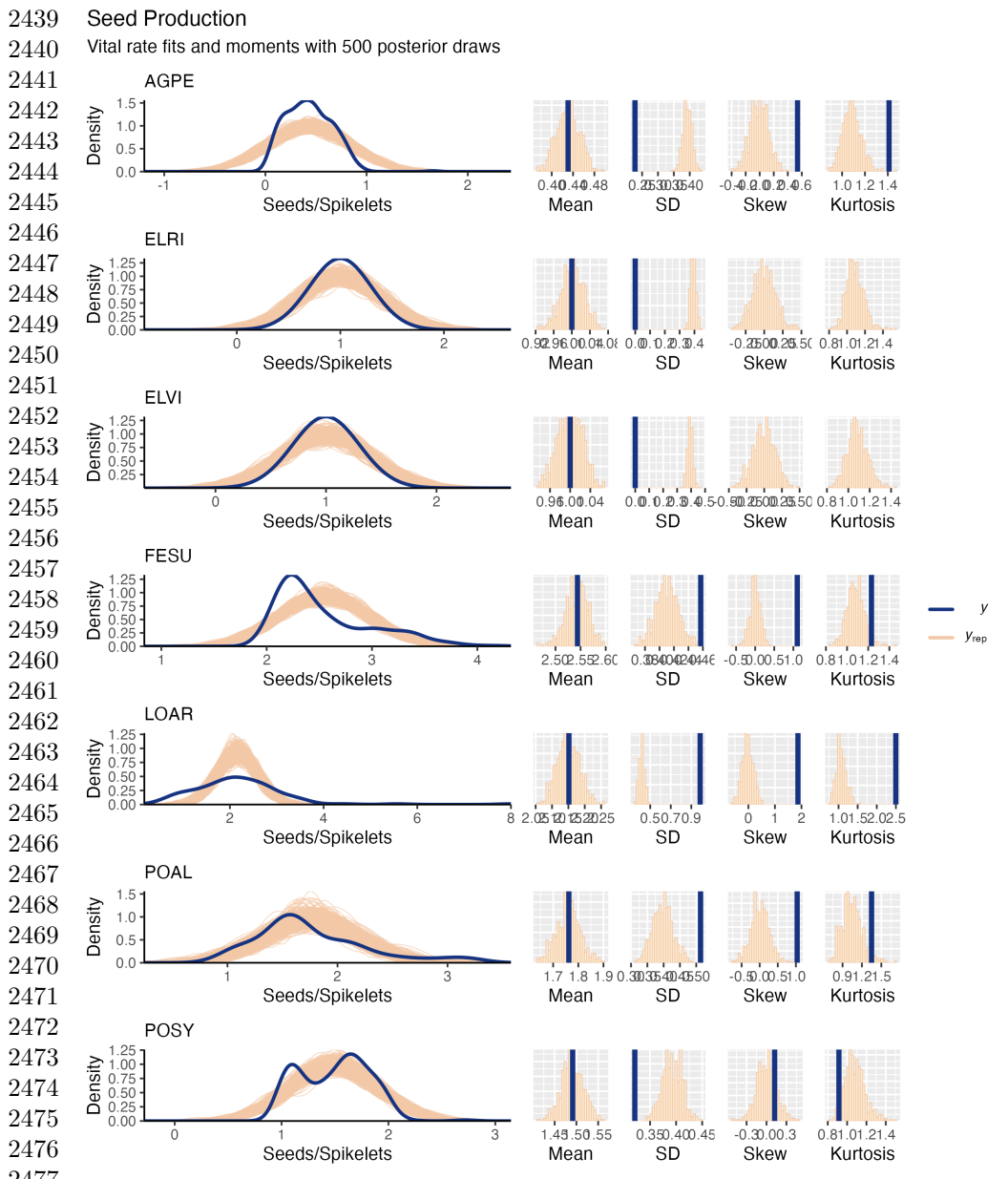


**Fig. S35** Posterior predictive check for statistical model of Spikelets/Inflorescence. Consistency between real data and simulated values indicates that fitted models describe the data well. Lines show density distributions of observed data (blue line) compared to data simulated from fitted models (tan lines) generated from 500 draws from posterior distributions of model parameters along with the distribution's moments.



2449 Fig. S36 Posterior predictive check for statistical model of Mean Seeds/Spikelet. Consistency  
 2450 between real data and simulated values indicates that fitted models describe the data well. Lines  
 2451 show density distributions of observed data (blue line) compared to data simulated from fitted mod-  
 2452 els (tan lines) generated from 500 draws from posterior distributions of model parameters along with  
 2453 the distribution's moments.

2454  
 2455  
 2456

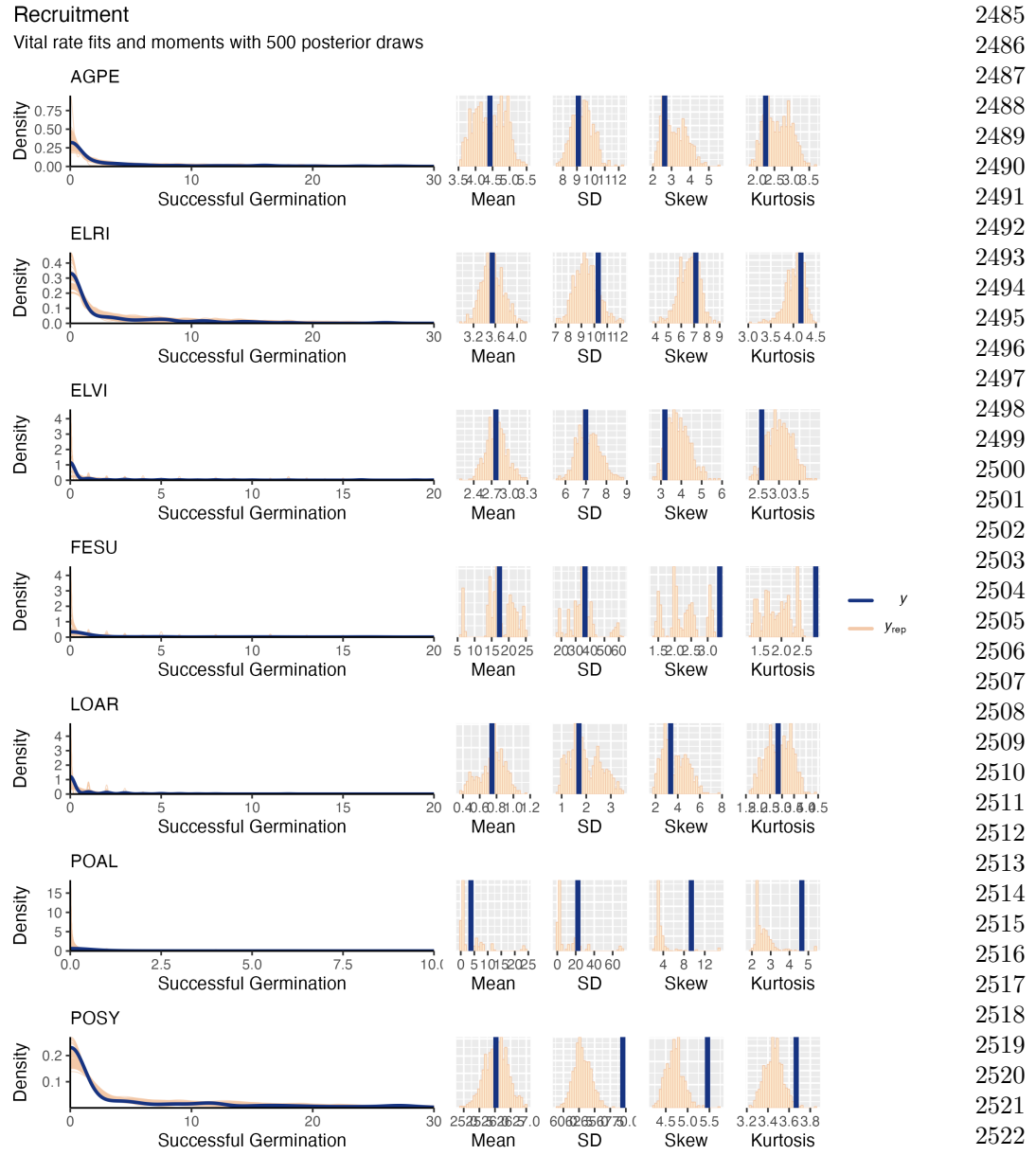
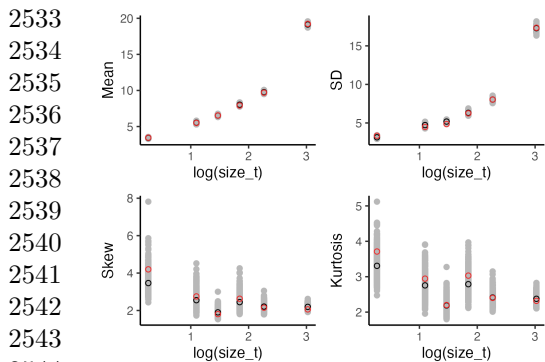


**Fig. S37** Posterior predictive check for statistical model of Recruitment. Consistency between real data and simulated values indicates that fitted models describe the data well. Lines show density distributions of observed data (blue line) compared to data simulated from fitted models (tan lines) generated from 500 draws from posterior distributions of model parameters along with the distribution's moments.

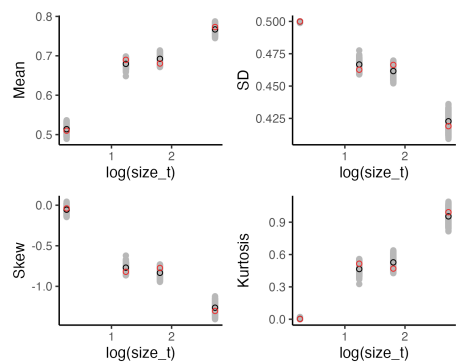
2485  
2486  
2487  
2488  
2489  
2490  
2491  
2492  
2493  
2494  
2495  
2496  
2497  
2498  
2499  
2500  
2501  
2502  
2503  
2504  
2505  
2506  
2507  
2508  
2509  
2510  
2511  
2512  
2513  
2514  
2515  
2516  
2517  
2518  
2519  
2520  
2521  
2522  
2523  
2524  
2525  
2526  
2527  
2528  
2529  
2530

2531 Size specific vital rate moments

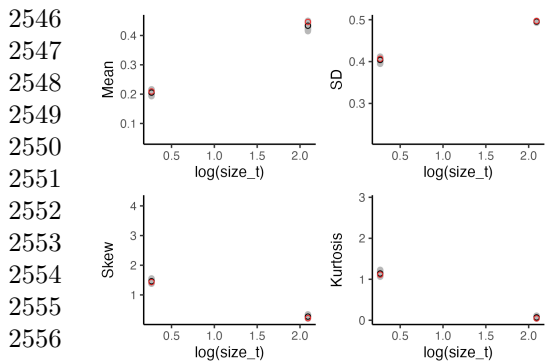
2532 Adult Growth



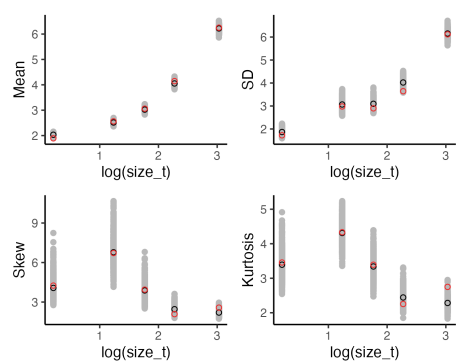
Adult Survival



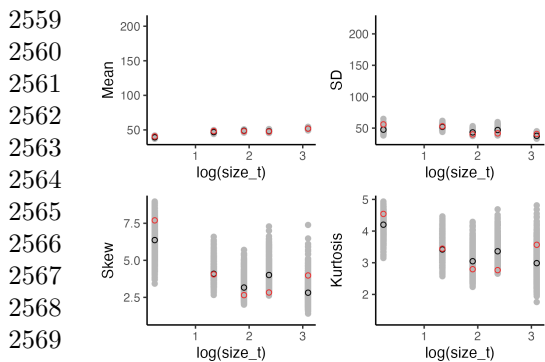
2545 Flowering Probability



Inflorescence Production



2558 Spikelets/Infl.



2572 **Fig. S38** Consistency between real data and fitted values across sizes indicates that the vital rate  
2573 models are accurately capturing size dependence. Graphs of posterior predictive check for mean and  
2574 higher moments of the vital rate models across size. Points show the value of statistical moments  
2575 binned across size for the observed data (red circles) compared to the simulated datasets (grey circles)  
2576 and the median of the simulated values (black circles) generated from 500 posterior draws from the  
2577 fitted model.

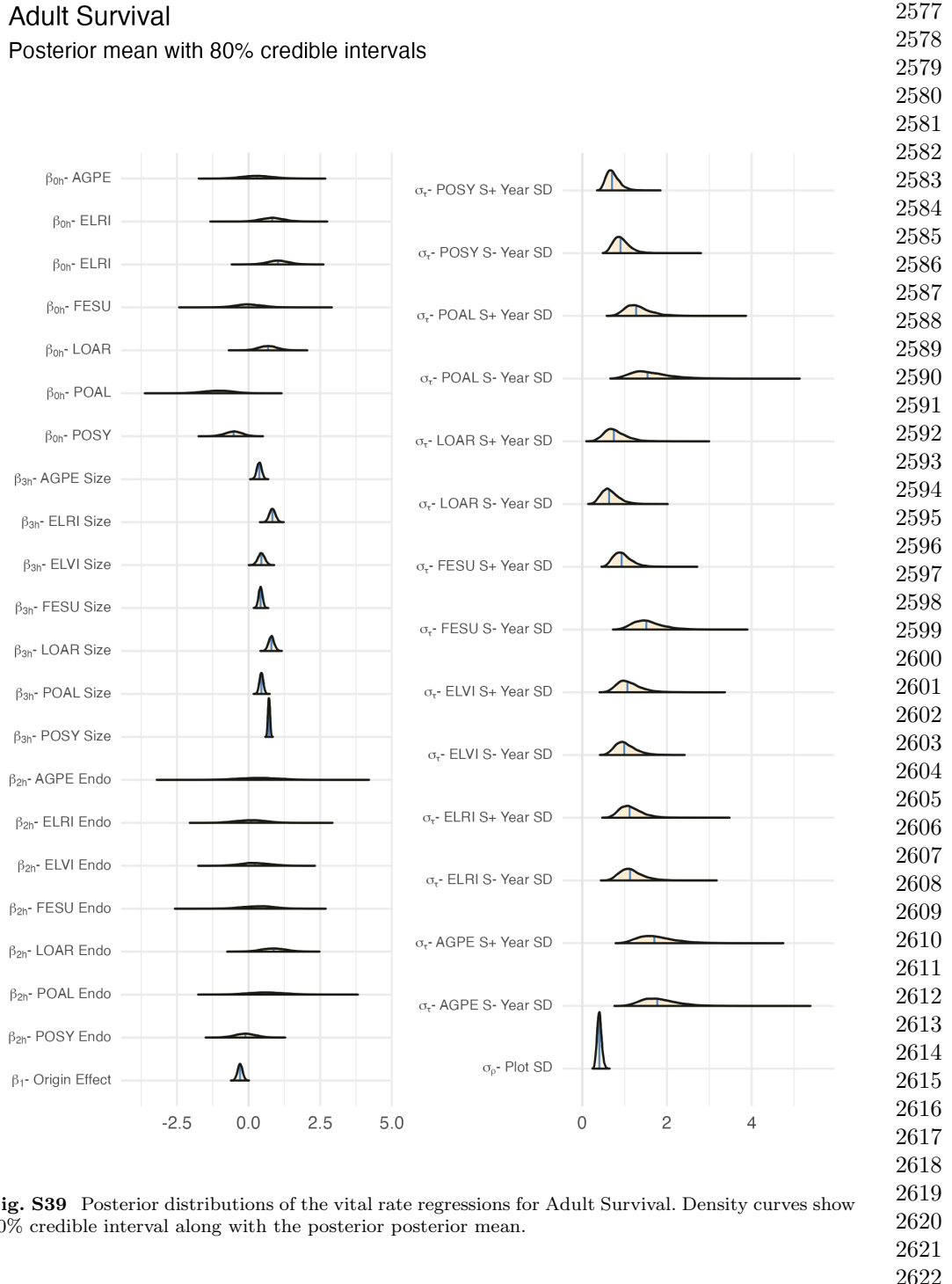


**Fig. S39** Posterior distributions of the vital rate regressions for Adult Survival. Density curves show 80% credible interval along with the posterior mean.

2623 Seedling Survival  
2624 Posterior mean with 80% credible intervals

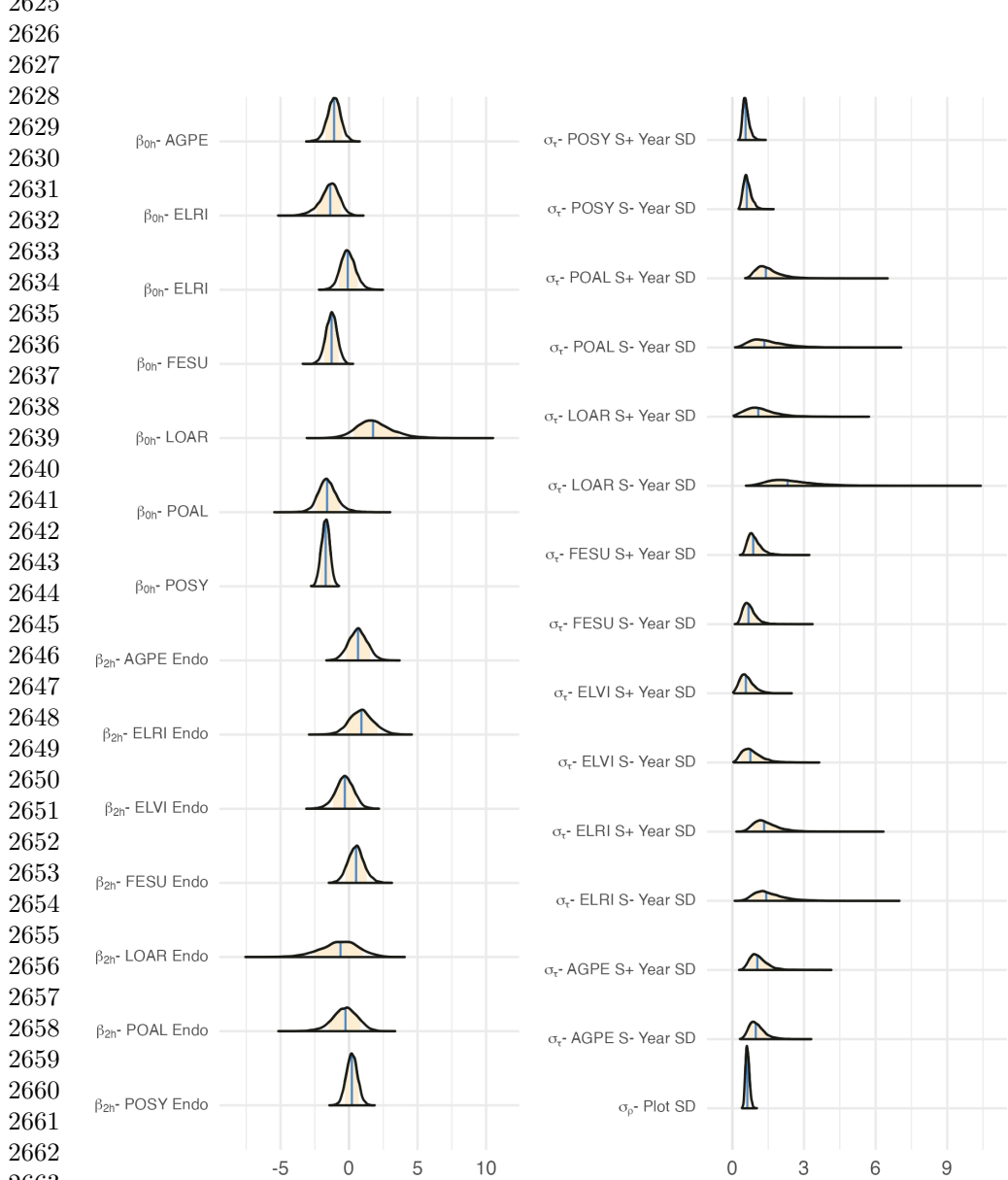
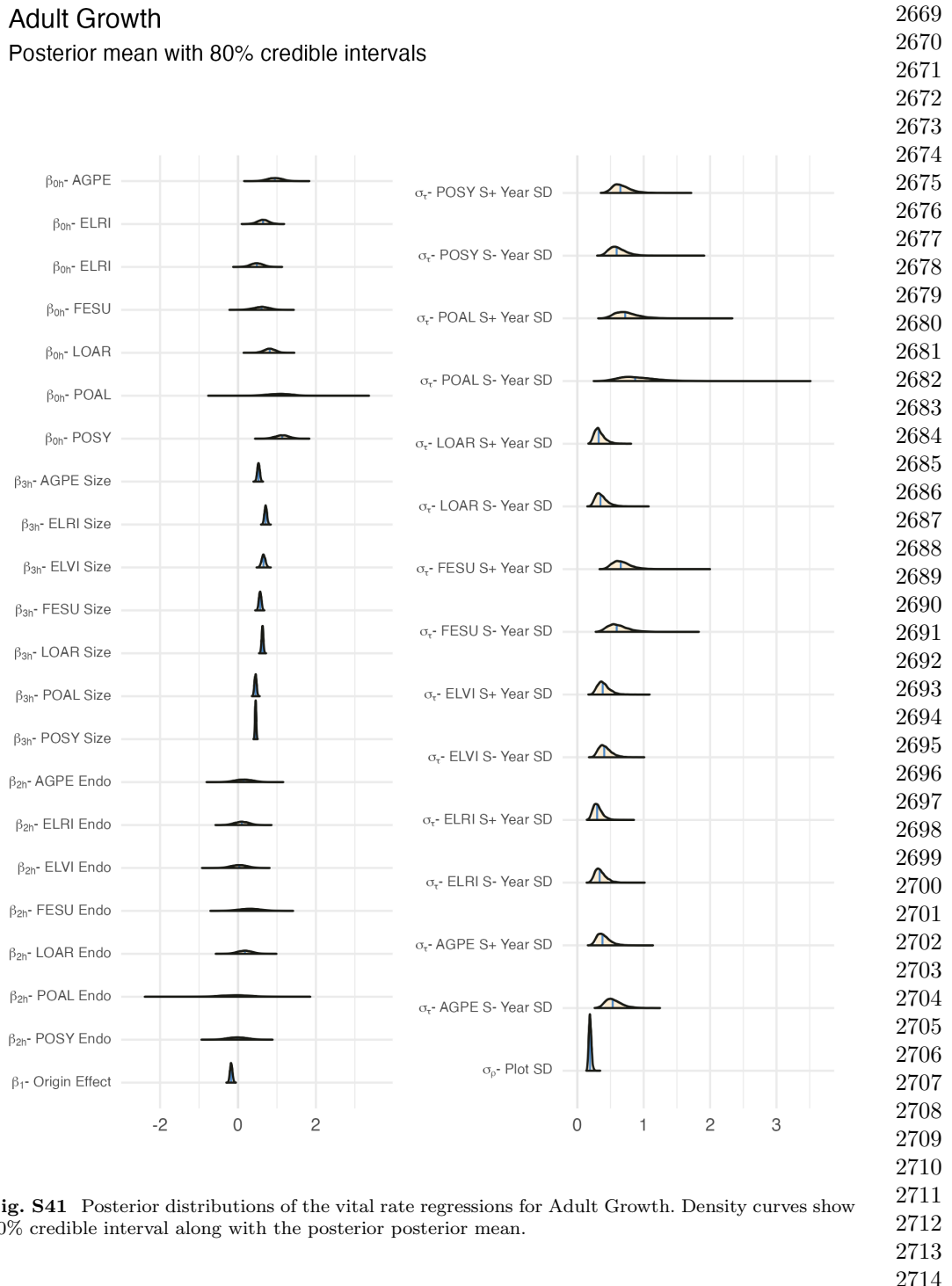


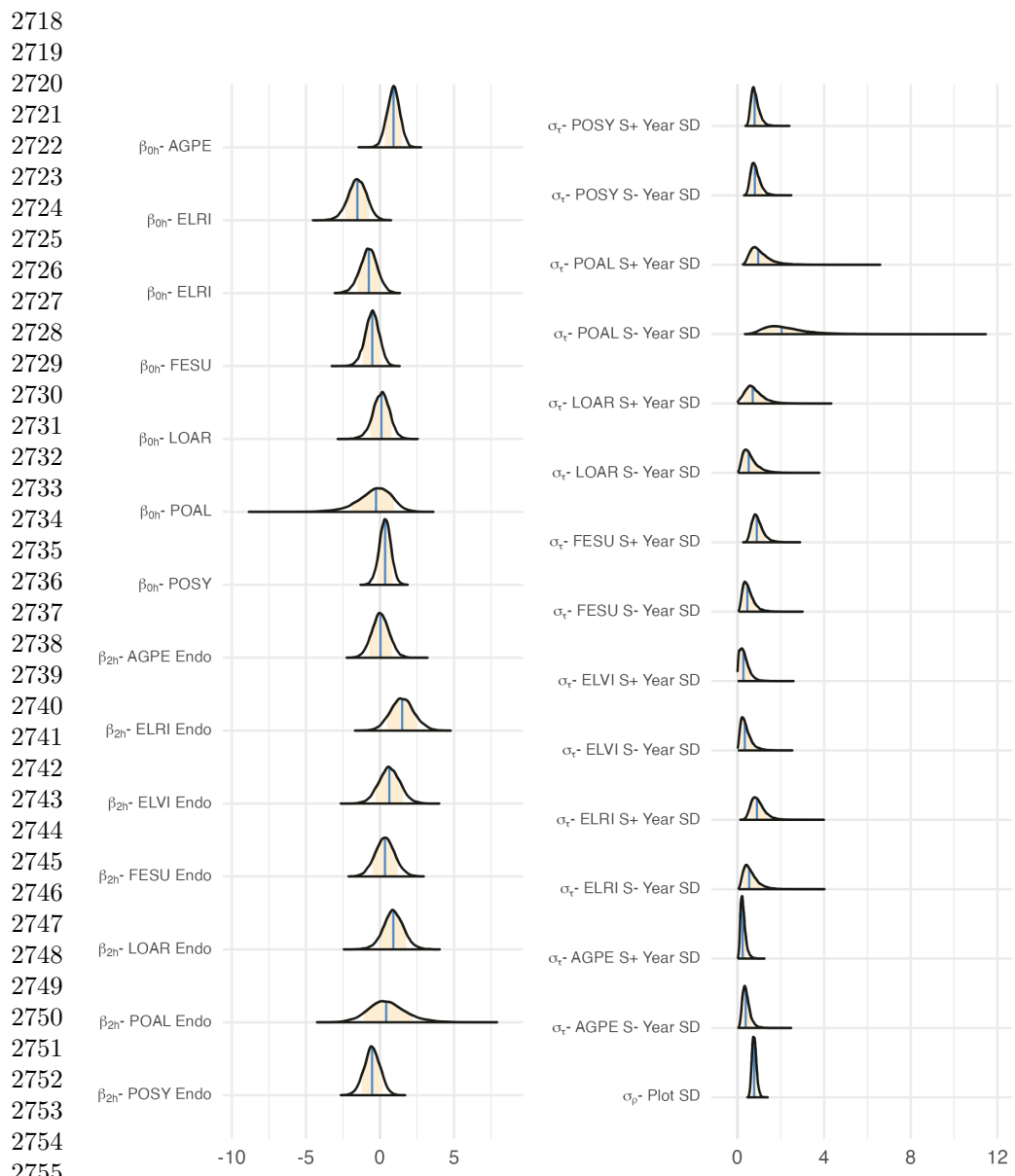
Fig. S40 Posterior distributions of the vital rate regressions for Seedling Survival. Density curves show 80% credible interval along with the posterior posterior mean.

2666  
2667  
2668



**Fig. S41** Posterior distributions of the vital rate regressions for Adult Growth. Density curves show 80% credible interval along with the posterior posterior mean.

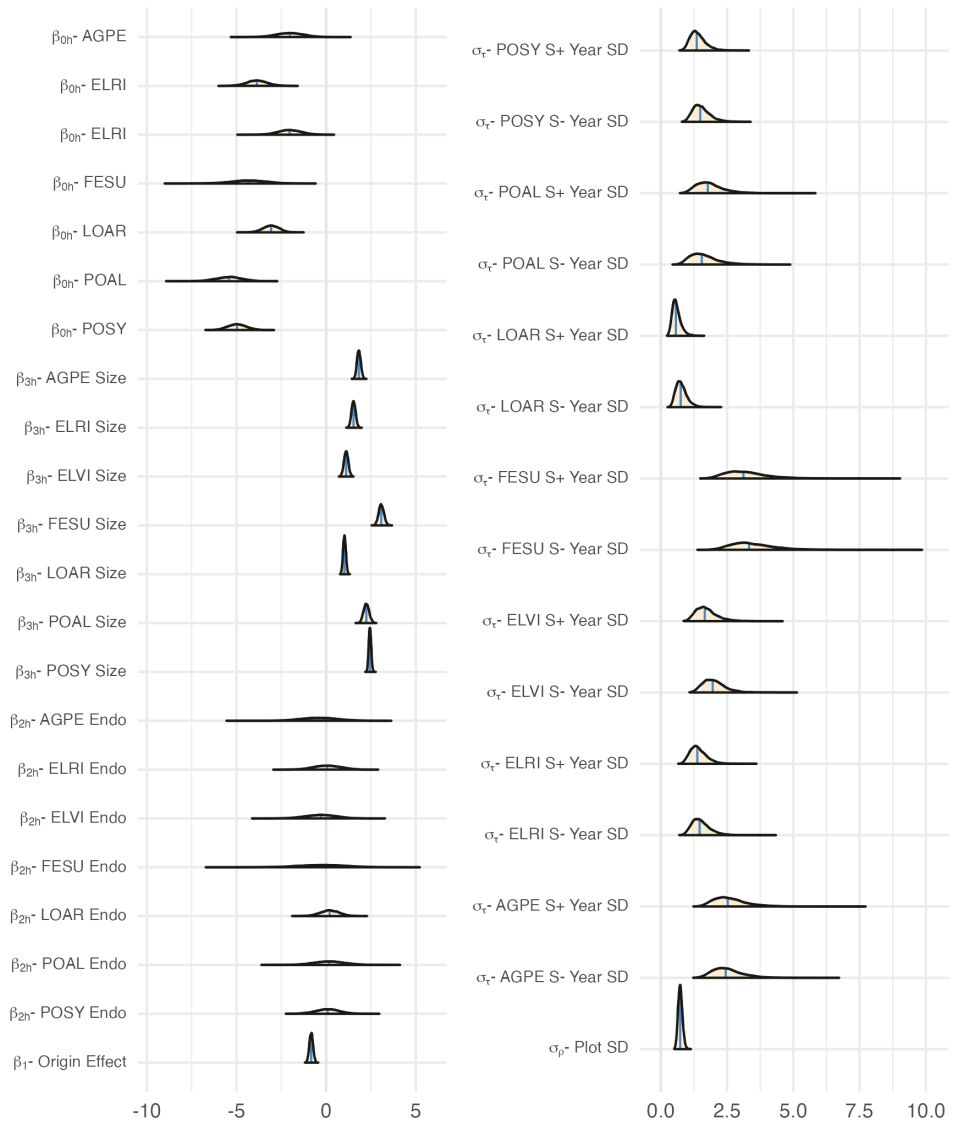
2715 Seedling Growth  
 2716 Posterior mean with 80% credible intervals  
 2717



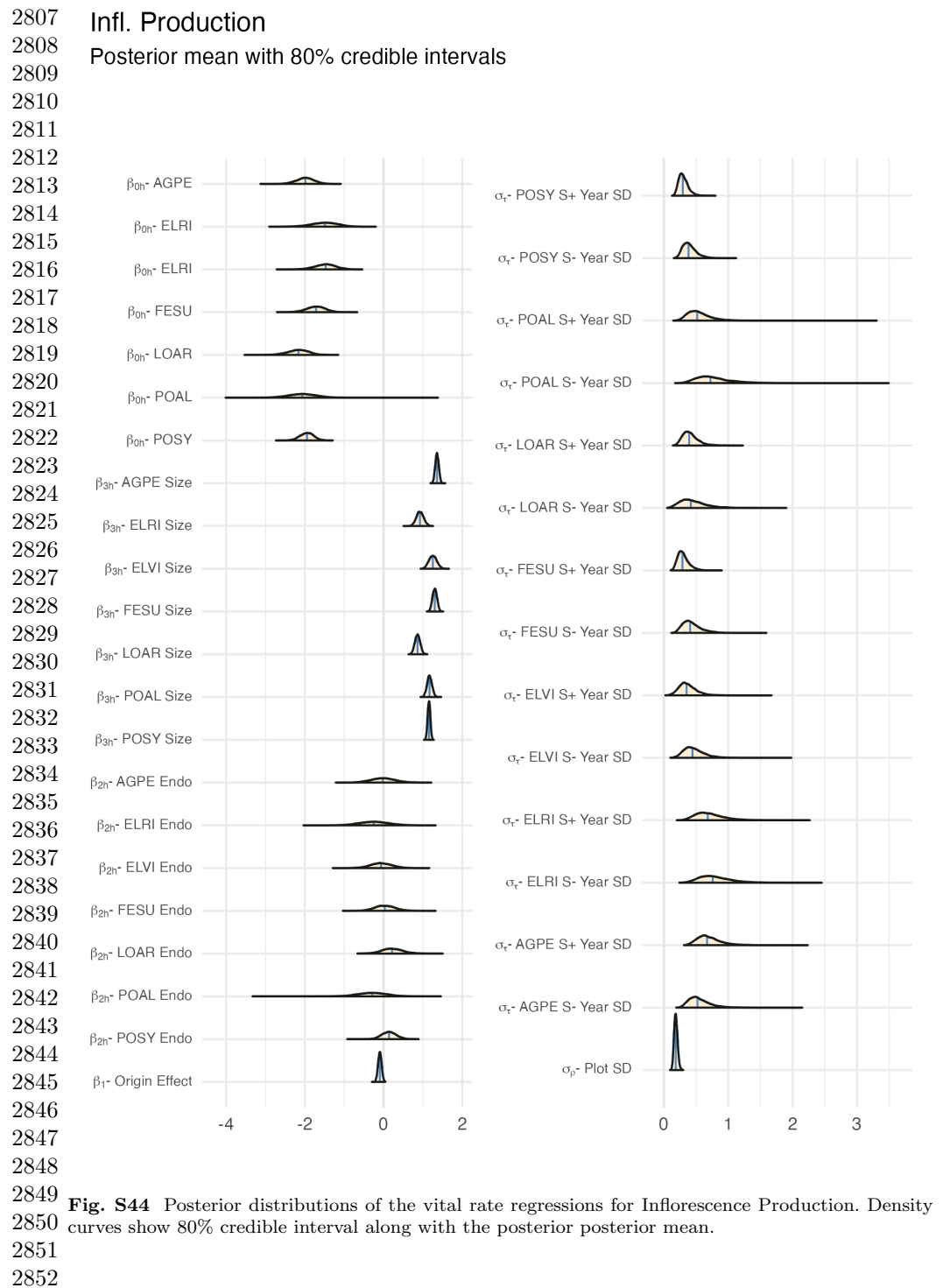
2757 **Fig. S42** Posterior distributions of the vital rate regressions for Seedling Growth. Density curves  
 2758 show 80% credible interval along with the posterior posterior mean.

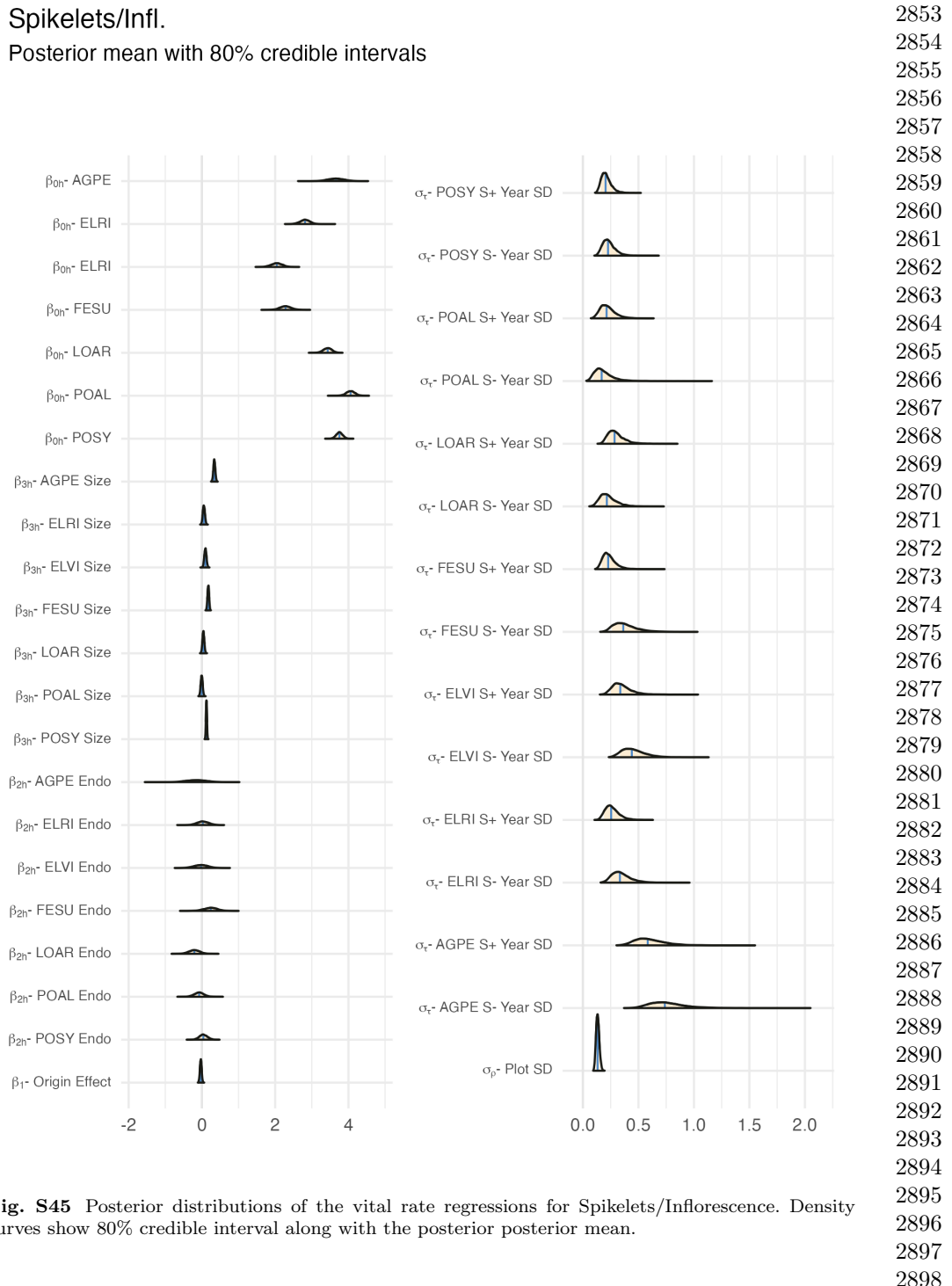
2759  
 2760

**Flowering Probability**  
Posterior mean with 80% credible intervals

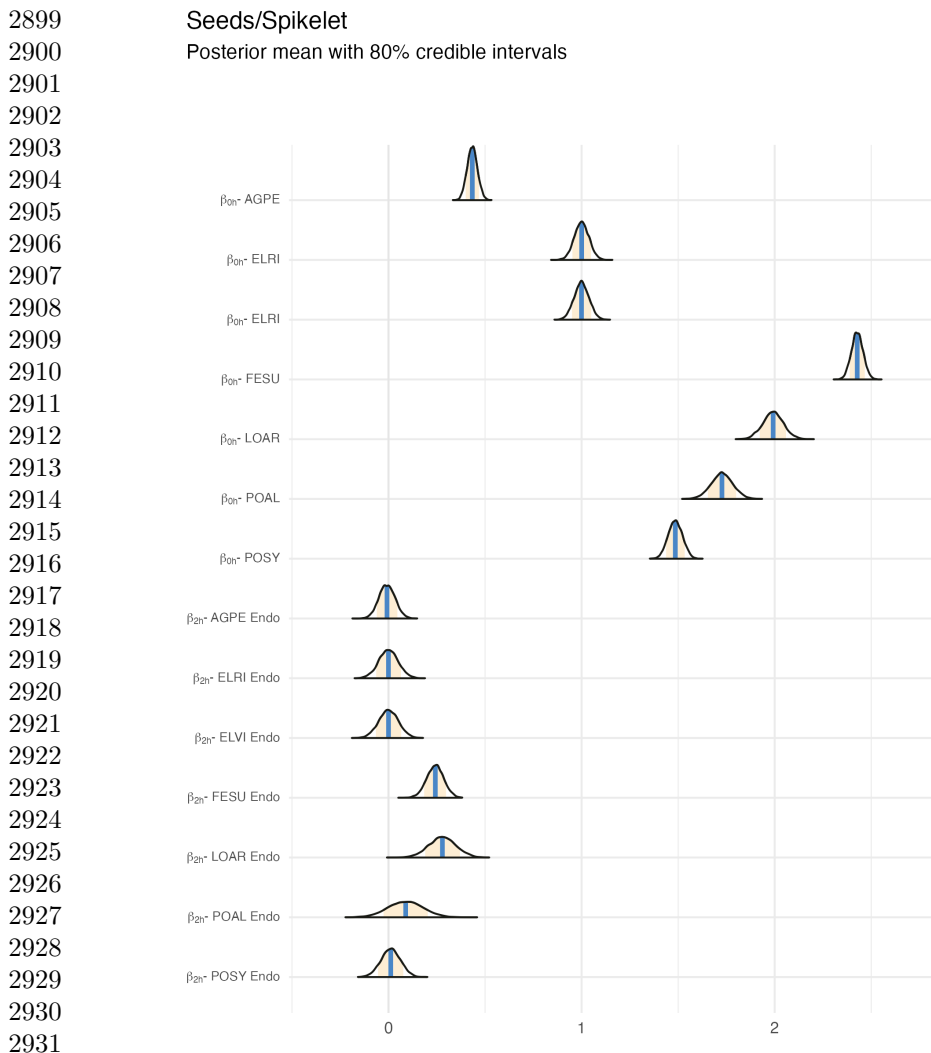


**Fig. S43** Posterior distributions of the vital rate regressions for Flowering Probability. Density curves show 80% credible interval along with the posterior posterior mean.

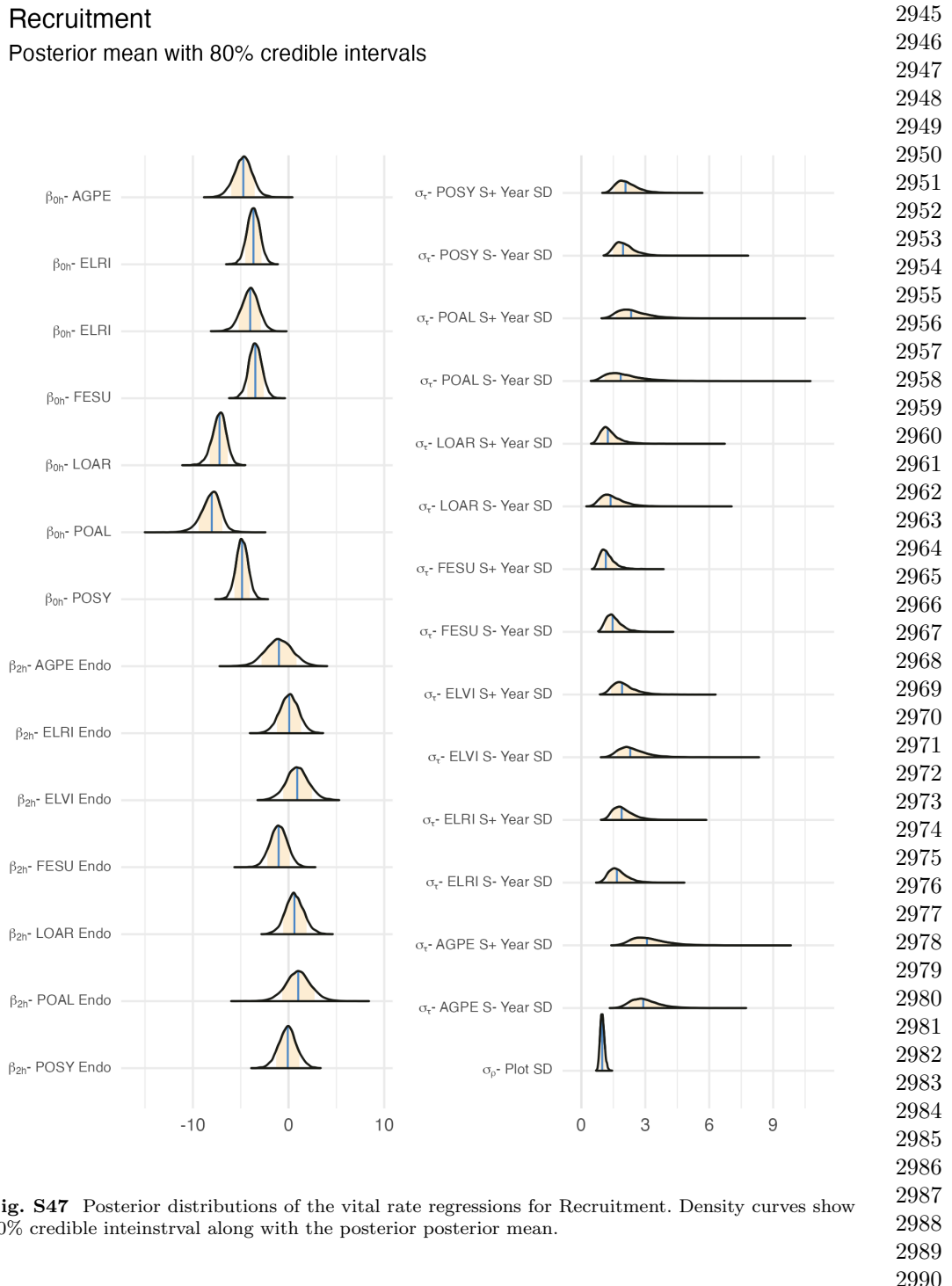




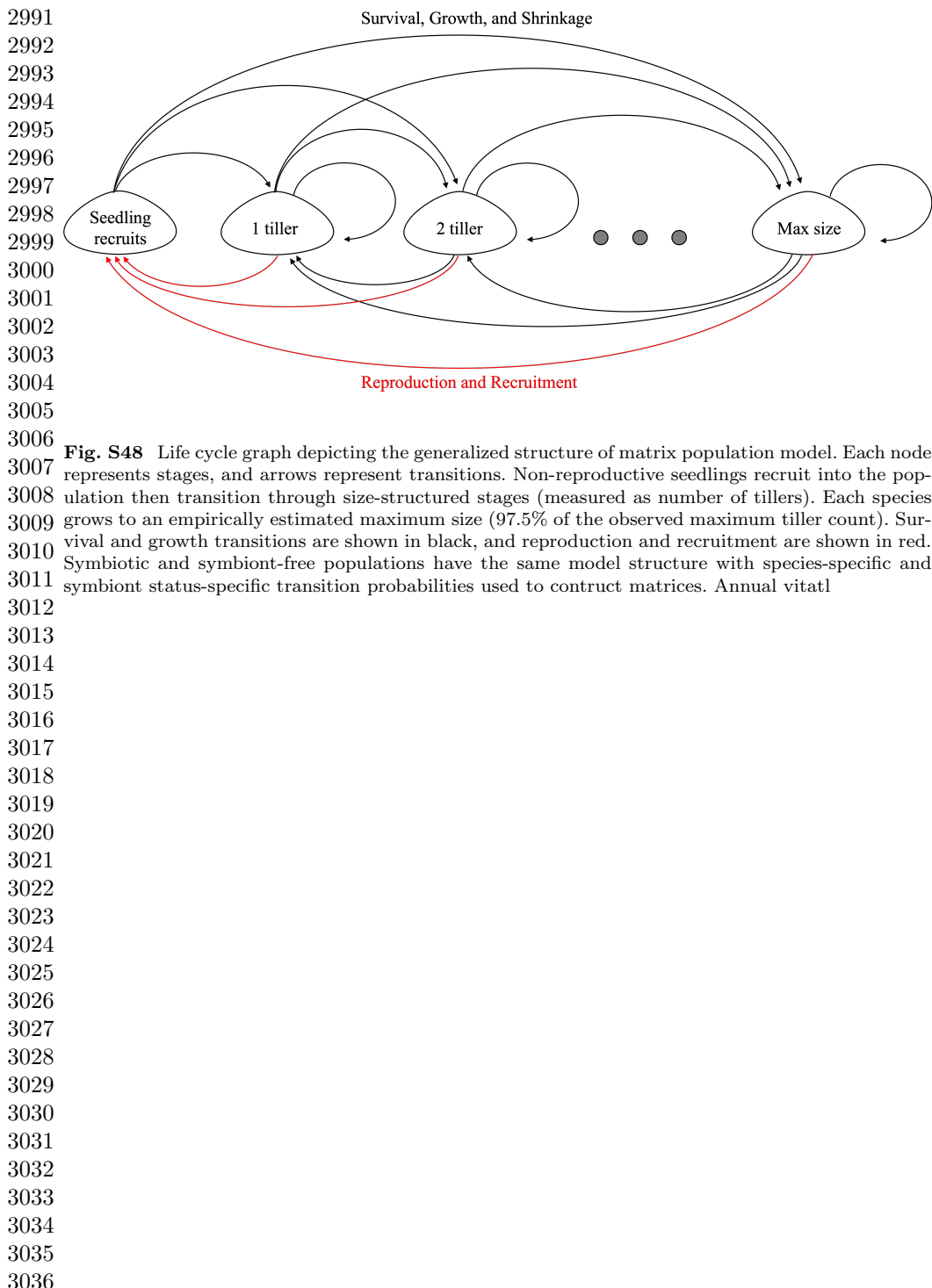
**Fig. S45** Posterior distributions of the vital rate regressions for Spikelets/Inflorescence. Density curves show 80% credible interval along with the posterior posterior mean.



2932 **Fig. S46** Posterior distributions of the vital rate regressions for Seeds/Spikelet. Density curves show  
 2933 80% credible interval along with the posterior posterior mean.  
 2934  
 2935  
 2936  
 2937  
 2938  
 2939  
 2940  
 2941  
 2942  
 2943  
 2944



**Fig. S47** Posterior distributions of the vital rate regressions for Recruitment. Density curves show 80% credible intervals along with the posterior mean.



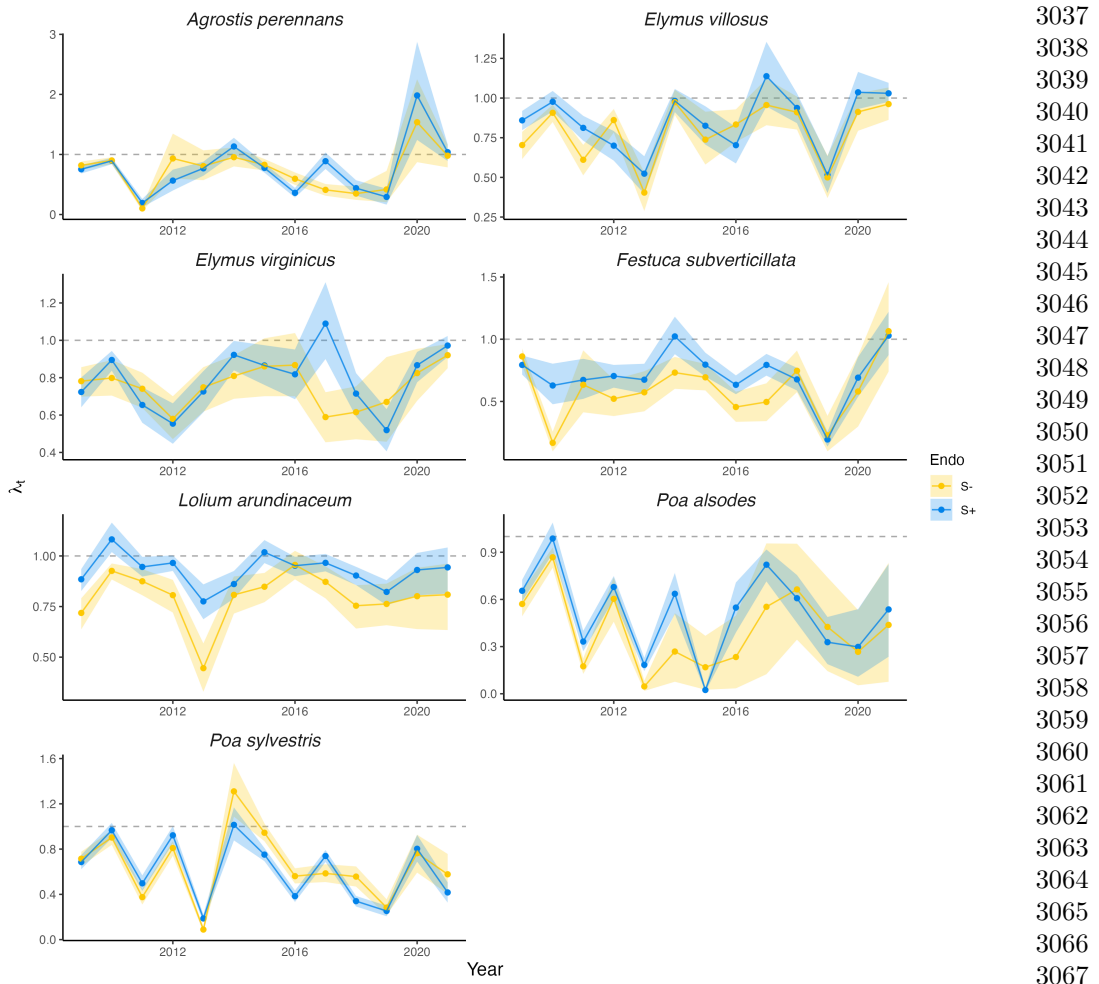
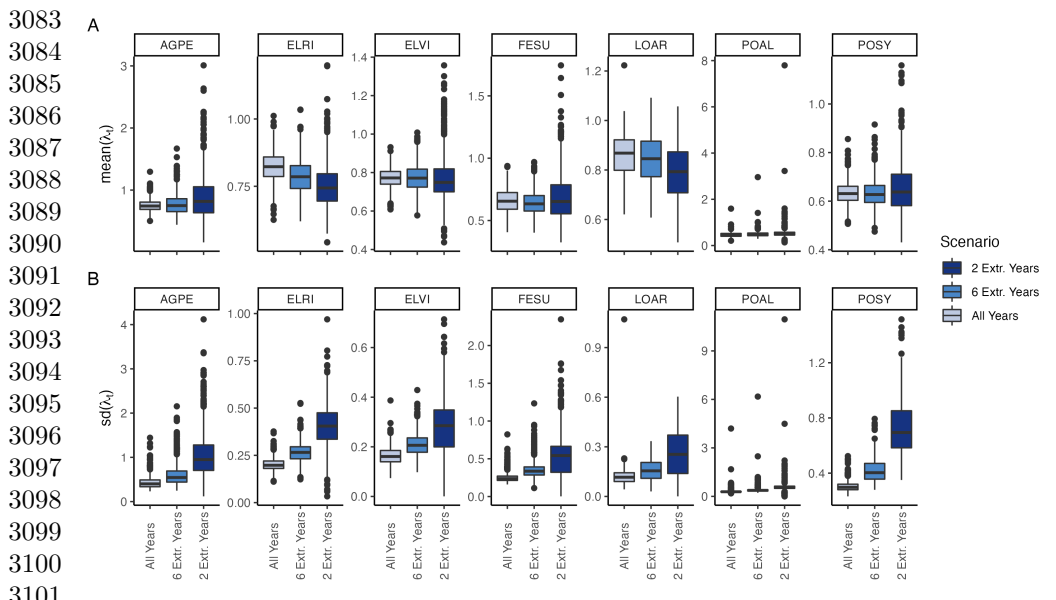


**Fig. S49** Annual growth rate values ( $\lambda_t$ ) over thirteen years. Mean values for symbiotic (blue) and symbiont-free (yellow) population growth rates are show along with 80% credible intervals. Dashed line at ( $\lambda_t = 1$ ) indicates stable population growth rate. All values are calculated from matrix models representing recruit plants.

3037  
3038  
3039  
3040  
3041  
3042  
3043  
3044  
3045  
3046  
3047  
3048  
3049  
3050  
3051  
3052  
3053  
3054  
3055  
3056  
3057  
3058  
3059  
3060  
3061  
3062  
3063  
3064  
3065  
3066  
3067  
3068  
3069  
3070  
3071  
3072  
3073  
3074  
3075  
3076  
3077  
3078  
3079  
3080  
3081  
3082



3103 **Fig. S50** (A) Mean and (B) standard deviation of annual growth rate values during simulation  
 3104 scenarios. Each scenario selects from observed transition matrixes, increasing the variance by selecting  
 3105 either all observed years, or a set (6 or 2 years) that have the highest and lowest growth rates for  
 3106 symbiont-free populations.

3106  
 3107  
 3108  
 3109  
 3110  
 3111  
 3112  
 3113  
 3114  
 3115  
 3116  
 3117  
 3118  
 3119  
 3120  
 3121  
 3122  
 3123  
 3124  
 3125  
 3126  
 3127  
 3128

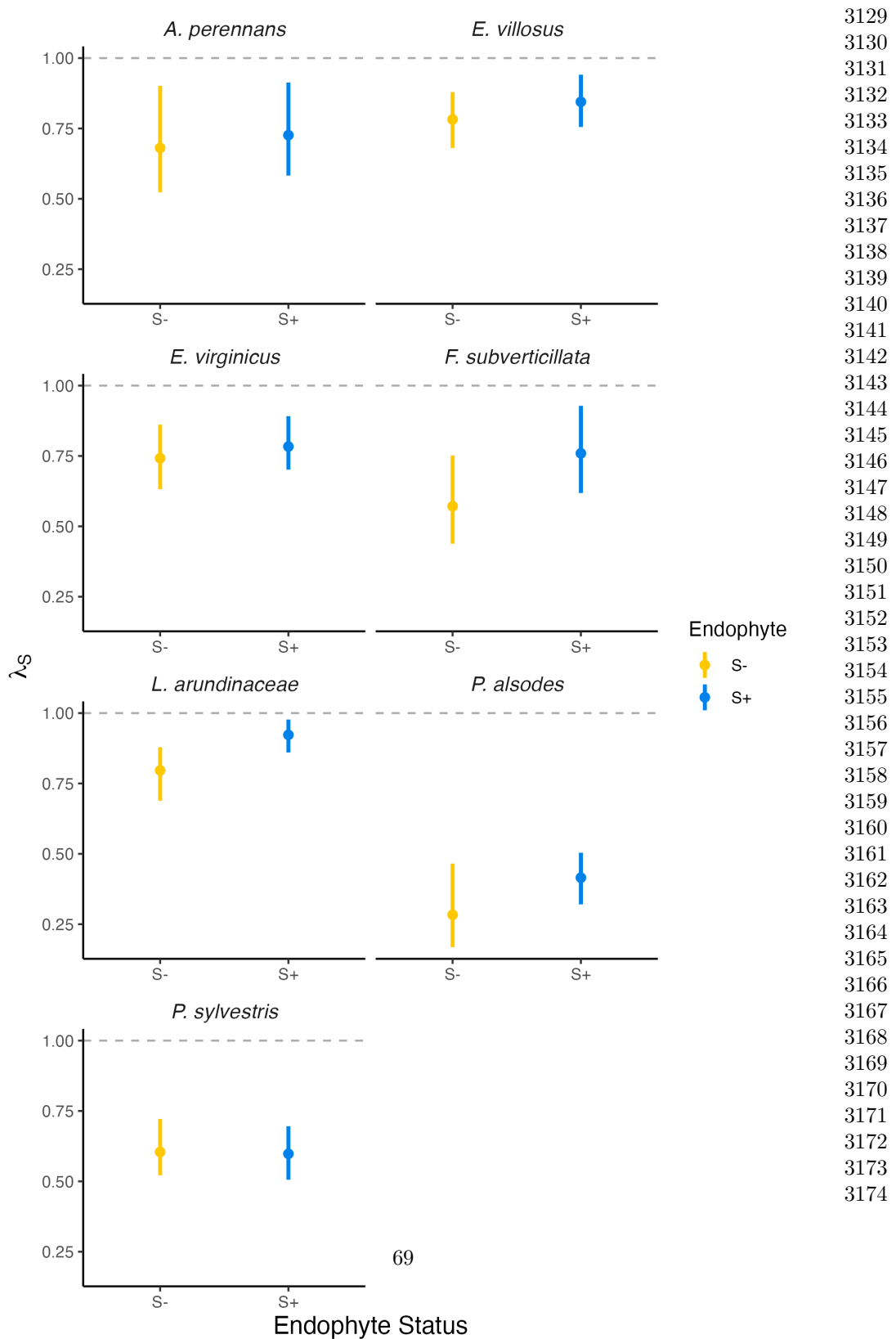


**Fig. S51** Stochastic population growth rates ( $\lambda_s$ ) for symbiotic (blue) and symbiont-free (yellow) populations. Points show posterior medians along with the 95% credible interval 50% and posterior medians. All values are calculated from matrix models representing recruit plants.

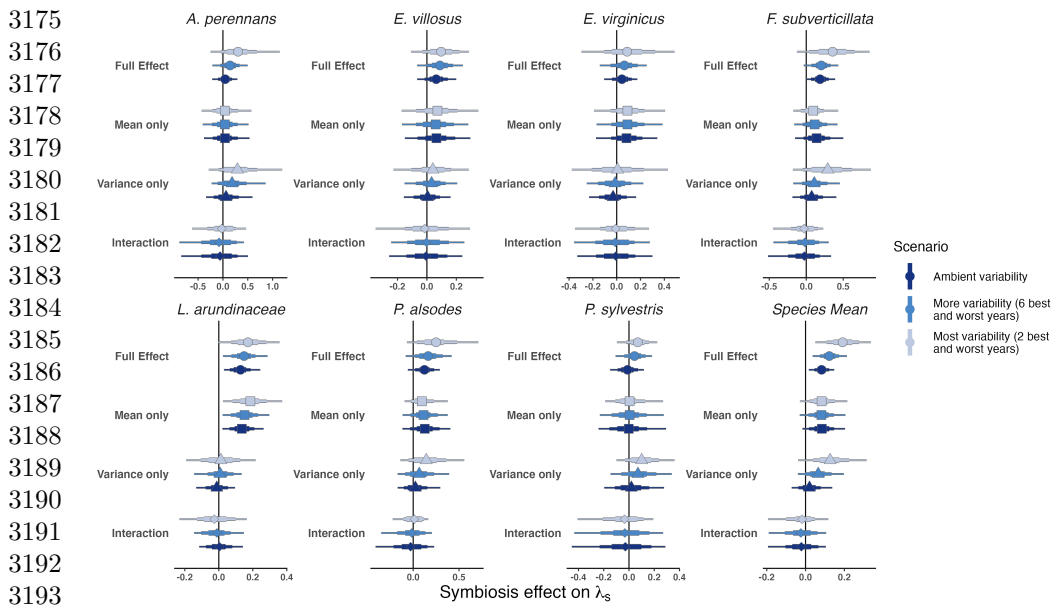
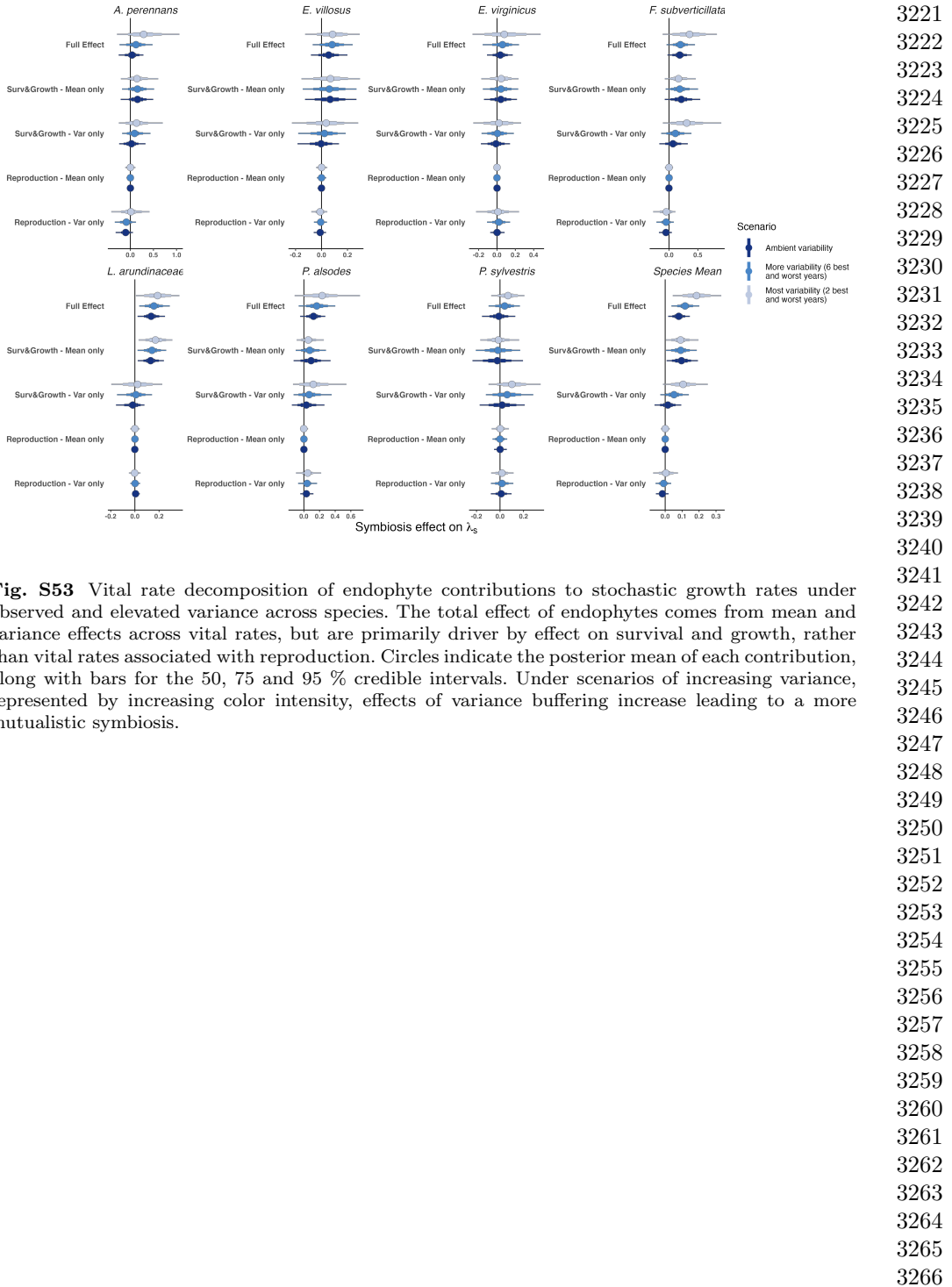


Fig. S52 Endophyte contributions to stochastic growth rates under observed and elevated variance across species. The total effect of endophytes (circle) comes from mean benefits (square) and variance buffering (triangle) as well as the interaction between mean and variance effects (diamond). Shapes indicate the posterior mean of each contribution, along with bars for the 50, 75 and 95 % credible intervals. Under scenarios of increasing variance, represented by increasing color intensity, effects of variance buffering increase leading to a more mutualistic symbiosis.

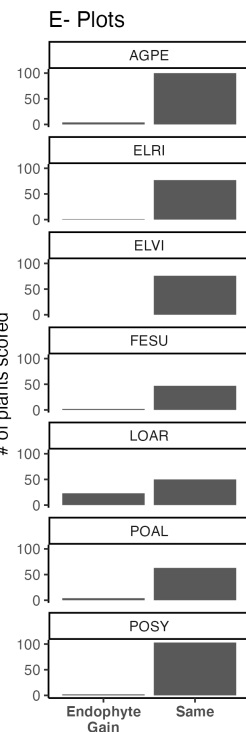
3195  
3196  
3197  
3198  
3199  
3200  
3201  
3202  
3203  
3204  
3205  
3206  
3207  
3208  
3209  
3210  
3211  
3212  
3213  
3214  
3215  
3216  
3217  
3218  
3219  
3220



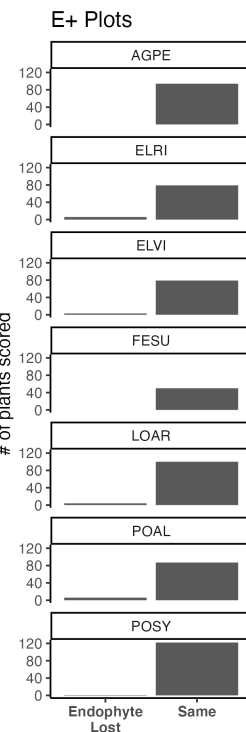
3267  
3268  
3269  
3270  
3271  
3272  
3273  
3274  
3275  
3276  
3277  
3278  
3279  
3280  
3281  
3282  
3283  
3284  
3285  
3286  
3287  
3288  
3289  
3290  
3291  
3292

#### Endophyte Status Checks

A



B



3293 **Fig. S54** Faithfulness of experimental plots to assigned endophyte status. Counts of plants scored  
3294 with leaf peels or seed squashes to check the faithfulness of recruits to the assigned plot-level endophyte  
3295 status. (A) Endophytic plants may be gained in initially S- plots, or (B) lost in initially S+ plots.

3296  
3297  
3298  
3299  
3300  
3301  
3302  
3303  
3304  
3305  
3306  
3307  
3308  
3309  
3310  
3311  
3312

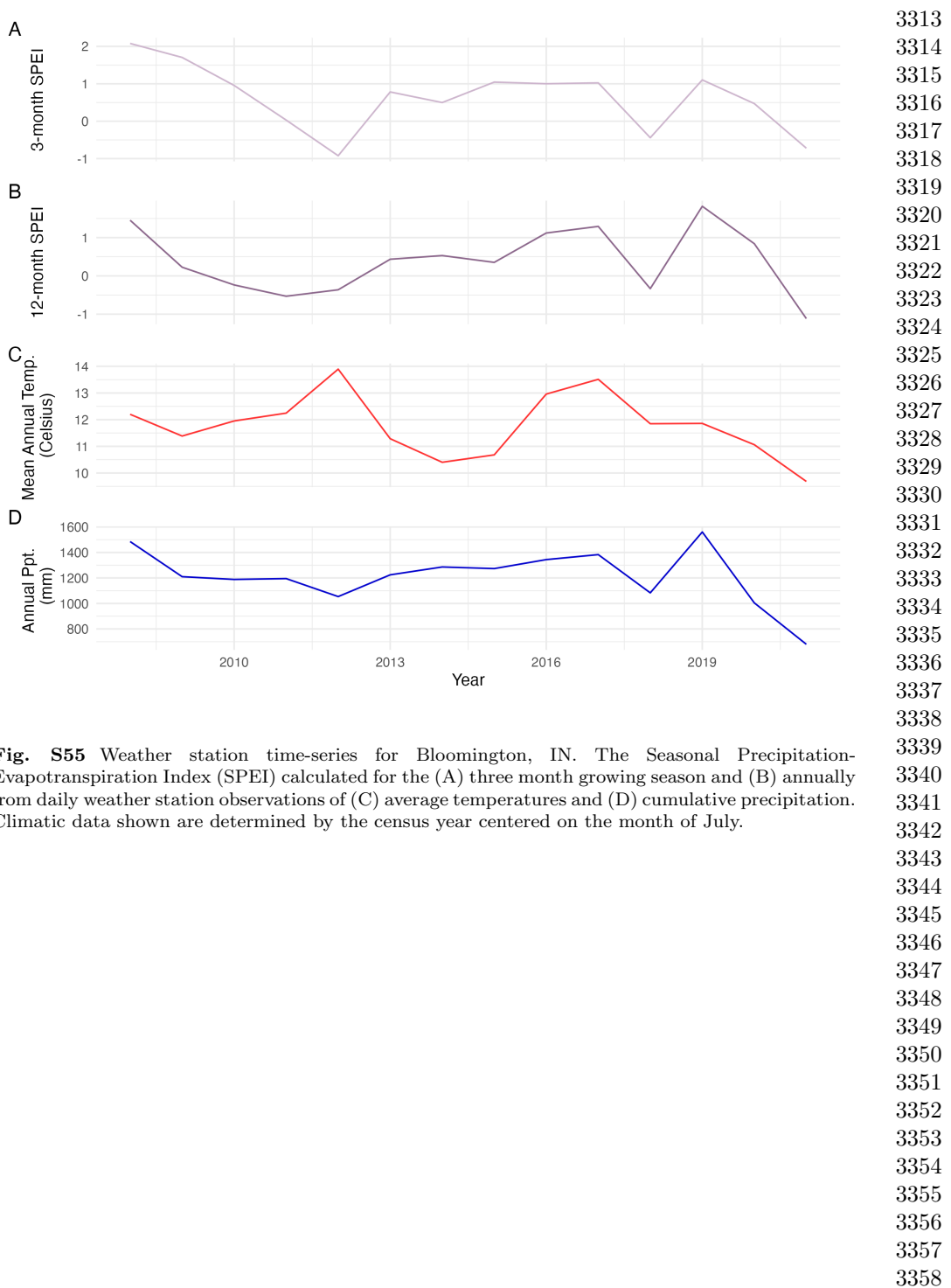


**Fig. S55** Weather station time-series for Bloomington, IN. The Seasonal Precipitation-Evapotranspiration Index (SPEI) calculated for the (A) three month growing season and (B) annually from daily weather station observations of (C) average temperatures and (D) cumulative precipitation. Climatic data shown are determined by the census year centered on the month of July.

3359

3360

3361

3362

3363

3364

3365

3366

3367

3368

3369

3370

3371

3372

3373

3374

3375

3376

3377

3378

3379

3380

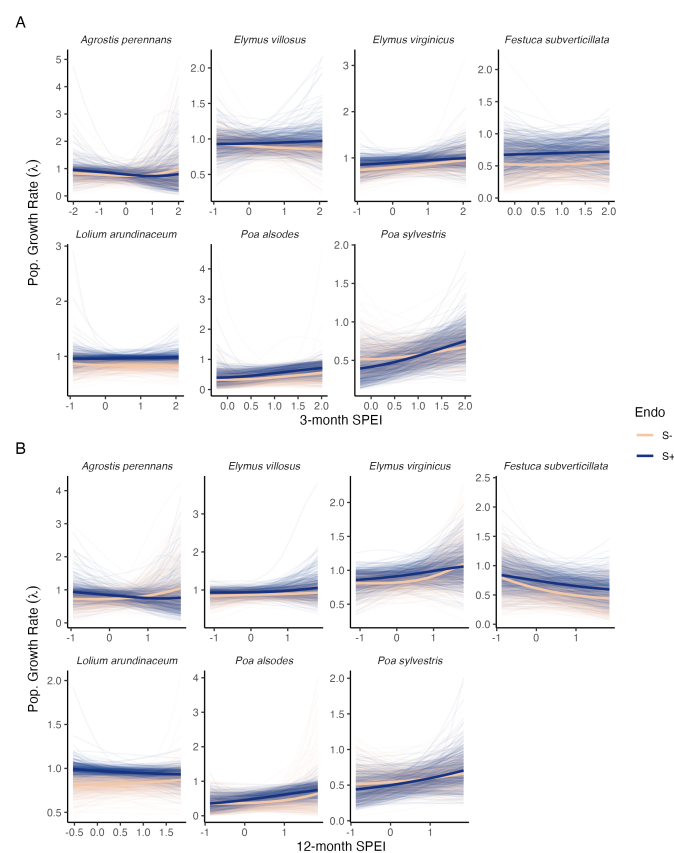
3381

3382

3383

3384

3385



3386 **Fig. S56** Predicted population growth rates across drought indices. Symbiotic (S+; blue) and  
 3387 symbiont-free (S-; tan) populations respond differently to climate as measured by the (A) 3-month  
 3388 SPEI and (B) 12-month SPEI. Thick lines represent the predicted mean growth rate and thin lines  
 3389 show 500 posterior draws.

3390

3391

3392

3393

3394

3395

3396

3397

3398

3399

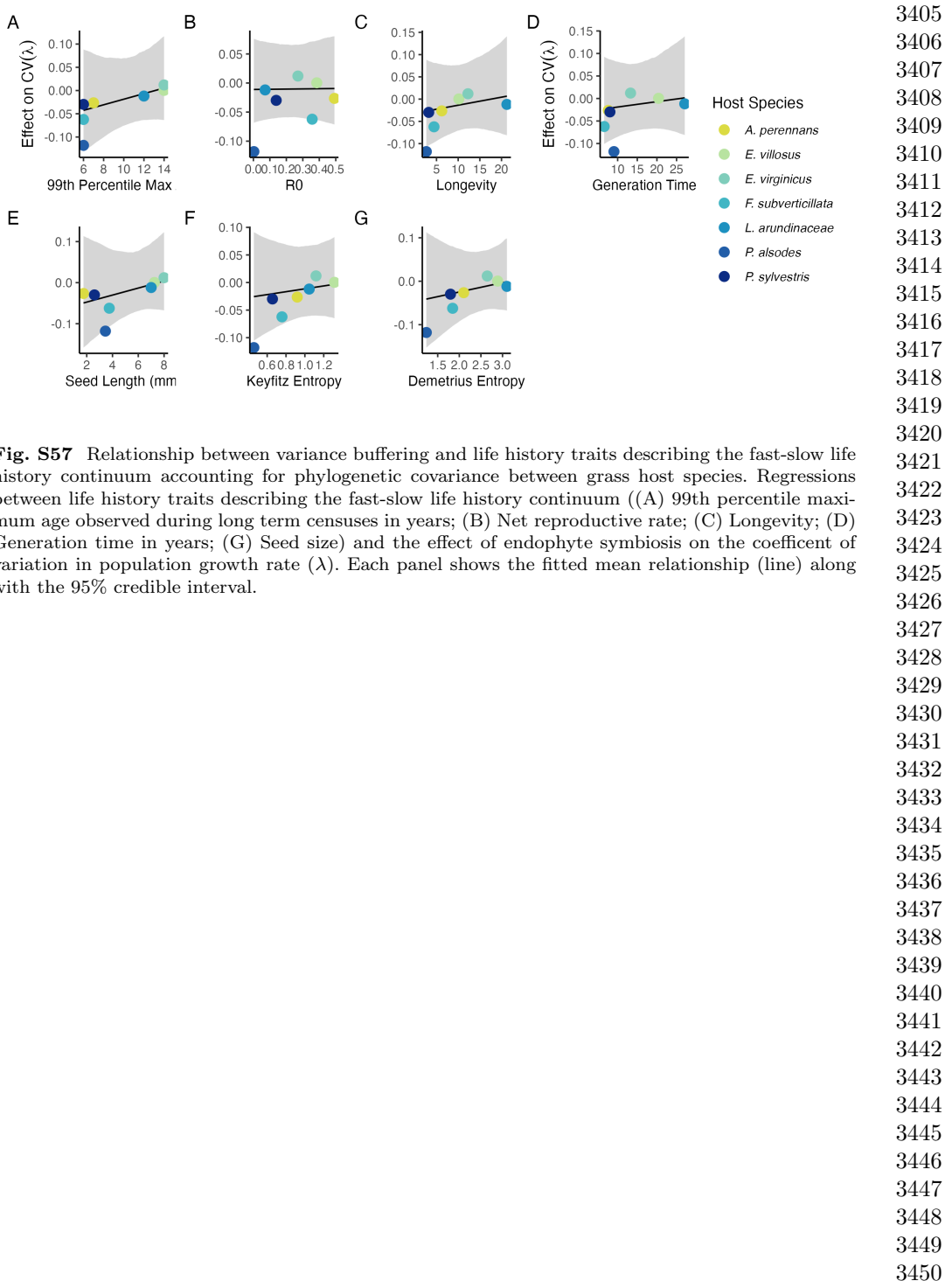
3400

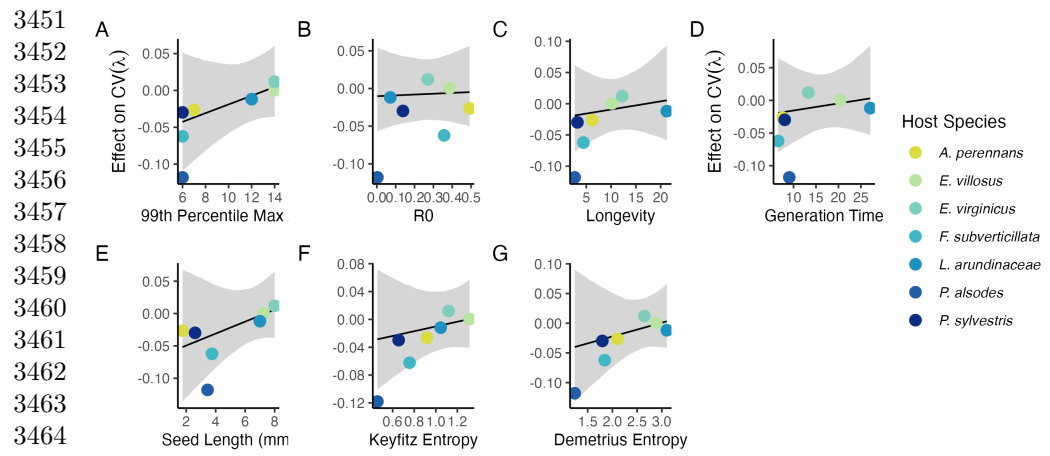
3401

3402

3403

3404





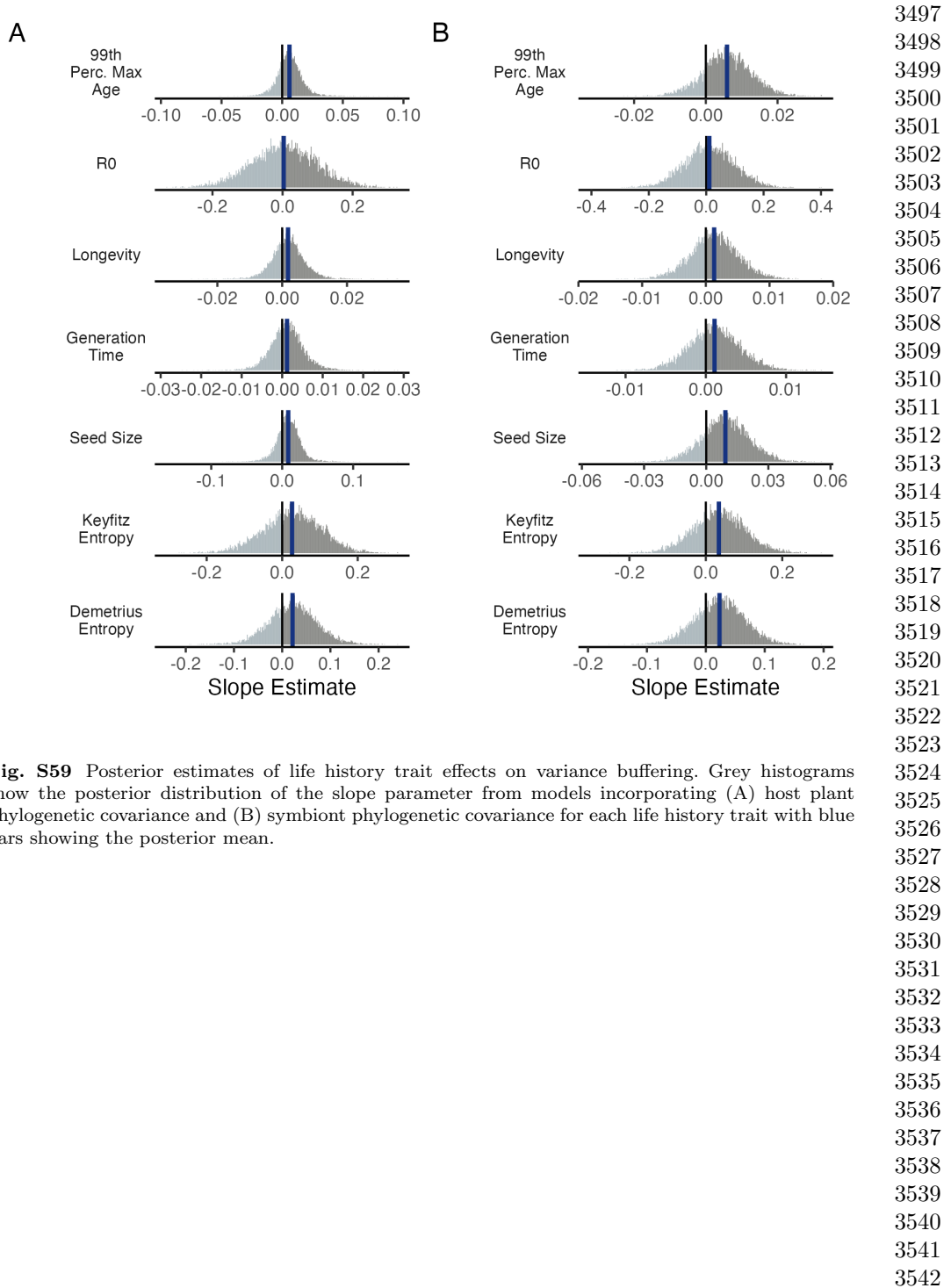


**Fig. S59** Posterior estimates of life history trait effects on variance buffering. Grey histograms show the posterior distribution of the slope parameter from models incorporating (A) host plant phylogenetic covariance and (B) symbiont phylogenetic covariance for each life history trait with blue bars showing the posterior mean.



<b>Supplemental Tables S1-S3</b>	3589
	3590
	3591
	3592
	3593
	3594
	3595
	3596
	3597
	3598
	3599
	3600
	3601
	3602
	3603
	3604
	3605
	3606
	3607
	3608
	3609
	3610
	3611
	3612
	3613
	3614
	3615
	3616
	3617
	3618
	3619
	3620
	3621
	3622
	3623
	3624
	3625
	3626
	3627
	3628
	3629
	3630
	3631
	3632
	3633
	3634

3635  
 3636  
 3637  
 3638  
 3639  
 3640  
 3641  
 3642  
 3643  
 3644  
 3645  
 3646  
 3647  
 3648  
 3649  
 3650  
 3651  
 3652  
 3653  
 3654  
 3655  
 3656  
 3657  
 3658  
 3659  
 3660  
 3661  
 3662  
 3663  
 3664  
 3665  
 3666  
 3667  
 3668  
 3669  
 3670  
 3671  
 3672  
 3673  
 3674  
 3675  
 3676  
 3677  
 3678  
 3679  
 3680

**Table S1** Summary of host-endophyte propagation and transplant methods

Host Species	Symbiont Species	Heat treatment duration (Temp.)	Transplant date
<i>Agrostis perennans</i>	<i>E. amarillans</i>	12 min. hot water bath (60 °C)	April 2008 (10 plots)
<i>Elymus villosus</i>	<i>E. elymi</i>	6 days drying oven (60 °C)	April 2008 (10 plots)
<i>Elymus virginicus</i>	<i>E. elymi</i> or <i>EviTG-1</i>	6 days drying oven (60 °C)	April 2008 (10 plots)
<i>Festuca subverticillata</i>	<i>E. starrii</i>	6 days drying oven (60 °C)	April 2008 (10 plots)
<i>Lolium arundinaceum</i>	<i>E. coenophiala</i>	6 days drying oven (60 °C)	Sept. 2007 (10 plots)
<i>Poa alsodes</i>	<i>E. alsodes</i>	7 days drying oven (60 °C)	Sept. 2007 (8 plots)/April 2008 (10 plots)
<i>Poa sylvestris</i>	<i>E. PsyTG-1</i>	7 days drying oven (60 °C)	Sept. 2007 (8 plots)/April 2008 (10 plots)

**Table S2** Summary of focal life history traits

Host Species	Observed max age (years)	99th percentile max age (years)	Generation time (years)	$R_0$	Longevity (years)	Seed length (mm.)	Keyfitz Entropy	Demetrius Entropy	Imperfect transmission rate (%)	Stromata Observed (% of indiv. per species)
<i>Agrostis perennans</i>	11	7	7.6	0.58	6.4	1.75	0.9	2.1	69.8	0.0
<i>Elymus villosus</i>	14	14	20.7	0.35	9.8	7.25	1.3	2.9	100	4.6
<i>Elymus virginicus</i>	14	14	13.4	0.25	12.5	8	1.1	2.6	100	0.6
<i>Festuca subverticillata</i>	9	6	6.6	0.28	4.3	3.75	0.8	1.8	42.7	0.0
<i>Lolium arundinaceum</i>	12*	12*	27.4	0.08	21.3	7	1.1	3.1	100	0.0
<i>Poa alsodes</i>	8	6	9.2	0.0033	2.6	3.45	0.5	1.2	99.9	0.0
<i>Poa sylvestris</i>	12	6	8.0	0.14	3.2	2.6	0.7	1.8	16.6	0.1
Page's $\lambda$ (host)	—	0.27	0.28	0.23	0.28	0.27	0.25	0.25	—	—
Page's $\lambda$ (symbiont)	—	0.63	0.63	0.63	0.63	0.62	0.62	0.62	—	—

\*Censuses for *L. arundinaceum* plots stopped after year 12 of the experiment.

3727  
 3728  
 3729  
 3730  
 3731  
 3732  
 3733  
 3734  
 3735  
 3736  
 3737  
 3738  
 3739  
 3740  
 3741  
 3742  
 3743  
 3744  
 3745  
 3746  
 3747  
 3748  
 3749  
 3750  
 3751  
 3752  
 3753  
 3754  
 3755  
 3756  
 3757  
 3758  
 3759  
 3760  
 3761  
 3762  
 3763  
 3764  
 3765  
 3766  
 3767  
 3768  
 3769  
 3770  
 3771  
 3772

**Table S3** Summary of host-endophyte drought sensitivities

Host Species	Effect on CV( $\lambda$ )	Effect on Mean( $\lambda$ )	$\frac{\Delta\lambda^-}{\Delta SPEI_3}$	$\frac{\Delta\lambda^+}{\Delta SPEI_3}$	3 month S- to S+ ratio	$\frac{\Delta\lambda^-}{\Delta SPEI_{12}}$	$\frac{\Delta\lambda^+}{\Delta SPEI_{12}}$	12 month S- to S+ ratio
<i>Agrostis perennans</i>	-0.0264	0.0441	0.03	-0.04	0.85	0.11	-0.06	1.82
<i>Elymus villosus</i>	0.0003	0.0509	-0.03	0.01	1.95	0.03	0.04	0.70
<i>Elymus virginicus</i>	0.0120	0.0578	0.07	0.05	1.50	0.10	0.07	1.42
<i>Festuca subverticillata</i>	-0.0622	0.1639	0.02	0.02	1.01	-0.13	-0.09	1.43
<i>Lolium arundinaceum</i>	-0.0118	0.1022	-0.01	0.01	1.32	0.03	-0.03	1.02
<i>Poa alsodes</i>	-0.1179	0.1282	0.10	0.14	0.71	0.11	0.14	0.73
<i>Poa sylvestris</i>	-0.0298	-0.0085	0.07	0.16	0.44	0.05	0.10	0.55

<b>References</b>	3773
[1] Seneviratne, S. <i>et al.</i> <i>Changes in climate extremes and their impacts on the natural physical environment</i> (Cambridge University Press, 2012).	3774
[2] IPCC. Climate change 2021: The physical science basis (2021). URL <a href="https://www.ipcc.ch/report/ar6/wg1/">https://www.ipcc.ch/report/ar6/wg1/</a> .	3775
[3] Clark, J. S. Why environmental scientists are becoming bayesians. <i>Ecology letters</i> <b>8</b> , 2–14 (2005).	3776
[4] Lewontin, R. C. & Cohen, D. On Population Growth in a Randomly Varying Environment. <i>Proceedings of the National Academy of Sciences</i> <b>62</b> , 1056–1060 (1969). URL <a href="https://www.pnas.org/content/62/4/1056">https://www.pnas.org/content/62/4/1056</a> . Publisher: National Academy of Sciences Section: Biological Sciences: Zoology.	3777
[5] Tuljapurkar, S. D. Population dynamics in variable environments. III. Evolutionary dynamics of r-selection. <i>Theoretical Population Biology</i> <b>21</b> , 141–165 (1982). URL <a href="http://www.sciencedirect.com/science/article/pii/0040580982900107">http://www.sciencedirect.com/science/article/pii/0040580982900107</a> .	3778
[6] Cohen, J. E. Comparative statics and stochastic dynamics of age-structured populations. <i>Theoretical population biology</i> <b>16</b> , 159–171 (1979).	3779
[7] Tuljapurkar, S. <i>Population dynamics in variable environments</i> Vol. 85 (Springer Science & Business Media, 2013).	3780
[8] Pfister, C. A. Patterns of variance in stage-structured populations: evolutionary predictions and ecological implications. <i>Proceedings of the National Academy of Sciences</i> <b>95</b> , 213–218 (1998).	3781
[9] Morris, W. F. <i>et al.</i> Longevity can buffer plant and animal populations against changing climatic variability. <i>Ecology</i> <b>89</b> , 19–25 (2008).	3782
[10] Compagnoni, A. <i>et al.</i> The effect of demographic correlations on the stochastic population dynamics of perennial plants. <i>Ecological Monographs</i> <b>86</b> , 480–494 (2016).	3783
[11] Ellis, M. M. & Crone, E. E. The role of transient dynamics in stochastic population growth for nine perennial plants. <i>Ecology</i> <b>94</b> , 1681–1686 (2013).	3784
[12] Murphy, G. I. Pattern in life history and the environment. <i>The American Naturalist</i> <b>102</b> , 391–403 (1968).	3785
[13] Compagnoni, A. <i>et al.</i> Herbaceous perennial plants with short generation time have stronger responses to climate anomalies than those with longer generation time. <i>Nature communications</i> <b>12</b> , 1–8 (2021).	3786

- 3819 [14] Le Coeur, C., Yoccoz, N. G., Salguero-Gómez, R. & Vindenes, Y. Life his-  
3820 tory adaptations to fluctuating environments: Combined effects of demographic  
3821 buffering and lability. *Ecology Letters* **25**, 2107–2119 (2022).
- 3822
- 3823 [15] Rodríguez-Caro, R. C. *et al.* The limits of demographic buffering in coping with  
3824 environmental variation. *Oikos* **130**, 1346–1358 (2021).
- 3825
- 3826 [16] Tuljapurkar, S. & Orzack, S. H. Population dynamics in variable environments i.  
3827 long-run growth rates and extinction. *Theoretical Population Biology* **18**, 314–342  
3828 (1980).
- 3829
- 3830 [17] Fieberg, J. & Ellner, S. P. Stochastic matrix models for conservation and  
3831 management: a comparative review of methods. *Ecology letters* **4**, 244–266 (2001).
- 3832
- 3833 [18] Menges, E. S. Applications of population viability analyses in plant conservation.  
3834 *Ecological Bulletins* 73–84 (2000).
- 3835
- 3836 [19] Kuparinen, A., Boit, A., Valdovinos, F. S., Lassaux, H. & Martinez, N. D.  
3837 Fishing-induced life-history changes degrade and destabilize harvested ecosys-  
3838 tems. *Scientific reports* **6**, 22245 (2016).
- 3839
- 3840 [20] Hilde, C. H. *et al.* The Demographic Buffering Hypothesis: Evidence and Chal-  
3841 lenges. *Trends in Ecology & Evolution* **0** (2020). URL [https://www.cell.com/trends/ecology-evolution/abstract/S0169-5347\(20\)30050-1](https://www.cell.com/trends/ecology-evolution/abstract/S0169-5347(20)30050-1). Publisher: Elsevier.
- 3842
- 3843 [21] Dybala, K. E., Gardali, T. & Eadie, J. M. Dependent vs. independent juvenile  
3844 survival: contrasting drivers of variation and the buffering effect of parental care.  
3845 *Ecology* **94**, 1584–1593 (2013).
- 3846
- 3847 [22] Colchero, F., Eckardt, W. & Stoinski, T. Evidence of demographic buffering in  
3848 an endangered great ape: Social buffering on immature survival and the role of  
3849 refined sex-age classes on population growth rate. *Journal of Animal Ecology* **90**,  
3850 1701–1713 (2021).
- 3851
- 3852 [23] Rodriguez, R., White Jr, J., Arnold, A. E. & Redman, a. R. a. Fungal endophytes:  
3853 diversity and functional roles. *New phytologist* **182**, 314–330 (2009).
- 3854
- 3855 [24] McFall-Ngai, M. *et al.* Animals in a bacterial world, a new imperative for the  
3856 life sciences. *Proceedings of the National Academy of Sciences* **110**, 3229–3236  
3857 (2013).
- 3858
- 3859 [25] Funkhouser, L. J. & Bordenstein, S. R. Mom knows best: the universality of  
3860 maternal microbial transmission. *PLoS biology* **11**, e1001631 (2013).
- 3861
- 3862 [26] Fine, P. E. Vectors and vertical transmission: an epidemiologic perspective.  
3863 *Annals of the New York Academy of Sciences* **266**, 173–194 (1975).
- 3864

- [27] Russell, J. A. & Moran, N. A. Costs and benefits of symbiont infection in aphids: variation among symbionts and across temperatures. *Proceedings of the Royal Society B: Biological Sciences* **273**, 603–610 (2006). 3865  
3866  
3867  
3868  
3869  
3870  
3871  
3872  
3873  
3874  
3875  
3876  
3877  
3878  
3879  
3880  
3881  
3882  
3883  
3884  
3885  
3886  
3887  
3888  
3889  
3890  
3891  
3892  
3893  
3894  
3895  
3896  
3897  
3898  
3899  
3900  
3901  
3902  
3903  
3904  
3905  
3906  
3907  
3908  
3909  
3910
- [28] Kivlin, S. N., Emery, S. M. & Rudgers, J. A. Fungal symbionts alter plant responses to global change. *American Journal of Botany* **100**, 1445–1457 (2013). 3865  
3866  
3867  
3868  
3869  
3870  
3871  
3872  
3873  
3874  
3875  
3876  
3877  
3878  
3879  
3880  
3881  
3882  
3883  
3884  
3885  
3886  
3887  
3888  
3889  
3890  
3891  
3892  
3893  
3894  
3895  
3896  
3897  
3898  
3899  
3900  
3901  
3902  
3903  
3904  
3905  
3906  
3907  
3908  
3909  
3910
- [29] Dunbar, H. E., Wilson, A. C. C., Ferguson, N. R. & Moran, N. A. Aphid thermal tolerance is governed by a point mutation in bacterial symbionts. *PLoS biology* **5**, e96 (2007). 3865  
3866  
3867  
3868  
3869  
3870  
3871  
3872  
3873  
3874  
3875  
3876  
3877  
3878  
3879  
3880  
3881  
3882  
3883  
3884  
3885  
3886  
3887  
3888  
3889  
3890  
3891  
3892  
3893  
3894  
3895  
3896  
3897  
3898  
3899  
3900  
3901  
3902  
3903  
3904  
3905  
3906  
3907  
3908  
3909  
3910
- [30] Reyna, R., Cooke, P., Grum, D., Cook, D. & Creamer, R. Detection and localization of the endophyte *undifilum oxytropis* in locoweed tissues. *Botany* **90**, 1229–1236 (2012). 3865  
3866  
3867  
3868  
3869  
3870  
3871  
3872  
3873  
3874  
3875  
3876  
3877  
3878  
3879  
3880  
3881  
3882  
3883  
3884  
3885  
3886  
3887  
3888  
3889  
3890  
3891  
3892  
3893  
3894  
3895  
3896  
3897  
3898  
3899  
3900  
3901  
3902  
3903  
3904  
3905  
3906  
3907  
3908  
3909  
3910
- [31] Saikonen, K., Gundel, P. E. & Helander, M. Chemical ecology mediated by fungal endophytes in grasses. *Journal of chemical ecology* **39**, 962–968 (2013). 3865  
3866  
3867  
3868  
3869  
3870  
3871  
3872  
3873  
3874  
3875  
3876  
3877  
3878  
3879  
3880  
3881  
3882  
3883  
3884  
3885  
3886  
3887  
3888  
3889  
3890  
3891  
3892  
3893  
3894  
3895  
3896  
3897  
3898  
3899  
3900  
3901  
3902  
3903  
3904  
3905  
3906  
3907  
3908  
3909  
3910
- [32] Neyaz, M., Gardner, D. R., Creamer, R. & Cook, D. Localization of the swainsonine-producing chaetothyriales symbiont in the seed and shoot apical meristem in its host *ipomoea carnea*. *Microorganisms* **10**, 545 (2022). 3865  
3866  
3867  
3868  
3869  
3870  
3871  
3872  
3873  
3874  
3875  
3876  
3877  
3878  
3879  
3880  
3881  
3882  
3883  
3884  
3885  
3886  
3887  
3888  
3889  
3890  
3891  
3892  
3893  
3894  
3895  
3896  
3897  
3898  
3899  
3900  
3901  
3902  
3903  
3904  
3905  
3906  
3907  
3908  
3909  
3910
- [33] Chamberlain, S. A., Bronstein, J. L. & Rudgers, J. A. How context dependent are species interactions? *Ecology letters* **17**, 881–890 (2014). 3865  
3866  
3867  
3868  
3869  
3870  
3871  
3872  
3873  
3874  
3875  
3876  
3877  
3878  
3879  
3880  
3881  
3882  
3883  
3884  
3885  
3886  
3887  
3888  
3889  
3890  
3891  
3892  
3893  
3894  
3895  
3896  
3897  
3898  
3899  
3900  
3901  
3902  
3903  
3904  
3905  
3906  
3907  
3908  
3909  
3910
- [34] Catford, J. A., Wilson, J. R., Pyšek, P., Hulme, P. E. & Duncan, R. P. Addressing context dependence in ecology. *Trends in Ecology & Evolution* **37**, 158–170 (2022). 3865  
3866  
3867  
3868  
3869  
3870  
3871  
3872  
3873  
3874  
3875  
3876  
3877  
3878  
3879  
3880  
3881  
3882  
3883  
3884  
3885  
3886  
3887  
3888  
3889  
3890  
3891  
3892  
3893  
3894  
3895  
3896  
3897  
3898  
3899  
3900  
3901  
3902  
3903  
3904  
3905  
3906  
3907  
3908  
3909  
3910
- [35] Jordano, P. Spatial and temporal variation in the avian-frugivore assemblage of *prunus mahaleb*: patterns and consequences. *Oikos* 479–491 (1994). 3865  
3866  
3867  
3868  
3869  
3870  
3871  
3872  
3873  
3874  
3875  
3876  
3877  
3878  
3879  
3880  
3881  
3882  
3883  
3884  
3885  
3886  
3887  
3888  
3889  
3890  
3891  
3892  
3893  
3894  
3895  
3896  
3897  
3898  
3899  
3900  
3901  
3902  
3903  
3904  
3905  
3906  
3907  
3908  
3909  
3910
- [36] Leuchtmann, A. Systematics, distribution, and host specificity of grass endophytes. *Natural toxins* **1**, 150–162 (1992). 3865  
3866  
3867  
3868  
3869  
3870  
3871  
3872  
3873  
3874  
3875  
3876  
3877  
3878  
3879  
3880  
3881  
3882  
3883  
3884  
3885  
3886  
3887  
3888  
3889  
3890  
3891  
3892  
3893  
3894  
3895  
3896  
3897  
3898  
3899  
3900  
3901  
3902  
3903  
3904  
3905  
3906  
3907  
3908  
3909  
3910
- [37] Cheplick, G. P., Faeth, S. & Faeth, S. H. *Ecology and evolution of the grass-endophyte symbiosis* (OUP USA, 2009). 3865  
3866  
3867  
3868  
3869  
3870  
3871  
3872  
3873  
3874  
3875  
3876  
3877  
3878  
3879  
3880  
3881  
3882  
3883  
3884  
3885  
3886  
3887  
3888  
3889  
3890  
3891  
3892  
3893  
3894  
3895  
3896  
3897  
3898  
3899  
3900  
3901  
3902  
3903  
3904  
3905  
3906  
3907  
3908  
3909  
3910
- [38] Brem, D. & Leuchtmann, A. Epichloë grass endophytes increase herbivore resistance in the woodland grass *brachypodium sylvaticum*. *Oecologia* **126**, 522–530 (2001). 3865  
3866  
3867  
3868  
3869  
3870  
3871  
3872  
3873  
3874  
3875  
3876  
3877  
3878  
3879  
3880  
3881  
3882  
3883  
3884  
3885  
3886  
3887  
3888  
3889  
3890  
3891  
3892  
3893  
3894  
3895  
3896  
3897  
3898  
3899  
3900  
3901  
3902  
3903  
3904  
3905  
3906  
3907  
3908  
3909  
3910
- [39] Decunta, F. A., Pérez, L. I., Malinowski, D. P., Molina-Montenegro, M. A. & Gundel, P. E. A systematic review on the effects of epichloë fungal endophytes on drought tolerance in cool-season grasses. *Frontiers in plant science* **12**, 644731 (2021). 3865  
3866  
3867  
3868  
3869  
3870  
3871  
3872  
3873  
3874  
3875  
3876  
3877  
3878  
3879  
3880  
3881  
3882  
3883  
3884  
3885  
3886  
3887  
3888  
3889  
3890  
3891  
3892  
3893  
3894  
3895  
3896  
3897  
3898  
3899  
3900  
3901  
3902  
3903  
3904  
3905  
3906  
3907  
3908  
3909  
3910

- 3911 [40] Bacon, C. W. & White, J. F. in *Stains, media, and procedures for analyzing*  
3912      *endophytes* 47–56 (CRC Press, 2018).
- 3913
- 3914 [41] Rudgers, J. A. & Swafford, A. L. Benefits of a fungal endophyte in *elymus*  
3915      *virginicus* decline under drought stress. *Basic and Applied Ecology* **10**, 43–51  
3916      (2009).
- 3917
- 3918 [42] Bultman, T. L., White Jr, J. F., Bowdish, T. I., Welch, A. M. & Johnston, J.  
3919      Mutualistic transfer of epichloë spermatia by phorbia flies. *Mycologia* **87**, 182–189  
3920      (1995).
- 3921
- 3922 [43] Stan Development Team. RStan: the R interface to Stan (2022). URL <https://mc-stan.org/>. R package version 2.21.7.
- 3923
- 3924 [44] Elderd, B. D. & Miller, T. E. Quantifying demographic uncertainty: Bayesian  
3925      methods for integral projection models. *Ecological Monographs* **86**, 125–144  
3926      (2016).
- 3927
- 3928 [45] Gabry, J., Simpson, D., Vehtari, A., Betancourt, M. & Gelman, A. Visualization  
3929      in bayesian workflow. *Journal of the Royal Statistical Society Series A: Statistics*  
3930      in Society **182**, 389–402 (2019).
- 3931
- 3932 [46] Brooks, S. P. & Gelman, A. General methods for monitoring convergence of  
3933      iterative simulations. *Journal of computational and graphical statistics* **7**, 434–455  
3934      (1998).
- 3935
- 3936 [47] Gelman, A. & Hill, J. *Data analysis using regression and multilevel/hierarchical*  
3937      *models* (Cambridge university press, 2006).
- 3938
- 3939 [48] Williams, J. L., Miller, T. E. & Ellner, S. P. Avoiding unintentional eviction from  
3940      integral projection models. *Ecology* **93**, 2008–2014 (2012).
- 3941
- 3942 [49] Jones, O. R. *et al.* Rcompadre and rage—two r packages to facilitate the use of  
3943      the compadre and comadre databases and calculation of life-history traits from  
3944      matrix population models. *Methods in Ecology and Evolution* **13**, 770–781 (2022).
- 3945
- 3946 [50] .
- 3947 [51] Bürkner, P.-C. brms: An R package for Bayesian multilevel models using Stan.  
3948      *Journal of Statistical Software* **80**, 1–28 (2017).
- 3949
- 3950 [52] Zanne, A. E. *et al.* Three keys to the radiation of angiosperms into freezing  
3951      environments. *Nature* **506**, 89–92 (2014).
- 3952
- 3953 [53] Leuchtmann, A., Bacon, C. W., Schardl, C. L., White Jr, J. F. & Tadych,  
3954      M. Nomenclatural realignment of neotyphodium species with genus epichloë.  
3955      *Mycologia* **106**, 202–215 (2014).
- 3956

- [54] Metcalf, C. J. E. *et al.* Statistical modelling of annual variation for inference on stochastic population dynamics using integral projection models. *Methods in Ecology and Evolution* **6**, 1007–1017 (2015). 3957  
3958  
3959  
3960  
3961  
3962  
3963  
3964  
3965  
3966  
3967  
3968  
3969  
3970  
3971  
3972  
3973  
3974  
3975  
3976  
3977  
3978  
3979  
3980  
3981  
3982  
3983  
3984  
3985  
3986  
3987  
3988  
3989  
3990  
3991  
3992  
3993  
3994  
3995  
3996  
3997  
3998  
3999  
4000  
4001  
4002
- [55] Caswell, H. Matrix population models: Construction, analysis, and interpretation. 2nd edn sinauer associates. *Inc., Sunderland, MA* (2001).
- [56] Rees, M. & Ellner, S. P. Integral projection models for populations in temporally varying environments. *Ecological Monographs* **79**, 575–594 (2009).
- [57] Rees, M. Evolutionary ecology of seed dormancy and seed size. *Philosophical Transactions of the Royal Society of London. Series B: Biological Sciences* **351**, 1299–1308 (1996).
- [58] Moles, A. T. & Westoby, M. Seedling survival and seed size: a synthesis of the literature. *Journal of Ecology* **92**, 372–383 (2004).
- [59] Afkhami, M. E. & Rudgers, J. A. Symbiosis lost: imperfect vertical transmission of fungal endophytes in grasses. *The American Naturalist* **172**, 405–416 (2008).
- [60] Jeschke, J. M. & Kokko, H. The roles of body size and phylogeny in fast and slow life histories. *Evolutionary Ecology* **23**, 867–878 (2009).
- [61] Vicente-Serrano, S. M., Beguería, S. & López-Moreno, J. I. A multiscalar drought index sensitive to global warming: the standardized precipitation evapotranspiration index. *Journal of climate* **23**, 1696–1718 (2010).
- [62] Rudgers, J. A. & Clay, K. An invasive plant–fungal mutualism reduces arthropod diversity. *Ecology Letters* **11**, 831–840 (2008).
- [63] Crawford, K. M., Land, J. M. & Rudgers, J. A. Fungal endophytes of native grasses decrease insect herbivore preference and performance. *Oecologia* **164**, 431–444 (2010).
- [64] Afkhami, M. E. & Strauss, S. Y. Native fungal endophytes suppress an exotic dominant and increase plant diversity over small and large spatial scales. *Ecology* **97**, 1159–1169 (2016).
- [65] Smith, E., Vaughan, G., Ketchum, R., McParland, D. & Burt, J. Symbiont community stability through severe coral bleaching in a thermally extreme lagoon. *Scientific Reports* **7**, 2428 (2017).
- [66] Dallas, J. W. & Warne, R. W. Captivity and animal microbiomes: potential roles of microbiota for influencing animal conservation. *Microbial Ecology* 1–19 (2022).
- [67] Wu, L. *et al.* Reduction of microbial diversity in grassland soil is driven by long-term climate warming. *Nature Microbiology* **7**, 1054–1062 (2022).

- 4003 [68] Ehrlén, J. & Morris, W. F. Predicting changes in the distribution and abundance  
4004 of species under environmental change. *Ecology letters* **18**, 303–314 (2015).
- 4005
- 4006 [69] Chamberlain, S., Hocking, D. & Anderson, B. Package ‘rnoaa’ (2022).
- 4007
- 4008 [70] Beguería, S. & Vicente-Serrano, S. M. Spei: calculation of the standardised  
4009 precipitation-evapotranspiration index. *R package version 1* (2013).
- 4010
- 4011
- 4012
- 4013
- 4014
- 4015
- 4016
- 4017
- 4018
- 4019
- 4020
- 4021
- 4022
- 4023
- 4024
- 4025
- 4026
- 4027
- 4028
- 4029
- 4030
- 4031
- 4032
- 4033
- 4034
- 4035
- 4036
- 4037
- 4038
- 4039
- 4040
- 4041
- 4042
- 4043
- 4044
- 4045
- 4046
- 4047
- 4048